

va

THE DETERMINATION OF LEAD IN BLOOD BY ATOMIC SPECTROSCOPY

BY

DAVID ALEXANDER CONOLLY, B.Sc., A.R.C.S.

A Thesis submitted for the Degree of Doctor of Philosophy,
University of London.

September 1973

Department of Chemistry,
Imperial College of Science and Technology,
London, SW7 2AY.

Abstract.

A variety of atom reservoirs for use in atomic absorption and atomic fluorescence spectrometry is reviewed. The efficacy of the Carbon Filament Atom Reservoir is related (theoretically) to certain features of its design and these relationships tested.

Methods for the determination of lead from pure aqueous samples by atomic absorption spectrometry and atomic fluorescence spectrometry with the C.F.A.R. are described and compared. The effects of some foreign ions on these methods are described.

Integration of the peak absorbance signals obtained from the C.F.A.R. is investigated and shown to offer no advantage over measurement of the peak height.

A method for the determination of lead in blood samples, by atomic absorption spectrometry with the C.F.A.R. is described.

Acknowledgements.

The work recorded in this thesis was carried out in the Chemistry Department of the Imperial College of Science and Technology between October 1969 and August 1972.

I owe a debt of thanks to Professor T.S. West for much advice and encouragement, to my colleagues in the Harwood Laboratory for many helpful discussions, to Dr. T. Delves of the Hospital for Sick Children, Great Ormond Street, London, for supplying blood samples and to the Ethyl Corporation Ltd. for financial assistance.

Finally I particularly wish to thank my wife, Lesley, for her invaluable help in preparing and typing this thesis.

Contents.

<u>Chapter One</u>	<u>Atom Reservoirs in Atomic Absorption Spectrometry and Atomic Fluorescence Spectrometry</u>	8
	<u>Atomic Absorption Spectrometry</u>	9
	Absorption Measurements	16
	Atomic Fluorescence Spectrometry	20
	Flame Atom Reservoirs	25
	Plasma Atom Reservoirs	30
	Furnace Atom Reservoirs	31
	Filament Atom Reservoirs	36
	Hollow Cathode Atom Reservoirs	40
	Laser based Atom Reservoirs	43
 <u>Chapter Two</u>	 <u>The Carbon Filament Atom Reservoir</u>	 44
	Basic Design	45
	Transience of the Atomic Vapour	48
	Heating Rate (Theoretical)	51
	Heating Rate (Experimental)	56
	Conclusions	63
 <u>Chapter Three</u>	 <u>The Determination of Lead on the Carbon Filament Atom Reservoir by Atomic Absorption Spectrometry.</u>	 67
	Delivery of small samples	68
	Instrumentation	70
	Monochromator	72
	Amplifier and Recorder	73
	Inert Atmosphere	80

	Power Supply	82
	Carbon Filament	83
	Hollow Cathode Lamp	86
	Optical Arrangement	86
	Method of Analysis	89
<u>Chapter Four</u>	<u>The Determination of Lead on the Carbon Filament Atom Reservoir by Atomic Fluorescence Spectrometry</u>	96
	Advantage of A.F.S.	97
	Instrumentation	97
	Method of Analysis	98
<u>Chapter Five</u>	<u>Interference Studies on the Carbon Filament Atom Reservoir</u>	103
	The Effect of Sodium and Potassium on Signals due to Atomic Lead	104
	The Variation of Interference with respect to Position of Light Path	106
	Selective Volatilisation of Elements from the Filament	106
<u>Chapter Six</u>	<u>Integrated Absorption Measurements with the Carbon Filament Atom Reservoir</u>	109
	Integrator	110
	Relationship between Integrated Signal and Heating Rate	112
	Method of Analysis	114

<u>Chapter Seven</u>	<u>The Determination of Lead in Blood</u>	118
	Lead Poisoning	119
	Problems arising from Blood Samples	120
	Controlled Heating	121
	Chemical Breakdown	121
	Dilution of Blood	123
	Method of Analysis	125
	Method of Standard Addition	127
	Conclusions	129
<u>References</u>		131

Errata.

- Chapter One p.26 for 'refractoy' read 'refractory',
p.43 for 'spectrometry' read 'spectrometric'.
- Chapter Three p.70 for 'arrnagements' read 'arrangements'.
p.83 for 'Before use in ...' read 'Before
use of ...'
- Chapter Five p.104 for 'corrspounding' read 'corresponding'.
- Chapter Seven p.122 for 'quatity' read 'quantity'.

Chapter One

Atom Reservoirs

in

Atomic Absorption Spectrometry

and

Atomic Fluorescence Spectrometry

The main concerns of this thesis are atomic absorption spectrometry (A.A.S.) and atomic fluorescence spectrometry (A.F.S.). A brief review of the theory of such measurements follows.

Atomic Absorption Spectrometry.

Free atoms can absorb electromagnetic radiation. This absorption is accompanied by a change in the energy state of an electron. The frequency of the absorbed radiation is determined by the separation of the electron energy levels.

$$\Delta E = h\nu \quad \underline{1.1}$$

where ΔE is the energy change associated with the electronic transition,

h is Planck's constant,

and ν is the frequency of the absorbed light.

The degree of absorption is described by an analogue of Lambert's Law.

$$I = I_0 \exp.(-k_\nu l) \quad \underline{1.2}$$

where I is the intensity of the transmitted light,

I_0 is the intensity of the incident light,

l is the absorption path length,

k_ν is the absorption coefficient at frequency ν ,

and $k_\nu \propto N \quad \underline{1.3}$

where N is the number of atoms in the light path

capable of absorbing radiation of frequency ν .

In fact absorption is observed not at a dis-

crete frequency, but over a small range i.e. the absorption has a finite width. If k_ν (which represents degree of absorption) is plotted against ν a typical result would be that shown in Fig. 1.1.

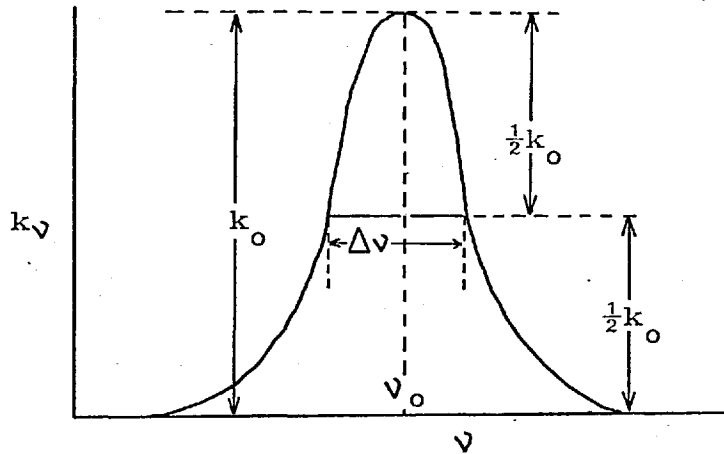


Fig. 1.1

k_0 is the maximum value of k ,

ν_0 is the value of ν at the peak,

$\Delta\nu$ is called the half width of the line and is the width at half the height of the line. (NOT half the width)

This finite thickness of the absorption line can be attributed to three main causes:-

i) Natural width,

ii) Doppler broadening,

iii) Lorentz broadening,

and to three minor causes:-

iv) Isotopic splitting, i.e. ν_0 varies slightly for different isotopes,

v) Zeeman splitting, i.e. an external magnetic field will split the electronic energy levels,

vi) Stark splitting, i.e. an external electric field

will split the electronic energy levels.

i) The natural width of an absorption line is due to the indeterminateness (after Heisenberg) of electron energy states, and can be calculated in terms of the lifetime of the excited state. The natural line profile is described by:-

$$k_{\nu} = \frac{k_0 \cdot (\Delta\nu_N)^2}{(\Delta\nu_N)^2 + 4(\nu - \nu_0)^2} \quad \underline{1.4}$$

where $\Delta\nu_N$ is the natural half width, i.e. the half width in the absence of any other effect. Generally $\Delta\nu_N$ is in the order of 10^{-5} nm., which is small in comparison with Doppler and Lorentz half widths.

ii) Since the atoms are moving with high, randomly distributed velocities, the Doppler effect (a shift of observed frequency which depends on the relative velocity of the object to the observer) appears not as a shift but as a broadening (i.e. a simultaneous shift in opposite directions) of the absorption profile. If a thermodynamic equilibrium (i.e. a Maxwellian distribution of velocities) is assumed, the broadened line profile is described by:-

$$k_{\nu} = k_0^D \cdot \exp. - \left[\frac{Ac^2}{2RT} \cdot \frac{(\nu - \nu_0)^2}{\nu_0^2} \right] \quad \underline{1.5}$$

where k_0^D is the maximum value of k_{ν} in the broadened profile. (Since the $\int_{-\infty}^{+\infty} k_{\nu} d\nu$ represents the energy absorbed, the peak value of k_0 must decrease as the profile is broadened).

\underline{A} is the atomic weight of the element observed,

c is the velocity of light,

R is the universal gas constant,

and T is the absolute temperature.

If

$$a) \quad k_{\nu} = \frac{1}{2} k_o^D, \quad \text{and}$$

$$b) \quad \nu - \nu_o = \frac{\Delta \nu_D}{2}$$

are substituted into equation 1.5, then

$$\Delta \nu_D = \frac{2\nu_o}{c} \cdot \left[\frac{2RT \ln 2}{\underline{A}} \right]^{\frac{1}{2}} \quad \underline{1.6}$$

results.

$\Delta \nu_D$ is called the Doppler half width and from the above a) and b) can be seen to be the width of the absorption line at half the height. k_o^D can be related to N (equation 1.3) from the classical (or the quantum) theory of electromagnetism:-

$$k_o^D = \frac{2e^2 (\pi \ln 2)^{\frac{1}{2}} N f}{mc \Delta \nu_D} \quad \underline{1.7}$$

where e is the charge on the electron,

m is the mass of the electron,

and f is the oscillator strength, which is an arbitrary factor in the classical theory, but in the quantum theory is related to the electronic transition probability and is constant for a given transition.

$\Delta \nu_D$ values range from roughly $5 \cdot 10^{-3} \text{ nm.}$ to $2 \cdot 10^{-3} \text{ nm.}$ in normal experimental conditions,

$$\text{i.e.} \quad \Delta \nu_D \gg \Delta \nu_N \quad \underline{1.8}$$

iii) Lorentz broadening is not fully understood, but depends on the presence of a foreign gas. Its effect is threefold:-

- a) to shift the peak of the absorption line,
- b) to broaden the absorption line,
- c) to introduce asymmetry about the peak of the absorption line.

Lorentz proposed a theory of molecular - atomic collisions which interrupt the intra-atomic process. This theory arrives at the following description of the line profile.

$$k_{\nu} = \frac{k_o^L (\Delta\nu_L)^2}{(\Delta\nu_L)^2 + 4(\nu - \nu_o)^2} \quad \underline{1.9}$$

where k_o^L is the maximum value of k_{ν} in the Lorentz broadened profile

and $\Delta\nu_L$ is the half width of the Lorentz broadened line, i.e. the Lorentz half width;

$$\text{also } k_o^L = \frac{2e^2 \cdot Nf}{mc \Delta\nu_L} \quad \underline{1.10}$$

This theory also provides an expression for $\Delta\nu_L$:-

$$\Delta\nu_L = 2.3026 \times 2.02 \times 10^{23} \sigma^2 P \left[\frac{2}{\pi RT} \left(\frac{1}{A} + \frac{1}{M} \right) \right]^{\frac{1}{2}} \quad \underline{1.11}$$

where $\pi\sigma$ is the effective collision cross-section,

M is the molecular weight of the foreign gas

and P is the partial pressure of the foreign gas.

Equation 1.11 agrees with experimental fact.

$$\Delta\nu_L \propto P \quad \underline{1.12}$$

The Lorentz theory however, explains neither the shift of the peak nor the asymmetry of the absorption profile.

Lindholm developed a theory (after Lenz and Weisskopf) of continuous atomic-molecular interaction which affects the phase of the intra-atomic process. The Lindholm theory accounts for the shift of the peak of the line and predicts

$$\frac{\Delta\nu_L}{\Delta\nu_S} = 2.77 \quad \underline{1.13}$$

where $\Delta\nu_S$ is the shift of the peak.

This prediction has been verified by experiments with nitrogen and argon as the foreign gas, but refuted by work with lighter gases. (1) Other attempts to decide between the Lorentz and Lindholm theories, e.g. by the study of the relationship between $\Delta\nu_L$ and temperature, have been indecisive.

The final profile of the absorption line, taking both Doppler and Lorentz broadening into account, is described by the Voigt equation. (2)

$$k_\nu = k_0^D \frac{a}{\pi} \int_{-\infty}^{+\infty} \frac{e^{-Y^2} dY}{a^2 + (\omega - Y)^2} \quad \underline{1.14}$$

$$\text{where } a = \frac{\Delta\nu_L \cdot [\ln 2]^{\frac{1}{2}}}{\Delta\nu_D}$$

$$\omega = \frac{2\Delta\nu_S \cdot [\ln 2]^{\frac{1}{2}}}{\Delta\nu_D}$$

$$Y = \frac{2\delta}{\Delta\nu_D}$$

This equation (1.14) is obtained when the Lorentz broadening is superimposed upon small elements of the Doppler profile. The term δ is the shift of each element under this treatment.

The isotopic, Zeeman and Stark effects are best considered in each particular case. They are frequently small in relation to the Doppler and Lorentz effects and are then ignored.

Summary.

Free atoms absorb radiation over a frequency range which is very small ($\approx 10^{-3}$ nm.) in comparison with molecular absorption bands. The shape of the absorption profile is dependent on many factors but the maximum value of the absorption coefficient is always proportional to the number of atoms in the light path capable of absorbing the radiation.

Absorption Measurements.

In all atomic absorption experiments the final measurement is of an electronically amplified signal from a photo-electron tube. More often than not the radiation falling on the photo-electron tube is modulated and the amplification involves a synchronous demodulation. It will be assumed that the end product of these processes is a true measure of the light intensity falling upon the photoelectric detector.

From the values of the incident light intensity, I_0 , and the transmitted light intensity, I , one of three functions may be calculated:-

- i) the integrated absorption coefficient,
- ii) the energy absorbed from a continuum source,
- iii) the relative absorption from a line source.

This last is by far the most convenient and frequently used function.

i) Integrated Absorption Coefficient.

This function is independent of the shape of the absorption profile and is directly proportional to the number of atoms in the light path capable of absorbing the radiation, and the oscillator strength.

$$K = \int_0^{\infty} k_{\nu} d\nu = \frac{\pi e^2 \cdot Nf}{mc} \quad \underline{1.15}$$

K is found by passing light from a continuum source through a known path length of free atoms and measuring I and I_0 at various values of ν .

Since, from equation 1.2,

$$k_{\nu} = \frac{1}{I} \ln \left(\frac{I_0}{I} \right) \quad \underline{1.16}$$

k_{ν} values are calculated and plotted as a function of ν . The value of K ($\int_0^{\infty} k_{\nu} d\nu$) is found graphically and a calibration curve of K vs. N constructed.

The technique requires a monochromator of exceptional resolving power (unless the absorption line is very broad). Fabry-Perot interferometers are capable of giving this necessary resolution, but very few other instruments. The 253.7 nm. mercury absorption line, broadened by very high pressures (10-50 atmospheres), has been examined in this manner.

ii) Total Energy Absorption.

By definition of intensity;

$$A_{\nu} = \int_0^{\infty} \frac{I_0 - I}{I_0} d\nu = \int_0^{\infty} \frac{1 - \frac{I}{I_0}}{1} d\nu \quad \underline{1.17}$$

where A_{ν} is the energy absorbed from the continuum spectrum by the absorption line centred on ν .

Therefore, from equation 1.2,

$$A_{\nu} = \int_0^{\infty} (1 - e^{-k_{\nu} l}) d\nu \quad \underline{1.18}$$

Two cases require separate treatment:-

a) If $k_{\nu} l \Rightarrow 0$,

$$\text{then } A_{\nu} = l \int_0^{\infty} k_{\nu} d\nu \quad \underline{1.19}$$

$$\text{i.e. } A_{\nu} = K \quad \underline{1.20}$$

$$A_{\nu} \propto Nfl \quad \underline{1.21}$$

b) If $k_{\nu} l$ is large,

$$\text{then } A_{\nu} = \left[\frac{2\pi e^2 \cdot N \cdot f \cdot l \cdot \Delta\nu}{mc} \right]^{\frac{1}{2}} \quad \underline{1.22}$$

$$\text{i.e.} \quad A \propto (Nf l)^{\frac{1}{2}} \quad \underline{1.23}$$

For case a) independence of the line profile is achieved, but not for case b).

iii) Relative Absorption from a Line Source;
the Walsh Method.

Measurements of the integrated absorption coefficient and the total energy absorbed from a continuum source would be difficult to use for routine analysis. Walsh⁽³⁾ reasoned that if a source produced an emission line narrower than the absorption line at the same peak frequency, then the absorption of that line by the atoms would give a direct measure of k_0 .

$$I = I_0 \exp.(-k_0 l) \quad \underline{1.2}$$

$$\log_{10} \frac{I_0}{I} = 2.3026 k_0 l \quad \underline{1.24}$$

The function $\log_{10} \frac{I_0}{I}$ Walsh called absorbance (A).

I

Even if the absorption line is broadened, the relation

$$A \propto k_0 \propto N \quad \underline{1.25}$$

remains true.

Walsh first used hollow cathode lamps (H.C.L.), which give very narrow atomic emission lines and demonstrated the above conclusion to be true. Hollow cathode lamps operate at a low pressure. Therefore the emission lines exhibit less Lorentz broadening than the absorption lines of atoms at atmospheric pressure (equation 1.12).

$$\Delta v_L \propto P$$

The lamps also operate at a temperature lower than

that of the atoms in a flame, so the Doppler broadening of the emission line is less than the Doppler broadening of the absorption profile (equation 1.6).

$$\Delta\nu_D \propto T^{\frac{1}{2}}$$

An additional (and very important) advantage of such narrow line sources is their selectivity. The atomic lines are so narrow that the possibility of overlap by the absorption line of another element is almost negligible; (only four such pairs of absorption lines have been reported).

Summary.

The relative absorption of a narrow atomic emission line from a hollow cathode lamp by an atomic vapour can be easily measured, using a low resolution monochromator to isolate the line of interest from other emission lines. If the emission line is narrower than the absorption profile and has the same peak frequency (this is usually the case) then the absorbance ($\log_{10} \frac{I}{I_0}$) is proportional to the number of atoms in

I

the vapour capable of absorbing the radiation. Positive spectral interference from foreign atoms is unlikely because the atomic absorption lines are very narrow.

As a result, A.A.S. is a selective, easy to use and sensitive method of trace analysis.

Atomic Fluorescence Spectrometry.

The phenomenon of atomic absorption is described by the quantum theory as the absorption, by the atom, of a quantum of electromagnetic energy (a photon) which causes, within that atom, an electronic transition from a lower to higher energy state. This higher energy state is unstable. Its lifetime varies between roughly 10^{-9} s. and 10^{-7} s. Any part of this electronic 'return' to the lower energy level (the ground state) which is accompanied by emission of radiation in the visible or ultra-violet regions of the spectrum is described as an atomic fluorescence process. The emitted radiation is called the fluorescence radiation. If the original excitation step does not involve any absorption of radiation (i.e. it is a thermal excitation) then the emitted radiation is not described as fluorescence nor is the phenomenon included in the category of atomic fluorescence.

Five distinct mechanisms of atomic fluorescence have been observed:-

i) Resonance Fluorescence.

This is the most simple. The excitation is a single step described by

$$\Delta E = h\nu \quad \underline{1.1}$$

and the return to the ground state is the reverse process. Therefore the frequency of the fluorescence is that of the absorbed radiation.

ii) Direct Line Fluorescence.

The atom is excited by resonance radiation to a higher excited state. Instead of a direct return

to the ground state, an electronic transition to an intermediate energy level occurs, which gives rise to fluorescence at a lower frequency than that of the absorbed radiation.

iii) Stepwise Fluorescence.

The atom is excited by radiation to a higher energy level than the first excited state. The atom undergoes radiationless transfer(s) to an intermediate energy level, then returns to the ground state by emitting resonance fluorescence radiation.

iv) Thermally Assisted Fluorescence.

The excitation process consists of two steps. The atom absorbs radiation and thermal energy to make two electronic transitions, then returns directly to a lower state by emitting a photon.

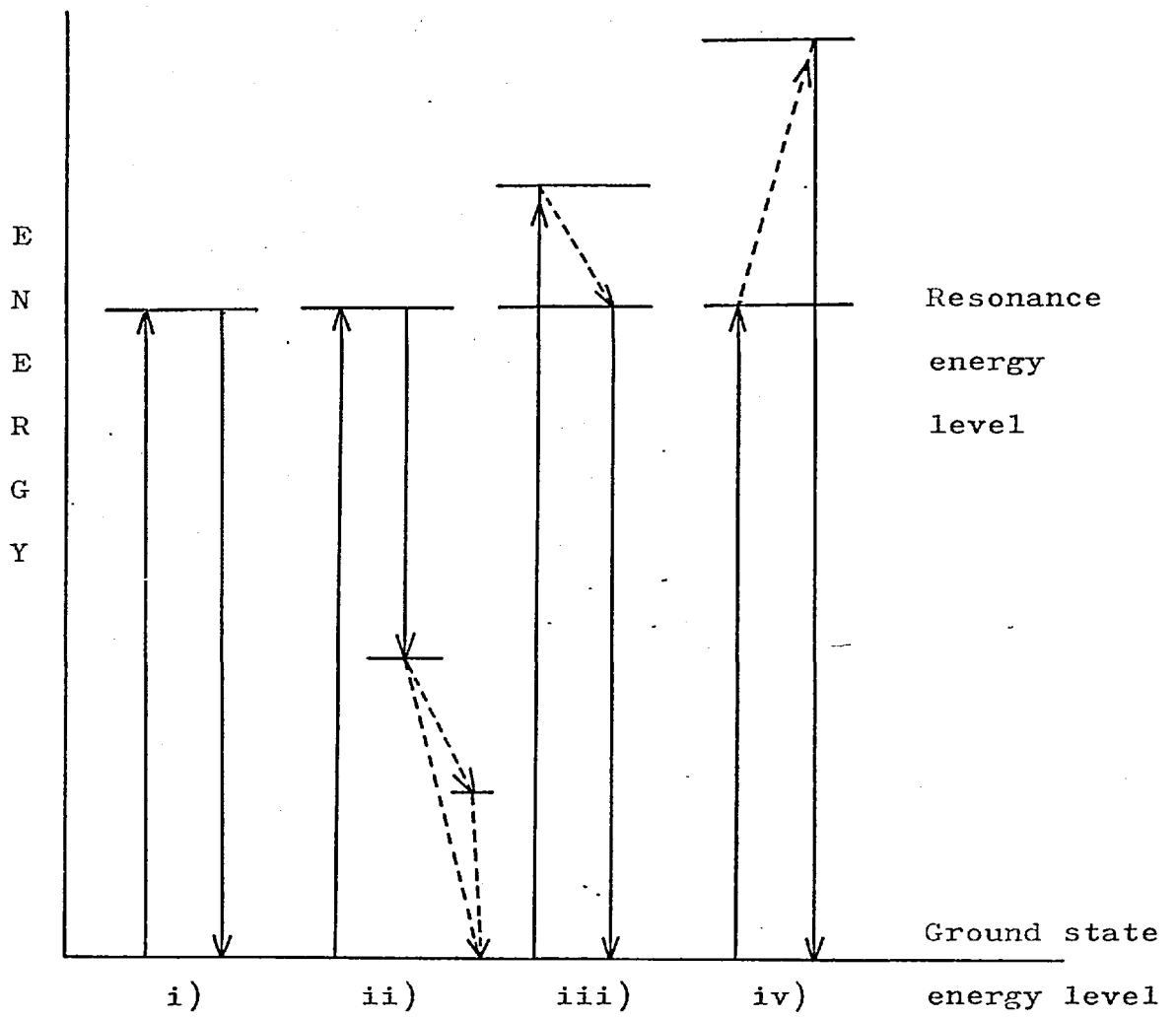
v) Sensitized Fluorescence.

This is a rare phenomenon involving interaction between atoms of different elements. An atom of one element absorbs its own resonance fluorescence radiation (e.g. mercury at 253.7nm.) then collides with a ground state atom of the other species (e.g. thallium) and an energy transfer occurs. This results in the second atom becoming excited and opens the possibility of deactivation by emission of radiation. (Thallium exhibits this behaviour by emitting at 535.0 nm. and 377.6 nm.)

The first four mechanisms are summarised in Figure 1.2.

Atomic fluorescence was observed by Mitchell and Zemansky⁽²⁾ in a quartz cell and by Nichols and

Figure 1.2



————— Energy changes involving emission or absorption of radiation.

----- Radiationless energy transfers.

Howes⁽⁴⁾ in a flame. Alkamade⁽⁵⁾ calculated the quantum efficiency of the sodium 589.0 nm. line in a flame. Robinson⁽⁶⁾ considered that atomic fluorescence could explain certain anomalies in line intensities observed in flame photometry. He suggested that certain emissions observed in flame photometry analysis are radiation induced as well as thermally induced, because these emissions are most intense not in the hottest flames, as predicted by the accepted theory of thermally induced emissions, but in flames which generate intense ultra-violet radiation. The same author corroborated this theory by observing an atomic fluorescence signal stimulated by an external ultra-violet source (a magnesium hollow cathode lamp). Alkamade⁽⁷⁾ considered the feasibility of A.F.S. as an alternative technique to A.A.S. and flame photometry. Winefordner⁽⁸⁾ proposed a simple theory of atomic fluorescence line intensities which included the basic relation:-

$$I_F \propto I_0 k_0 \phi \quad \underline{1.26}$$

where I_F is the fluorescence line intensity,

I_0 is the intensity of the incident radiation at the frequency absorbed,

ϕ is the quantum efficiency of the fluorescence, i.e. the fraction of the excited atoms which fluoresce

and k_0 is the absorption coefficient at the centre of the absorption band.

Therefore,

$$k_0 \propto N$$

$$\text{i.e. } I_F \propto N$$

Winefordner, Staab, Mansfield, Veillon and Parsons⁽⁹⁻¹²⁾ and Dagnall, Thompson, West and Young⁽¹³⁻¹⁷⁾ soon established A.F.S. as a potentially important method for trace analysis capable, given suitable spectral sources, of greater sensitivity than A.A.S.

Alkamade⁽¹⁸⁾, Hoomayers⁽¹⁹⁾ and Winefordner⁽²⁰⁻²³⁾ have more recently published detailed theoretical analyses of A.F.S.

It may be stated here that A.F.S. contains the inherent selectivity of A.A.S. (when narrow line sources are used for excitation) with the sensitivity of emission methods. (i.e. A small signal which may be electronically amplified is measured against a background which, in an ideal case, approaches zero, whereas in A.A.S. a small difference between two large signals is measured.)

Atom Reservoirs.

All methods of analysis by atomic spectrometry, (i.e thermal emission spectrometry, A.A.S. and A.F.S.) depend on the production of a vapour of free atoms. Consequently much research has been carried out in the field of atom reservoirs.

Most atom reservoirs can be included in one of the following categories:-

- a) Chemical flames.
- b) R.F. or microwave induced plasmas.
- c) Furnaces.
- d) Filaments.
- e) Hollow cathode spluttering devices.
- f) Laser microprobes.

a) Flames.

The technique of atomic spectrometry in chemical analysis is sometimes referred to as flame spectrometry, which indicates how frequently a flame is used as the atom reservoir, especially in routine analysis. The flame has many properties to commend its use in this manner.

A long history of flame technology has provided a choice of safe, reliable flames of use to the analytical chemist.

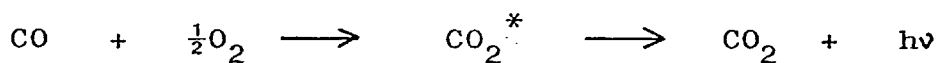
The air/hydrogen flame is a relatively low temperature flame with a very low 'noise' level. That is, the background emission from the flame is steady and not very intense (except at the hydroxy band wavelengths [ca. 310nm.]). It has been used for the ana-

lysis of easily atomized elements e.g. arsenic, selenium and tin, where the matrix is free from elements that are difficult to atomize. (It is usually the case that the composition of the matrix is just as important as the nature of the analyte in choosing the flame).

Air/propane is a similar mixture which reaches a higher temperature and enjoys a more widespread use.

Other elements e.g. cobalt, require a hotter flame to effect the dissociation of their salts and may be analysed in an air/acetylene mixture. Yet other elements, particularly those which form refractory oxides, e.g. aluminium and molybdenum, are most efficiently atomized in the reducing (cyanogen) zone of a fuel rich nitrous oxide/acetylene flame^(24,25).

A major disadvantage of flames, which has recently been minimised, is the emission band ranging from 320nm. to 700nm., caused by the chemiluminescence of carbon monoxide:-



and the emission bands centred on 281.1 nm. and 306.4 nm., due to the hydroxy group. These emissions are greatly diminished by shielding the flame from atmospheric oxygen with either a silica tube or with a flow of inert gas (nitrogen or argon) about the burner.⁽²⁶⁾ This removal of atmospheric oxygen from the flame also enables elements whose resonance lines lie in the vacuum ultra-violet region of the

spectrum, e.g. phosphorus and sulphur, to be studied in fuel rich shielded flames.

The Lambert-Beer Law suggests that the sensitivity (N.E.U.) of an analysis would be improved by observing the atoms in a long flame. Several attempts to produce and use long path flames have been made. (27-29) Most of these systems suffer from the formation of a deposit of carbon particles upon the viewing windows whenever either a hydrocarbon flame is used or an organic solvent is aspirated into an air/hydrogen flame. An ingenious solution to this problem has been suggested by Hingle, Kirkbright and West (29) who drew off a part of a separated flame into a side arm for observation. (Figure 1.3)

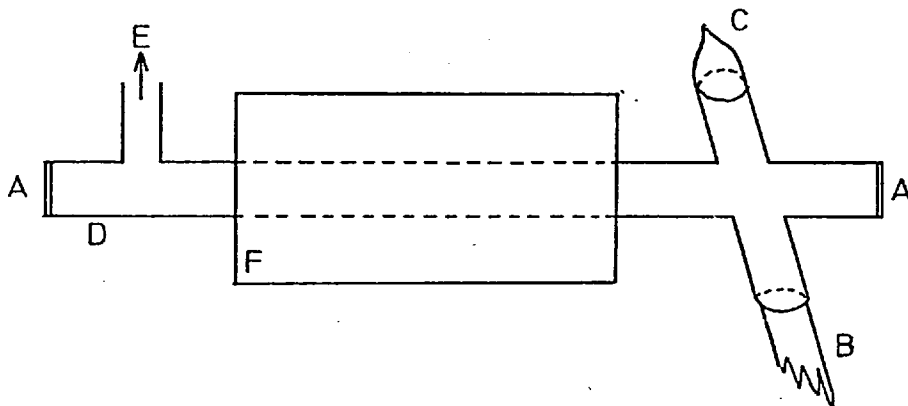


Figure 1.3 (from Ref.29)

- A Silica windows
- B Burner
- C Secondary zone of flame
- D Side arm; length 400 mm.
- E Gentle suction applied
- F Tube furnace; T = ca. 1000°C.

The major disadvantages associated with the use of chemical flames as atom reservoirs lie in the method of introducing the sample. The sample, which must be in the form of a solution, is nebulised by a pneumatic or ultrasonic nebuliser into the support gas and thus into the flame. This method of transporting the sample to the flame is almost unrivalled in commercial instruments; yet it normally results in less than ten percent of the analyte reaching the flame. Furthermore, the fraction of the analyte which finally reaches the viewing area has been 'diluted' by the expansion of the flame gases (owing to both increase in temperature and chemical reaction).

The use of a flame as the atom reservoir in atomic spectrometry is limited by several other considerations.

- i) Flames contain polyatomic molecules which quench atomic fluorescence.
- ii) Samples are restricted to a limited range of liquids. Viscous liquids, liquids which may extinguish the flame or those which may corrode the nebuliser-burner unit are all excluded, together with solids.
- iii) A relatively large sample (usually at least 10ml.) is required.
- iv) Large volumes of waste gases are produced. The danger from radioactive samples, or samples which could form poisonous gases is considerable.
- v) Flames are unable to excite much thermal

emission in elements whose resonance lines are below 320 nm.

Several attempts to avoid the inefficient sampling of the nebuliser-flame system without losing the advantages of the flame have been made. Total consumption burners have been used in thermal emission analysis, but the turbulence associated with such flames makes them unsuitable for A.A.S. or A.F.S. These techniques have mainly used pre-mixed laminar flow flames. White⁽³⁰⁾ and Danielson and Ulfendahl⁽³¹⁾ have used a platinum wire loop to hold a microlitre sample and introduce it mechanically to the flame. Delves⁽³²⁾ modified this idea by substituting a nickel sampling cup for the platinum loop and positioning a horizontal silica tube above the sampling cup. The silica tube has an opening to allow the atomic vapour an entrance, but excludes virtually all the flame gases, which sometimes absorb or emit light at an inconvenient frequency. The nickel cup allows samples larger than one microlitre to be used and also facilitates pre-treatment of the sample (Delves oxidised blood samples with hydrogen peroxide in this manner). Delves work on blood samples has been well corroborated.⁽³³⁻³⁷⁾ Clark, Dagnall and West^(38,39), however, have shown that the technique is useful only for easily atomized samples and that foreign elements interfere seriously, i.e. matrix effects are very significant.

b) Radio frequency or microwave induced plasmas.

The essential function of the flame in atomic spectrometry is to provide energy

- i) to vaporise the solvent,
- ii) to vaporise the matrix and analyte,
- iii) to atomize the analyte,
- iv) to excite the analyte atoms in thermal emission analysis.

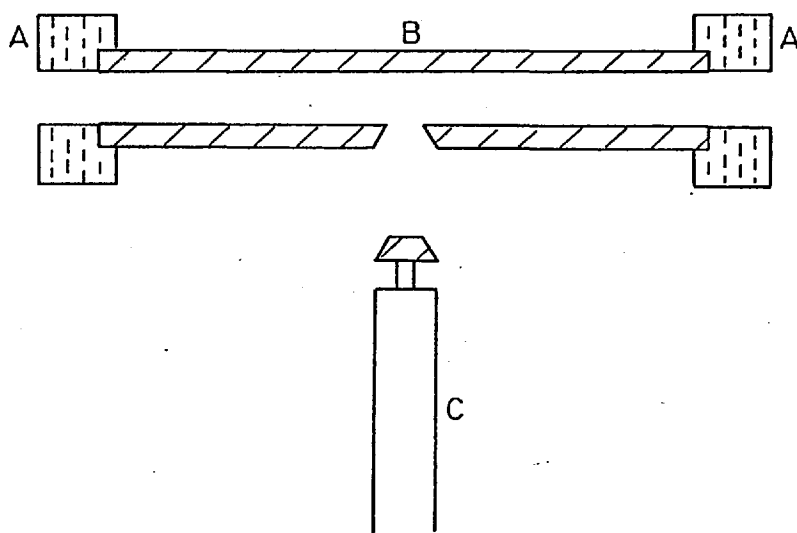
An alternative source of energy can be tapped by using a radio frequency (R.F.) or a microwave induced plasma. A plasma (i.e. an ionized gas) is capable of absorbing energy from the radio frequency or the microwave regions of the spectrum, and therefore has been considered as an alternative atom reservoir for several years. R.F. and microwave induced plasmas of inert gases (nitrogen or argon) provide an ideal chemical environment for the production of free atoms, especially when elements which form refractory oxides are present in the sample (as analyte or matrix). The electronic excitation temperature of such a plasma can be very high (ca. 10,000 K) so the thermal emission lines are very intense. Several workers have made use of this.⁽⁴⁰⁻⁴⁹⁾ The sample may be introduced to the plasma as a nebulised spray from a solution,⁽⁴⁰⁻⁴⁵⁾ but an excess of solvent can extinguish the plasma. Alternatively a fine powder can be supported on the gas stream.⁽⁴⁵⁻⁴⁷⁾ It is also possible to vaporise the sample into the gas stream from an electrically heated metal loop.^(48,49) The inert atmosphere, the high electronic excitation

temperature and the adaptability of the system of sample introduction give the R.F. and microwave induced plasmas a potentially large advantage over chemical flames, which should be realised in the future.

c) Furnaces.

A considerable number of furnace devices have been designed to overcome the problems of inefficient nebulisation, sample dilution, the need for large samples in a favourable liquid form, the unfavourable chemical environment, background noise and dangerous waste gases, normally associated with flame atom reservoirs. (54-56) King, (57) an astronomer who was interested in atomic absorption phenomena observed in solar and stellar spectra, described a graphite furnace atom reservoir as early as 1908. L'vov and his co-workers have used similar graphite furnaces and have published extensive atomic absorption studies over the past eleven years. (58-66) The L'vov furnace consists of a graphite tube 30 to 50 mm. in length, with an internal diameter of 2.5 or 3.0 mm., held in a sealed chamber which can be purged with argon. The sample (liquid or solid) is introduced on a shaped graphite rod which fits into an orifice in the graphite tube. (Figure 1.4). The atomization is accomplished by resistance heating. The temperature of the furnace, the nature and pressure of the atmosphere can be easily controlled. By using a high pressure argon atmosphere, diffusion of the atomic vapour through the walls is reduced. This diffusion is further

Figure 1.4 (from Ref. 65)



- A Graphite supports and contacts.
- B Graphite tube.
- C Shaped graphite rod to hold sample and act as an electrode.

reduced by lining both the inside and outside of the tube with pyrographite, so a steady-state atomic vapour is obtained. The pyrographite also contributes an evenness of heating to the system. The atomic absorption spectra of fortysix elements have been investigated using this apparatus, including phosphorus, sulphur and iodine (whose resonance lines lie in the vacuum ultra-violet spectrum).

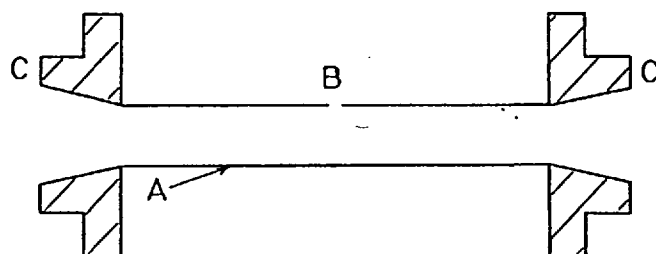
Very low sensitivities have been obtained (sensitivity here is taken to mean the size of sample required to obtain a signal of 1% absorption), ranging from 10^{-10} g. for boron and sulphur, to 3×10^{-14} g. for beryllium and zinc. Oscillator strengths, Lorentz half

widths of resonance lines and atomic diffusion coefficients have also been measured.

L'vov's furnace is, as stated above, held in a sealed chamber, purged with argon. This fact prohibits rapid analysis of a large number of samples.

A graphite tube furnace, which can be used more quickly than the L'vov furnace, has been described by Massmann.^(67,68) Argon is blown through and around the tube, 55 mm. long with internal diameter 6.5 mm. and 1.5 mm. wall thickness, to protect the white hot carbon and the free atoms from atmospheric oxygen. (Figure 1.5)

Figure 1.5 (from Ref. 67)



A Graphite tube.

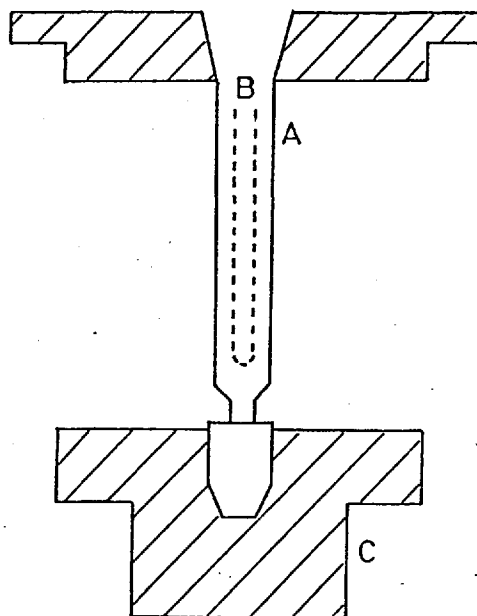
B Orifice for sample introduction.

C Steel supports and electrical contacts.

The same author has also described a cup shaped graphite cuvette, 40 mm. long. with internal diameter 6.5 mm. and 1.5 mm wall thickness, for use in A.F.S. (Figure 1.6).⁽⁶⁷⁾

In the absorption mode, the sample is introduced through an orifice 2 mm. in diameter in the top

Figure 1.6 (from Ref. 67)



- A Graphite cuvette.
- B Slit to observe fluorescence.
- C Steel supports and electrical contacts.

centre of the tube via a micropipette. The optical pathway is along the centre of the tube. In the fluorescence mode the sample is inserted through the open top of the cuvette. The atoms are irradiated through the open top and the fluorescence radiation is observed through a slit in the side of the cuvette. Liquid samples from $5 \mu\text{l.}$ to $200 \mu\text{l.}$ and solid samples up to 1 mg. have been used.

The furnace is rapidly heated to 2600°C by passing up to 400 amps at low voltages.

A commercially available version of the Massmann furnace (the Perkin-Elmer H.G.A. 70) has been used by Manning and Fernández⁽⁶⁹⁾ to determine copper in milk, with no pre-treatment of the sample. Segar

and Gonzalez⁽⁷⁰⁾ attempted to use the H.G.A.70 for trace metal analysis in sea water, but discovered that interference from the major constituent salts was large and that it was not possible to separate the constituents by sequential vaporisation. Norval and Butler⁽⁷¹⁾ have used a Massmann type furnace to determine lead in blood, without any inert gas protection. The graphite tube is oxidised and must be replaced after each heating. Omang^(80,81) has used an H.G.A.70 to determine lead filtered from air, as well as vanadium and nickel in oils.

Woodriff⁽⁷²⁻⁷⁷⁾ and his co-workers have used a graphite furnace, 150 mm. in length, internal diameter 7 mm., which is resistance heated from an arc-welder. The sample is introduced in a carbon cup (rather like the L'vov furnace) or is nebulised, usually from a methanol solution, and is carried into the furnace with the inert gas.

Headridge and Smith^(78,79) have described a small graphite tube, 75 mm. long, internal diameter 15 mm., which is heated by an induction coil. The sample (mainly solid alloys) is introduced by L'vov's method. This furnace is heated to merely 1350°C in routine use, but this is sufficient for the volatile alloys which it is used to analyse. Traces of bismuth and cadmium in lead and zinc based alloys have been determined as a matter of routine.

Pemsler, Rapperport and Adler^(82,83) have described a furnace into which sealed quartz tubes fit. The sealed quartz tubes contain the samples,

which are similar to those investigated by Headridge and Smith (see above).

Recently Winefordner and his co-workers^(84,85) have published a preliminary description of a platinum furnace designed to give a very low noise level, for use in A.F.S. studies.

d) Filaments.

The major alternative flameless atom reservoir to some form of furnace is some form of filament. A filament atom reservoir, as far as this thesis is concerned, is a graphite or metal conductor which may be resistance heated to atomize the sample, which is NOT then confined, but is rapidly lost from the viewing path. Such a system is simpler to use than a furnace. A filament has one major disadvantage compared to a furnace, and that is the rapid cooling of the atomic vapour after losing contact with the filament surface. This sometimes leads to chemical interferences and matrix effects, and a need for fast response amplifiers to follow the analytical signal.

West and Williams⁽⁸⁶⁾ first reported the use of a filament atom reservoir in A.A.S. and A.F.S. Using the fluorescence mode they detected silver and magnesium down to 3×10^{-11} g. and 10^{-16} g. respectively, by heating small samples (5 μ l.) placed via a syringe micropipette in a notch carved in a graphite filament, 20 mm. in length, 2mm. in diameter. The filament was held between stainless steel electrodes, enclosed in a glass cell which could be purged with argon. However,

this prototype carbon filament atom reservoir (C.F.A.R.) resulted in low precision and was soon modified. (87,88)

The important changes in design were as follows:-

- i) A solid brass base was incorporated to impart greater physical stability.
- ii) A water cooling system for the electrodes was added.
- iii) A box packed with alternate plane and crinkled metal strips was fitted directly beneath the filament, thus greatly increasing the protection afforded to the white hot carbon.

The increased protection for the filament allowed the removal of the glass envelope from the C.F.A.R. in some circumstances.

The precision obtained from the C.F.A.R was considerably improved by these modifications, and by the replacement of the syringe micropipette with Drummond microcaps (and later by Marburg Eppendorf micropipettes).

West and his co-workers⁽⁸⁹⁻⁹¹⁾ showed that above the filament the atomic vapour diminishes rapidly and no atomic signal is observed more than 7 or 8 mm. above the filament. With the less volatile elements the cloud of atomic vapour disappears even closer to the filament. Furthermore the same authors showed that large excesses of foreign ions interfere negatively. (i.e. reduce the A.F. or A.A.signal) The nature of this interference seems to be complex, but has been shown to include a vapour phase interaction. Attempts to remove this interference by observing only that section of the

light which passes very close to the filament, in conjunction with a fast response amplifier have been generally successful. (91,93,95)

Aggett and West⁽⁹²⁾ examined metal chelates dissolved in organic solvents (which could cause problems in a flame atom reservoir) and showed that the solvent could be evaporated and the chelate sometimes broken down by controlled heating prior to the atomization. Ebdon, Kirkbright and West^(93,94) have used the C.F.A.R. to determine manganese (medium volatility) and iron (low volatility). Jackson and West have determined nickel⁽⁹⁵⁾ and vanadium⁽⁹⁶⁾ impurities in titanium pigments with the C.F.A.R. Osborne and West⁽⁹⁷⁾ have determined cobalt, extracted as a trace from soils. Lead in blood can be determined on the C.F.A.R. as is shown in this thesis.

Matousek and his co-workers⁽⁹⁸⁻¹⁰²⁾ have used a modification, now commercially available as the Varian Carbon Rod Atomizer, of the original C.F.A.R. The Carbon Rod Atomizer differs from the C.F.A.R. in two main ways:-

- i) A 5 mm. diameter filament or rod which, for use in the absorption mode, has a transverse hole bored through the centre, replaces the original filament.
- ii) The argon is replaced by a stream of hydrogen which ignites when the filament is heated and provides a hot atmosphere above the filament. This same group of workers has applied this device to the practical analysis problems of determining lead in petroleum products,⁽¹⁰⁰⁾ and volatile metals in blood^(101,102)

and have claimed exceptionally low detection limits. These detection limits have been criticised by Winefordner and his colleagues as unjustified extrapolations rather than real measurements. Using the same equipment Winefordner obtained detection limits one order of magnitude higher than Matousek. Bratzel and Chakrabarti have also used the Varian Carbon Rod Atomizer to analyse petroleum products⁽¹⁰⁴⁾ and geological samples.⁽¹⁰⁵⁾

The advantages of the Carbon Rod Atomizer over the C.F.A.R. may be disputed. The transverse bore through the filament, which is intended to reduce the rapid cooling of the atomic vapour, raises the cost of the filaments considerably, complicates the sample introduction procedure and makes it impossible to effectively shield the monochromator slit from the incandescent carbon. This in turn means that modulated light sources and tuned demodulating amplifiers must be used. Using the C.F.A.R. the monochromator slit can be shielded from the incandescent carbon and D.C. lamps and amplifiers can be used. The use of a hydrogen diffusion flame to maintain a high temperature above the filament is claimed to reduce matrix effects, but the method of restricted field viewing suggested by Jackson and West⁽⁹⁵⁾ seems to be a far more elegant way to reduce matrix effects. The whole idea of re-introducing a flame into a system which has been designed to overcome problems caused by flames seems, to this author, ill-founded.

Bratzel, Dagnall and Winefordner^(106,107)

have used platinum and tungsten loops as filament atom reservoirs for A.F.S. The sample, in solution, is applied to the loop via a 1 μ l. micropipette or by dipping the loop into the solution. This latter method, a surprisingly precise way of taking a sample, gives a reproducibility of 8%. The solvent is evaporated by gentle heat, then the sample is atomized into the surrounding argon stream. The atomic fluorescence is observed immediately above the loop. Only volatile elements have so far been studied and chemical interferences from sulphate and phosphate radicals have been observed.

Donega and Burgess⁽¹⁰⁸⁾ have atomized samples from tantalum, tungsten and graphite boats, 50 mm. long and 6 mm. wide, supported on copper electrodes in a sealed chamber. The chamber can be purged with an inert gas and the pressure adjusted to any desired value. The boats can hold samples up to 100 μ l. Since the absolute sensitivities (i.e. the mass of the element required to produce a 1% absorption signal) are of the same order as those reported by West, solutions at greater dilution will be analysable. However no information about matrix effects or chemical interferences has yet been published.

e) Hollow cathode spluttering devices.

In 1959 Walsh⁽¹⁰⁹⁾ reported that the atomic vapour produced in a hollow cathode spluttering

device extends beyond the cathode. He suggested two uses for this this phenomenon:-

- i) the hollow cathode spluttering device could be used as an atom reservoir,
- ii) the Walsh-Sullivan type high intensity hollow cathode lamp.

The following year the same author described the use of a hollow cathode lamp as an atom reservoir.⁽¹¹⁰⁾ The metal sample was machined to a hollow cylinder, 40 mm. in length with internal diameter 12 mm. When held with a steel clip in a sealed chamber with argon filler gas at a pressure of 1 mm. of mercury, the sample becomes a hollow cathode. The surface may be cleaned by passing about 60 mA. current for four minutes. Fresh filler gas can then be admitted (still argon at a pressure of 1 mm. of mercury), the discharge repeated and the absorption measurement made. Walsh observed the atomic absorption of silver at 338.3 nm. from an alloy containing 0.05% silver and obtained a relative standard deviation of 7% for a number of replicate readings. The ability of this device to operate in the absence of any gases which absorb vacuum ultra-violet radiation was utilised to determine phosphorous (in copper) down to 1000 p.p.m. and silicon (in steel and aluminium) down to 0.1%.⁽¹¹¹⁾

Massmann has described a similar device which he has used to determine volatile metals present in iron.⁽¹¹²⁾ This technique is, ofcourse, limited to metal samples which can be made into the

hollow cathode. Goleb and Brody ⁽¹¹³⁾ evaporated the sample onto an aluminium hollow cathode. They pointed out that the atoms in the reservoir will emit as well as absorb radiation and made corrections for this. However, they discovered many examples of chemical interference. Goleb ⁽¹¹⁴⁾ successfully adapted the Walsh method for use with uranium hollow cathodes in isotope analysis. Ivanov, Gusinsky and Jesikov ⁽¹¹⁵⁾ attempted a variation of Goleb and Brody's method. They evaporated the sample onto a graphite hollow cathode or onto a fine molybdenum wire which was placed along the central axis of the cathode.

Massmann ⁽¹¹⁶⁾ developed a hollow cathode spluttering device, for use with metal samples, which could be used at high temperature (to reduce chemical interference). A graphite tube, 30 mm. in length with an internal diameter of 7 mm., is supported by a cylindrical graphite electrode which passes through the wall of the cathode (rather like the L'vov furnace). The sample is placed on this carrier electrode and a discharge operated at a power of up to 1 kW. By using a modulated discharge, at 50 Hz., and a rotating sector in front of the monochromator slit, the atomic absorption may be measured during the discharge free period. Hence emission from the sample and continuum emission from the cathode itself are not seen. Massmann found it necessary to integrate (with respect to time) the measured absorption signals.

f)

Lasers.

Mossotti, Laqua and Hagenah⁽¹¹⁷⁾ used a pulsed laser microprobe to atomize the surface of a solid sample, into the light path of an atomic absorption spectrometer. They discovered that matrix effects were enormous and concluded that (at that time) the technique was unsuitable for quantitative analysis.

Summary.

The various modes of atomic spectrometry provide very useful techniques for trace analysis. For the vast majority of analyses performed by atomic spectrometry methods, a chemical flame is used as the atom reservoir. Notwithstanding the several disadvantages of flames, they remain the most practical atom reservoir for routine analysis.

Various non-flame atom reservoirs have been devised to meet the requirements of particular analytical problems. Each device has its own merits and failings and a general critical comparison would be of little value. It remains the task of the analytical chemist to decide which technique offers most advantages in a particular situation.

The following pages describe the design and use of a carbon filament atom reservoir to solve the problem of the determination of lead in blood.

Chapter Two

The Carbon Filament Atom Reservoir-

The carbon filament atom reservoir (C.F.A.R.) is designed to produce a transitory atomic vapour by rapid heating of a small sample in an inert gas atmosphere. The speed and ease of operation have been major considerations in the design.

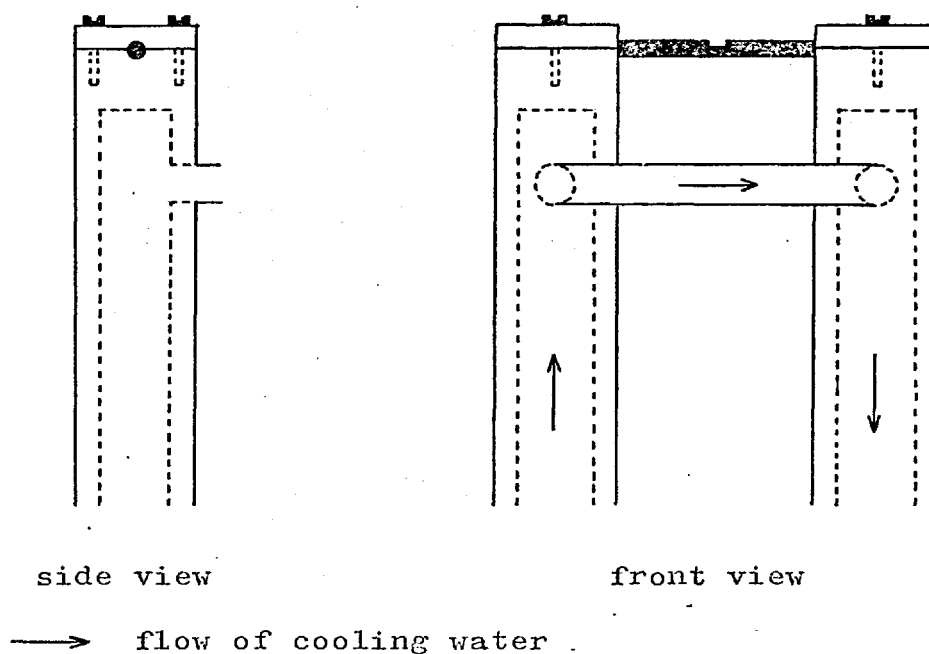
The filament itself is made of graphite. The shape of the filament is cylindrical and the dimensions vary. Filaments with diameters between 2mm. and 5mm., and with lengths between 5mm. and 60mm. have been used. A small notch is usually filed in the middle of the filament to hold the sample. The filament is supported between two stainless steel electrodes. These are hollow water cooled cylinders (diameter 13 mm. and height 60 mm.) with caps held in place by screws. The tops of the electrodes and the underside of the caps are grooved to hold the filament. Great care must be taken to align the grooves correctly, to save the filament from mechanical stress.

The cooling water, which enters through the base of one electrode, flows to the other electrode via an insulating plastic tube. (See Figure 2.1)

One electrode is insulated with mica from the brass base in which both electrodes are fixed. The other is in contact with the base. The whole assembly is mounted directly into a saddle on the optical bar of a spectrometer.

Power is supplied from the mains via a 1.2 kilowatt stepdown transformer and a Variac variable transformer, so that the potential difference across the filament may be varied between zero and twelve

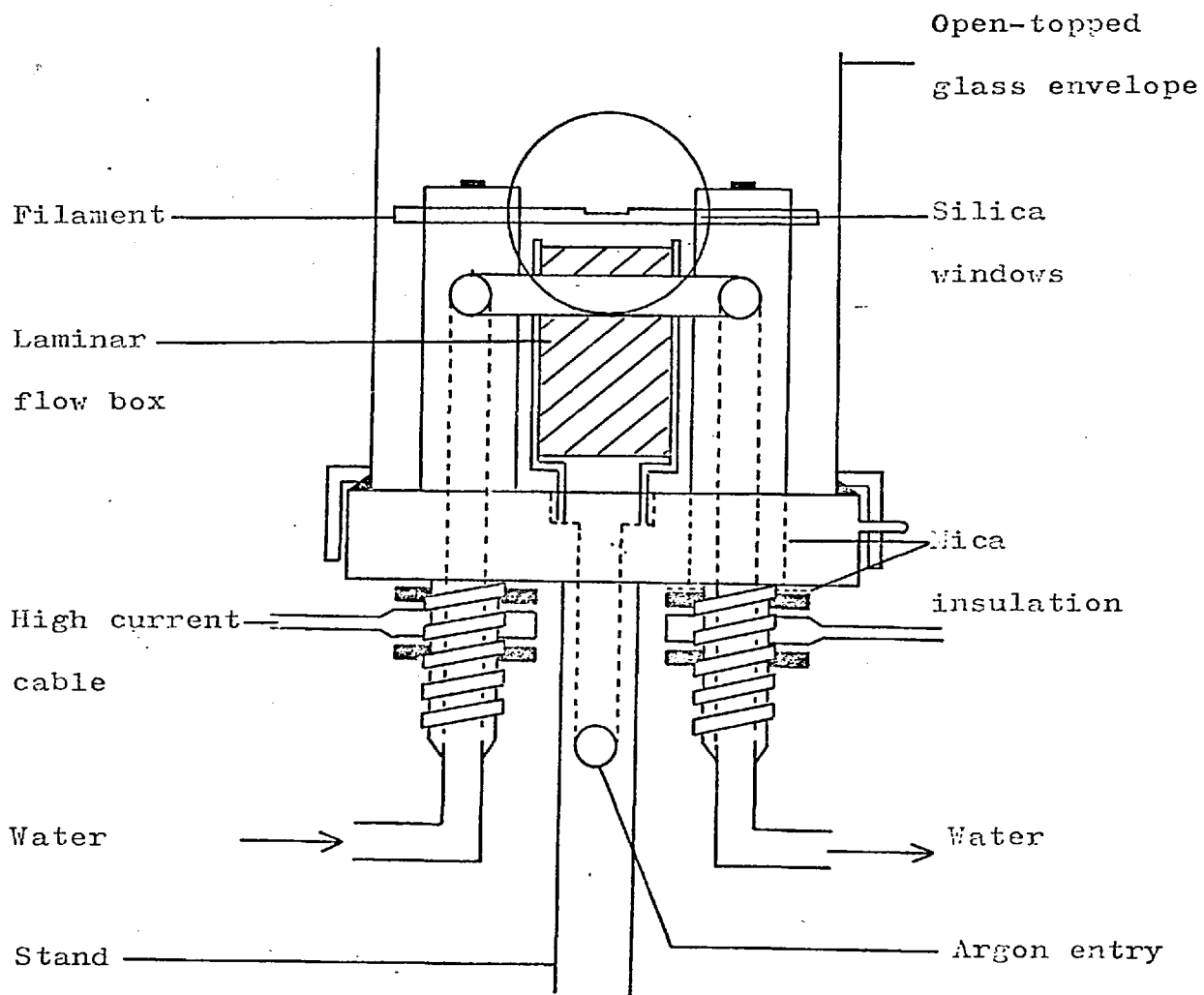
Figure 2.1



volts. The maximum load current is approximately seventy amps.

The atmosphere of inert gas, nitrogen or argon, is supplied from a cylinder via a large aspirator which absorbs any pressure fluctuations, and a Rotameter flow gauge, to a box placed just below the filament. This box is packed with plane and corrugated metal strips, arranged alternately, so that the gas flow around the filament is laminar.

In early experiments the filament, electrodes and base were encased in a glass envelope, with silica windows in the optical path, to ensure the protection of the incandescent filament and the atomic vapour from atmospheric oxygen. Later the envelope was removed since the flow of the inert gas was sufficient to prevent oxygen diffusing to the filament surface. Still later it was discovered that the surface of the fila-

Figure 2.2

ment was subject to attack from atmospheric oxygen near to the electrodes, because the sides of the laminar flow box obstruct the flow of inert gas. This effect was only noticed when the filament was kept at red heat for periods of one or more minutes (e.g. when ashing a blood sample). An open-topped glass envelope was found to be adequate to protect the filament in these conditions. The open-topped glass envelope does not reduce the ease of operation of the C.F.A.R. The design of the C.F.A.R. which was finally used is shown in Figure 2.2.

The Transience of the Atomic Vapour.

The atoms produced on the filament are 'seen' by the photomultiplier tube for a short period of time during which they occupy a particular space. This space will be referred to as the observed volume.

The strength of the absorbance or fluorescence signal at any instant depends on the number of free atoms of the analyte present in the observed volume at that instant. This signal has been related to the total number of atoms of analyte in the sample, by L'vov. (1)

Two parameters are considered; firstly the integral of the analytical signal over all the time of the signal and secondly the peak value of the analytical signal.

Let

- N_0 = the total number of atoms of analyte
in the sample,
- N = the number of atoms of analyte present
in the observed volume at any instant,
- N_p = the peak value of N ,

- τ_1 = the duration of the process of atomization
of the sample,
 τ_2 = the average time spent in the observed
volume by a single atom of the analyte,
 τ_3 = the total duration of the absorbance or
fluorescence signal,
 x = the absorbance or fluorescence signal at
any instant,
 x_p = the peak value of x .

Then L'vov has shown that

$$\int_0^{\tau_3} N dt \approx N_0 \tau_2 \quad \underline{2.1}$$

$$\therefore A \int_0^{\tau_3} x dt \approx N_0 \tau_2 \quad \underline{2.2}$$

where A is a constant.

$$\therefore \int_0^{\tau_3} x dt \propto N_0 \quad \underline{2.3}$$

if τ_2 is fixed.

i.e. The integral of the absorbance or fluorescence signal over the duration of the signal is proportional (to a first approximation, at least) to the total number of atoms of analyte, provided τ_2 is fixed. Secondly this integral signal is independent of τ_1 .

Equation 2.4 has also been derived by L'vov⁽¹⁾.

$$N_p = \frac{N_0 \tau_2}{\tau_1} (1 - e^{-\frac{\tau_1}{\tau_2}}) \quad \underline{2.4}$$

If τ_1/τ_2 tends to zero then equation 2.4 can be reduced to

$$N_p = N_0 \quad \underline{2.5}$$

If however τ_2 is ten times greater than τ_1

$$\text{i.e. } \frac{\tau_1}{\tau_2} = 0.1 \quad \underline{2.6}$$

$$\text{then } N_p = 0.95 N_0 \quad \underline{2.7}$$

$$\text{If } \frac{\tau_1}{\tau_2} = 0.2 \quad \underline{2.8}$$

$$\text{then } N_p = 0.90 N_o \quad \underline{2.9}$$

As long as the term τ_1 / τ_2 is fixed then

$$N_p \propto N_o \quad \underline{2.10}$$

$$\therefore x_p \propto N_o \quad \underline{2.11}$$

i.e. The peak absorbance or fluorescence signal is proportional to the total number of atoms of analyte provided the parameter τ_1 / τ_2 is fixed. The peak analytical signal reaches its maximum value at the minimum value of the parameter τ_1 / τ_2 .

To sum up:

- i) The integrated absorbance or fluorescence signal is to a first approximation, proportional to the mass of analyte and is independent of τ_1 .
- ii) The peak absorbance or fluorescence signal is proportional to the mass of analyte but is also dependent on τ_1 .

The definition of τ_1 was 'the duration of the atomization process'. It has been shown⁽¹⁾ that the atomization of a sample takes place over a range of about 100 - 200 degrees Kelvin. Thus τ_1 may be minimised by employing a large rate of increase of the temperature of the filament over the temperature range in which the atomization occurs.

This dependence of peak absorbance signal upon the heating rate of the filament has been used by Jackson and West⁽⁹⁶⁾ and Osborne and West⁽⁹⁷⁾. These authors have used high rates of heating to increase significantly the peak absorbance signals due to vanadium

and cobalt respectively.

The rate of change of temperature of the filament over the atomization temperature range is clearly a critical factor in the operation of the C.F.A.R. The direct measurement of this parameter is difficult. Continuous measurement of the temperature of the filament with a thermocouple, as described in this chapter, is restricted to temperatures below about 1800 K. Measurement of higher temperatures with an optical pyrometer, also described here, is restricted to steady temperatures since a substantial time is required to take a single reading with this type of instrument.

An approach can be made to estimating the rate of change of temperature of the filament from a consideration of the thermodynamics of the system.

The factors which affect the rate of change of temperature of the filament are:-

- i) the electrical power supplied,
- ii) the power loss by radiation,
- iii) the power loss by convection,
- iv) the power loss by conduction,
- v) the heat capacity of the filament.

The power generated in the filament is given by:-

$$P_I = \frac{V^2}{R_\theta} \tag{2.12}$$

where V = the applied potential difference,

R_θ = the resistance of the filament at θ K

and $R_\theta = R_{273} \cdot f(\theta) \cdot \frac{1}{\pi r^2}$ 2.13

where R_{273} = the specific resistivity of the filament material at 273 K.,

$f(\theta)$ represents the temperature dependence of the specific resistivity of the filament material. This function is not known in analytic terms, but is shown graphically in Figure 2.3. (Data from Morganite Co. Ltd.),

l = length of the filament between the electrodes,

r = radius of the filament.

Equation 2.12 can be re-written

$$P_I = \frac{V^2 \cdot \pi \cdot r^2}{R_{273} \cdot f(\theta) \cdot l} \quad 2.14$$

The radiation power loss is given by the Stefan-Boltzmann Law:-

$$P_{II} = 2\pi r l \sigma \epsilon (\theta^4 - T^4) \quad 2.15$$

where σ = the Stefan-Boltzmann constant,

ϵ = the emissivity of the filament,

T = the background radiation temperature.

The convection power loss is given by:-

$$P_{III} = 2\pi r l b (\theta - \theta_0) \quad 2.16$$

where b is an arbitrary constant

and θ_0 = the initial temperature of the inert gas.

The heat diffusion equation⁽¹¹⁸⁾ (equation 2.17) may be applied to the filament.

$$k \left(\frac{\partial^2 \theta}{\partial x^2} \right) + \left(\frac{\partial^2 \theta}{\partial y^2} \right) + \left(\frac{\partial^2 \theta}{\partial z^2} \right) - c \left(\frac{\partial \theta}{\partial t} \right) = -K^* \quad 2.17$$

where k = the specific thermal conductivity of the filament,

Figure 2.3

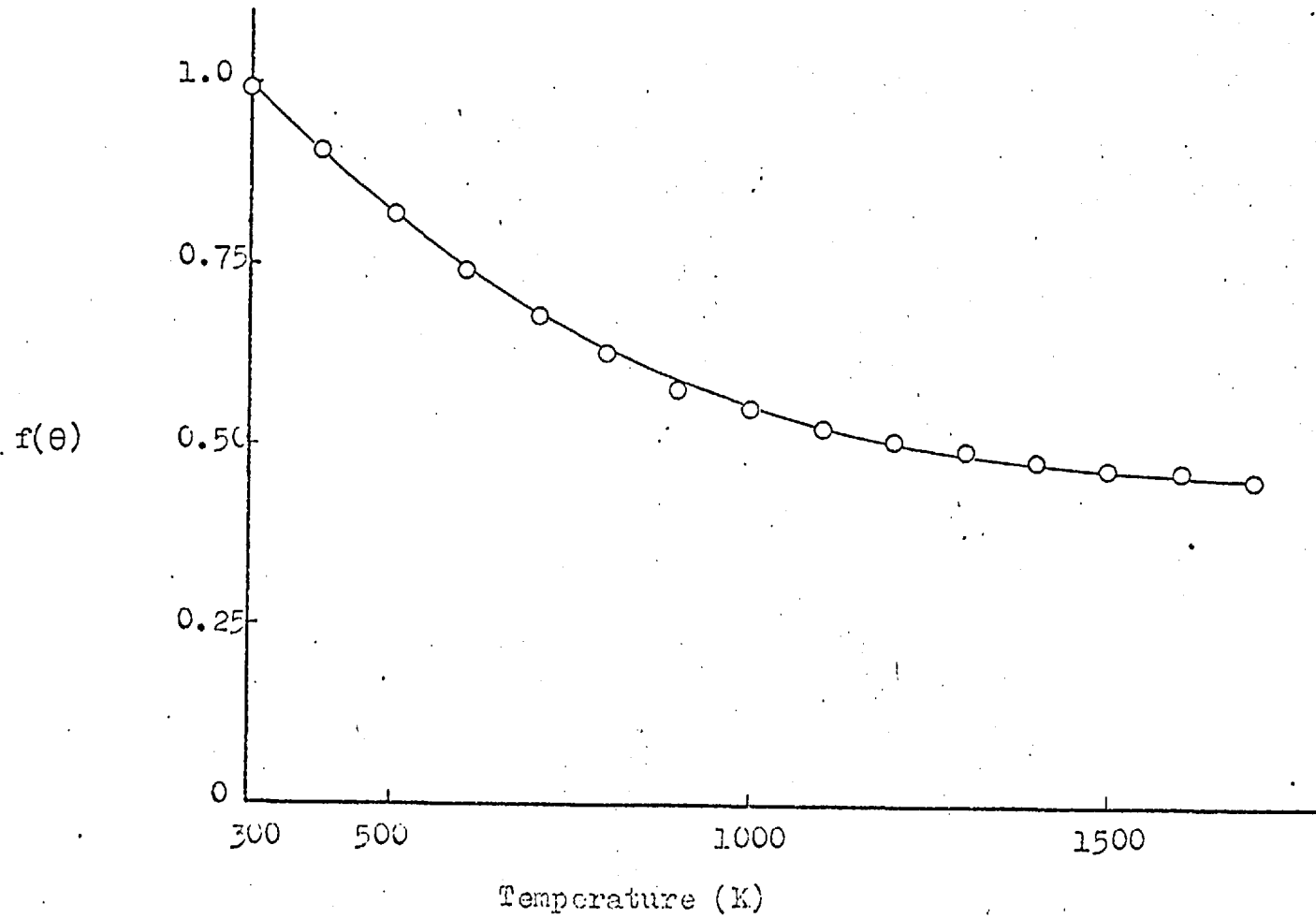


Figure 2.3

θ = the absolute temperature at any point
 (x, y, z) in the filament at any time,
 x, y, z are the Cartesian coordinates of the
 system. It is convenient to choose the
 x -axis as the axis of the filament.
 t is the time coordinate,
 ρ = the density of the filament,
 c = the specific heat of the filament,
 K^* = the net power generated per unit volume,
 at any point in the filament.

Since power is generated homogeneously in the
 filament, we can assume that near the middle of the
 filament

$$\left(\frac{\partial^2 \theta}{\partial y^2}\right) = \left(\frac{\partial^2 \theta}{\partial z^2}\right) = 0 \quad \underline{2.18}$$

$$\therefore \left(\frac{\partial^2 \theta}{\partial x^2}\right)_t - \rho c \left(\frac{\partial \theta}{\partial t}\right)_x = -K^* \quad \underline{2.19}$$

But

$$\pi r^2 1 K^* = \frac{v^2 \pi r^2}{R_{273} f(\theta) l} - 2\pi r l \sigma \epsilon (\theta^4 - T^4) - 2\pi r l b(\theta - \theta_0) \quad \underline{2.20}$$

Therefore

$$\left(\frac{\partial^2 \theta}{\partial x^2}\right)_t - \rho c \left(\frac{\partial \theta}{\partial t}\right)_x = \frac{2}{r} \left[\sigma \epsilon (\theta^4 - T^4) + b(\theta - \theta_0) \right] - \frac{v^2}{R_{273} f(\theta) l^2} \quad \underline{2.21}$$

The attempt to solve equation 2.21 by normal analytical
 methods meets with serious difficulties from two sources.
 Firstly the term $f(\theta)$ is not known in an analytic form.
 Secondly the boundary conditions which are needed to

calculate the constants of integration are unknown.

However it is possible to investigate the function $\frac{d\theta}{dt}$ without solving equation 2.21. By consid-

ering only the centre of the filament (where the sample is in fact placed) it may be assumed that

$$\frac{d\theta}{dt} = \left(\frac{\partial \theta}{\partial t} \right)_x \quad \underline{2.22}$$

Then inspection of equation 2.21 suggests that $\frac{d\theta}{dt}$ may

be increased by:-

- a) increasing V,
- b) reducing R_{273} ,
- c) reducing l,
- d) increasing r.

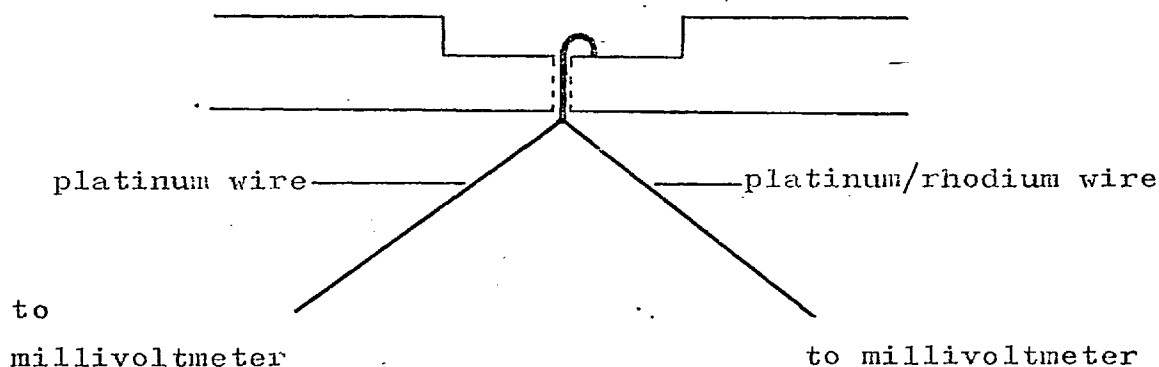
Investigation of the rate of heating of the filament by experiment presents difficulties, as have been mentioned. However both a platinum - platinum/rhodium thermocouple and an optical pyrometer have been used to obtain some information about the heating rate of the filament.

Experimental

- i) The Pt - Pt/Rh thermocouple.

The thermocouple was constructed by spot welding the final five millimetres of a length of platinum wire to the final five millimetres of a length of platinum/rhodium alloy wire. (13% rhodium). The other ends of the two wires were connected to the terminals of a recording millivoltmeter.

In order to keep the thermocouple 'probe' in firm contact with the filament it was necessary to drill a transverse hole, with a 0.2 mm. diameter drill bit, through the centre of the filament. The thermocouple probe was then inserted into and through this hole and bent into a hook where it emerged. The platinum and platinum/rhodium wires were then subjected to a slight tension. (See Figure 2.4) The potential difference generated in Figure 2.4



the thermocouple was continuously recorded by the millivoltmeter and was converted to the temperature excess of the filament over the ambient temperature by means of a calibration graph from data in the Handbook of Physics and Chemistry.

ii) The optical pyrometer.

A Leeds and Northrop optical pyrometer was focused on the notch at the middle of the filament, from a distance of approximately two feet. A period of between one half minute and two minutes after switching

the power on was allowed to elapse in order for the filament to reach its equilibrium temperature. The intensity of the pyrometer filament was adjusted to match the intensity of the carbon filament and the temperature read directly from the pyrometer.

Results and Discussion.

The temperature - time curves measured with the thermocouple, for a typical filament (length 26 mm., radius 1.6 mm., $R_{273} = 1.66 \times 10^{-2}$ ohm.mm.) at four rather low applied potential differences are shown in Figure 2.5. The curve Number (1) was obtained by applying a potential difference of three volts (3 V.) across the filament, Number (2) by applying 2.4 volts, Number (3) by applying 1.9 volts and Number (4) by applying 1.5 volts.

The rate of change of temperature of the filament is shown as a function of temperature in Figure 2.6. The curves (1) to (4) in Figures 2.5 and 2.6 correspond. The rates of change of temperature in Figure 2.6 were calculated from Figure 2.5.

Figure 2.6 shows clearly that the rate of increase in temperature of the filament, at any given temperature, is increased by increasing the applied potential difference across the filament. Figures 2.5 and 2.6 also show that the circumstances which produce a high equilibrium temperature also produce a relatively high rate of increase of temperature, at a given temperature. Thus the trend of result obtained by using the optical pyrometer, which concerns the equilibrium temperature of the filament can be applied to the rate of increase

Figure 2.5

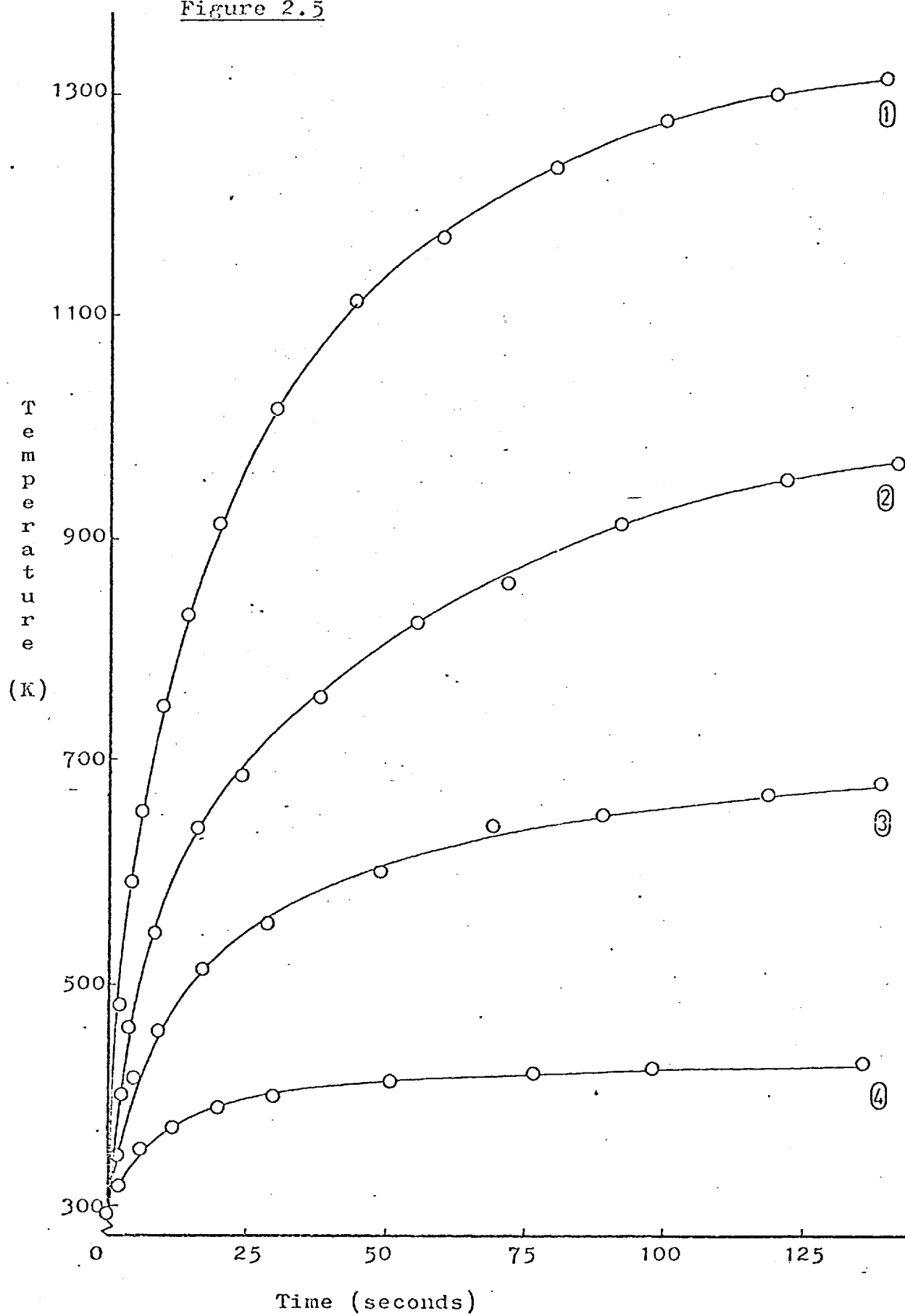
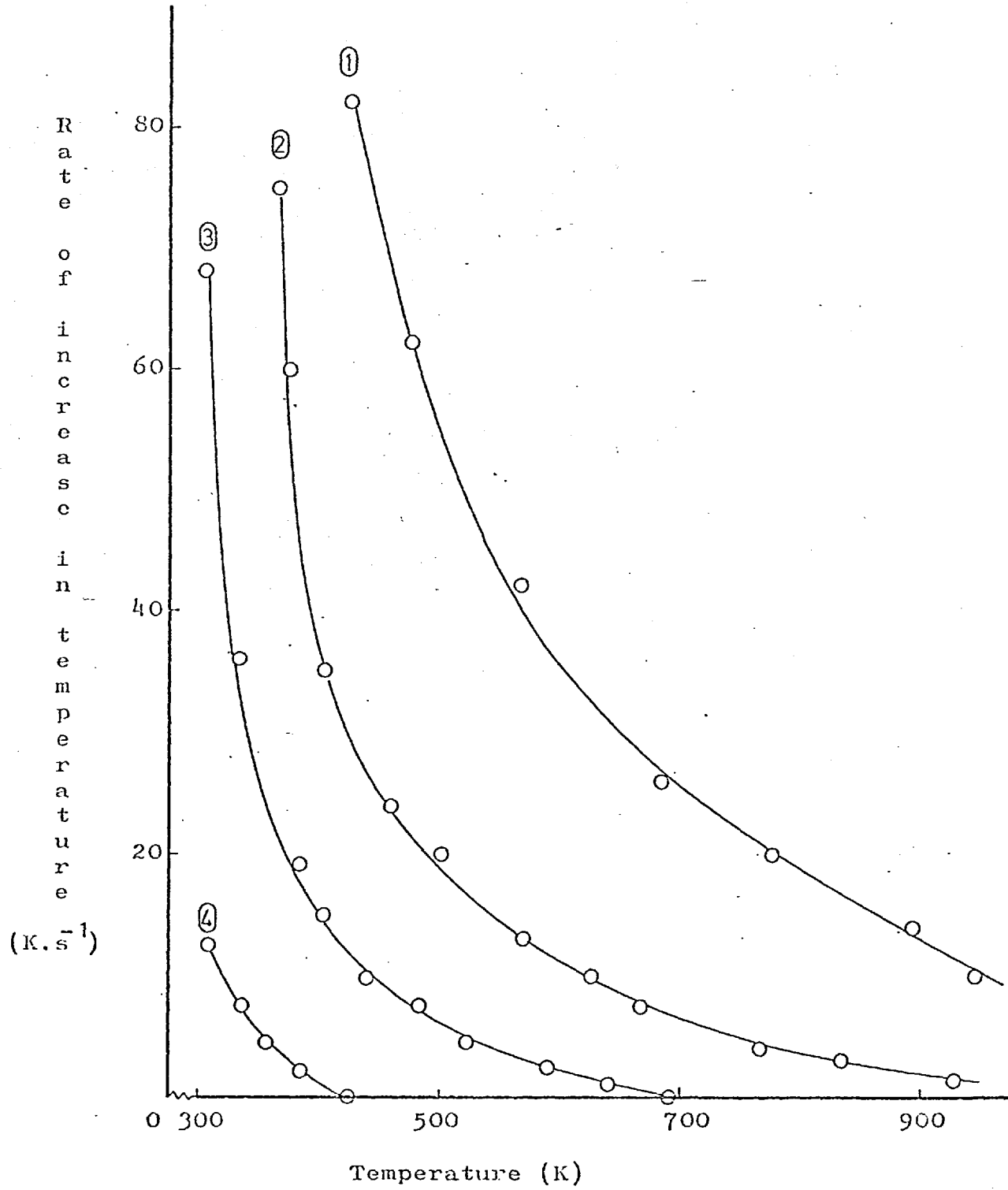


Figure 2.6



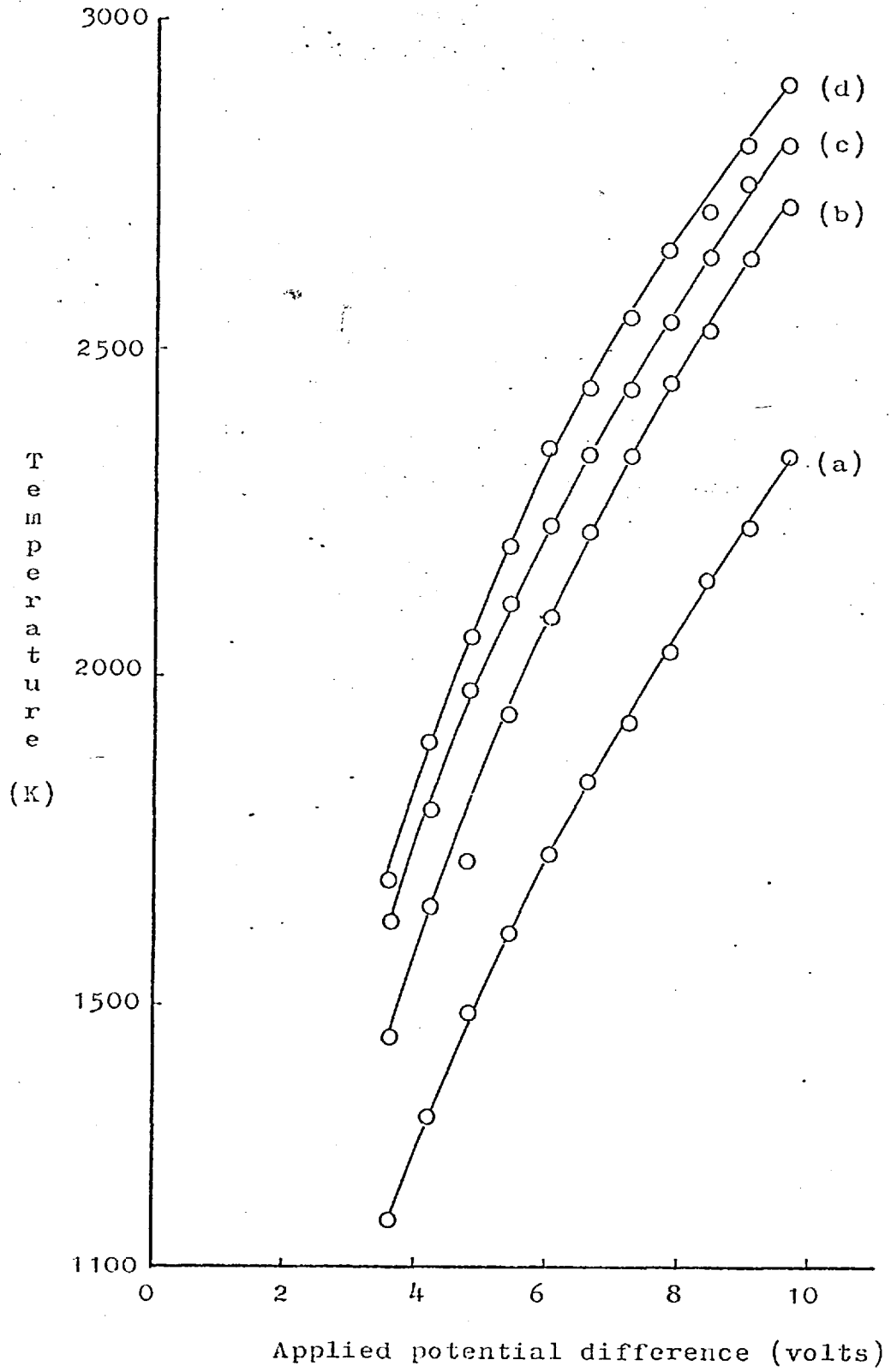
of temperature, at a given temperature.

Figure 2.7 shows how the equilibrium temperature reached by a filament, measured with the optical pyrometer, varies with the applied potential difference, for filaments with four different specific resistivities. Curve(a) represents a filament with $R_{273} = 2.7 \times 10^{-2}$ ohm.mm., curve (b) a filament with $R_{273} = 1.66 \times 10^{-2}$ ohm.mm., curve (c) a filament with $R_{273} = 0.7 \times 10^{-2}$ ohm.mm., and curve (d) a filament with $R_{273} = 0.25 \times 10^{-2}$ ohm.mm. Clearly the equilibrium temperature of a filament, and therefore the rate of increase in temperature, at a given temperature, is increased by reducing the specific resistivity of the filament.

The effects of altering the radius and the length of the filament were not investigated because K.W.Jackson and A.C.Oborne working in the Harwood Laboratory at the same time as this author performed these investigations. Jackson showed that the rate of increase in temperature of a filament was significantly increased by reducing the length of the filament between the steel electrodes. Osborne corroborated this result and also demonstrated that a reduction in the radius of the filament resulted in an increase in the rate of increase in temperature.

The effects of varying the applied potential difference, the specific resistivity and the length of the filament predicted by inspection of equation 2.21 have been corroborated. The prediction concerning the effect of varying the radius of the filament has been contradicted.

Figure 2.7



Equation 2.21 was derived by considering the middle part of the filament. The part of the filament in contact with the steel electrodes was not considered. Any attempt to analyse the heat transfer between the filament and the electrodes must assume that the heat is very rapidly removed by the cooling water so that the heat flux depends only upon the temperature of the filament and not upon the heat previously absorbed by the electrodes, base and water. i.e. The rate of cooling of the filament when the power is switched off should depend on the instantaneous temperature, but not upon the initial temperature of the filament. Figure 2.8 shows the temperature - time curves, measured with the thermocouple, for a cooling filament, from four initial temperatures. Figure 2.9 shows the rate of loss of temperature vs. temperature curves calculated from Figure 2.8. If the rate of cooling of the filament did not depend on the initial temperature then the four curves in Figure 2.9 should all be superimposed. Since this is clearly not the case, analysis of the heat flow into the electrodes has not been attempted. However a partial explanation of the relationship between the radius of the filament and the rate of increase in temperature, may be seen in the fact that the heat flow into the electrodes will depend very much on the area of contact between the electrodes and the filament.

The C.F.A.R. used in the investigation of the element lead, reported in the remainder of this thesis is shown in Figure 2.2. The filament used had a radius of 1.6 mm. and a specific resistivity of 1.66×10^{-2} ohm.mm. at 273°K. The separation between the electrodes (i.e. the

Figure 2.8

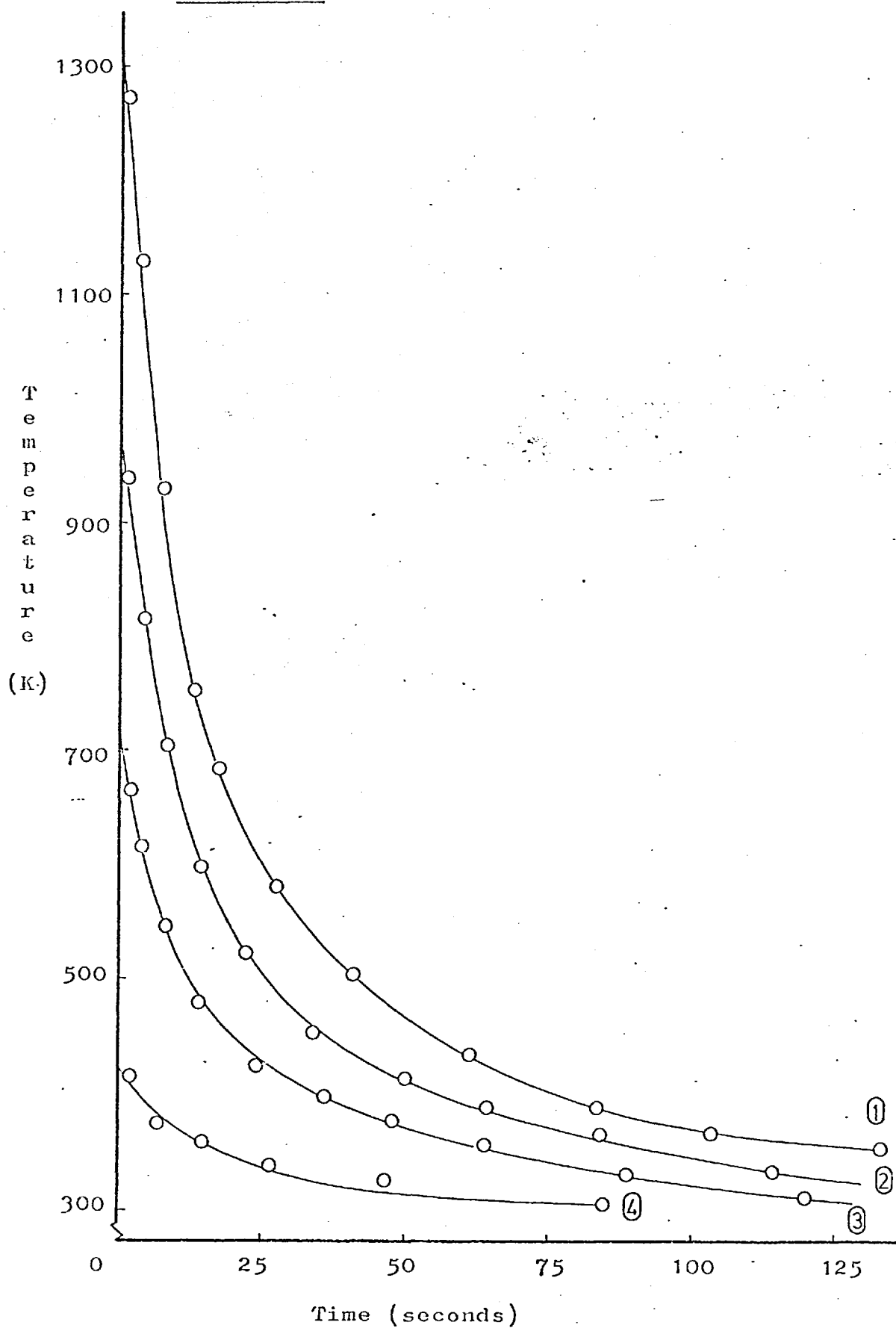
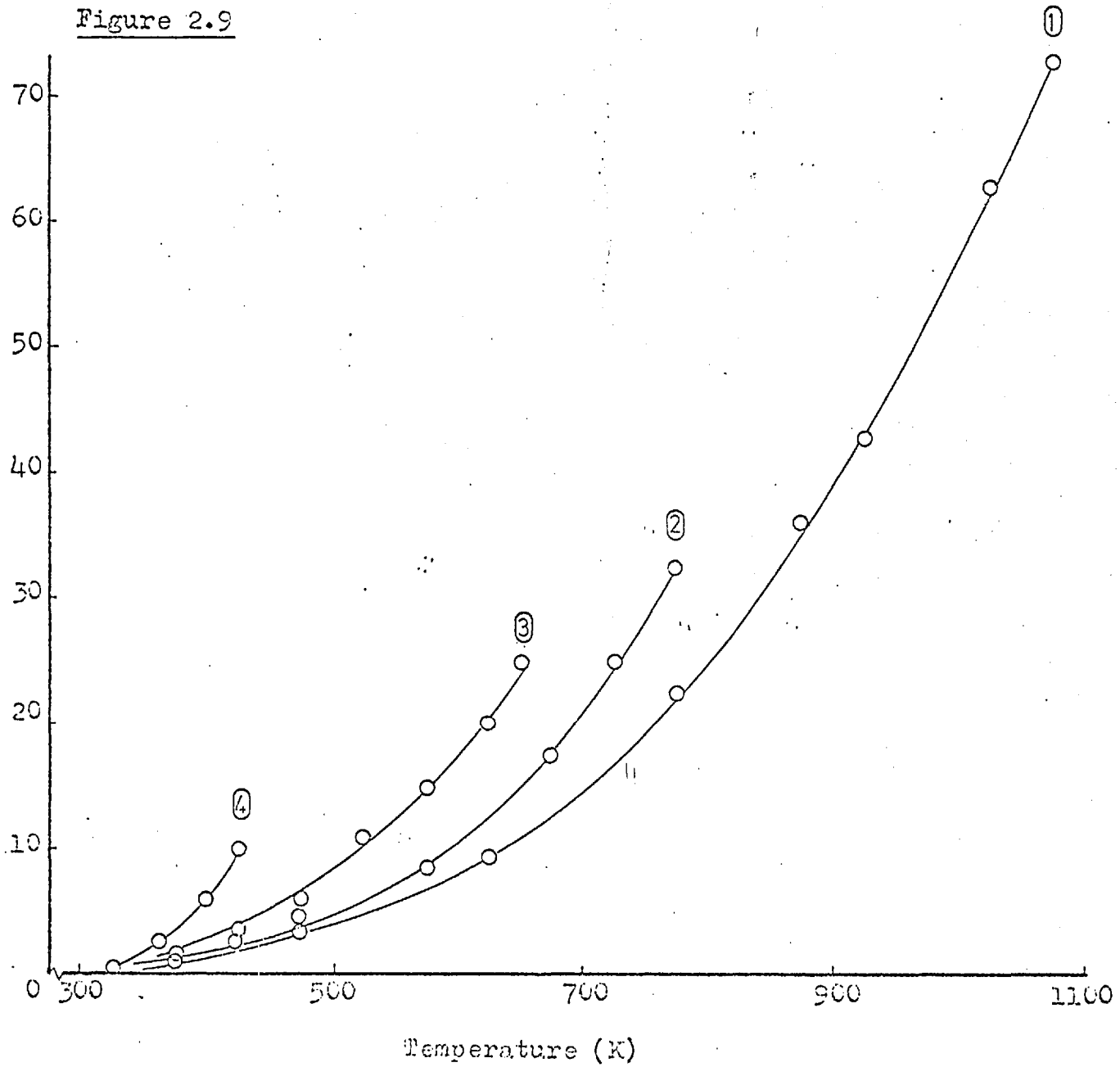


Figure 2.9

Rate of
fall in
temperature
(K.s⁻¹)



effective length of the filament) was 26 mm.

Chapter Three

The Determination of Lead —
on the
Carbon Filament Atom Reservoir
by
Atomic Absorption Spectrometry

Delivery of small samples.

One of the major advantages of the C.F.A.R. over the conventional flame atom reservoir is its capacity for handling very small samples. In normal practice a liquid sample of between one and five microlitres is used. Four instruments have been used to deliver a measured sample to the filament:-

i) An all glass syringe.

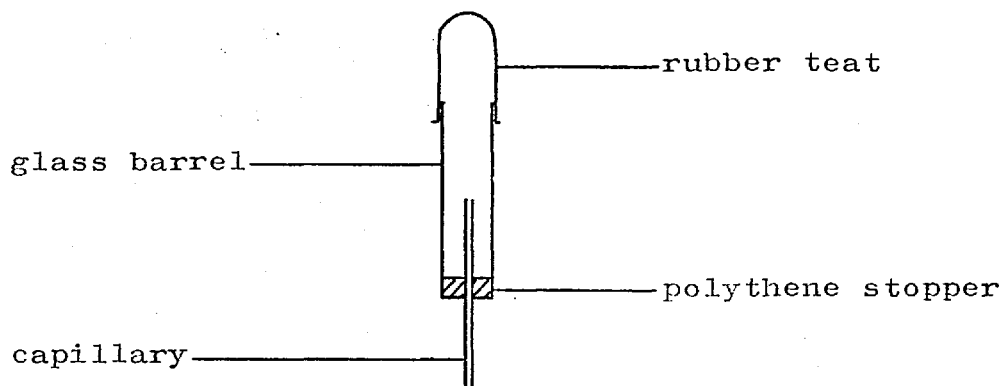
All the parts of the syringe which come into contact with the sample are glass, to avoid contamination from a metal surface. The plunger of this syringe is controlled by a micrometer screw, which ensures accurate control of the volume of sample delivered but is awkward to use. The weight of the micrometer screw makes it difficult to balance the syringe with the point unmoving above the centre of the C.F.A.R.

ii) A Hamilton syringe.

This is designed to introduce the sample to a gas-liquid chromatography column. It has a stainless steel needle and plunger and a glass barrel. The metal parts introduce a risk of contamination. (Gold-plated needles and plungers have been used by American workers.⁽¹⁰²⁾) The plunger, which fits exactly into the glass barrel, is a very thin steel rod. If the plunger is slightly bent it jams in the barrel and renders the instrument useless. Repair is difficult.

iii) A Drummond Micropipette.

This is a very simple instrument, shown in Figure 3.1. The glass capillary is designed to hold

Figure 3.1

either one, two or five microlitres. The sample is drawn into the capillary until it is filled. Any excess liquid drawn in flows through the capillary into the glass barrel. The contents of the capillary are deposited on the C.F.A.R. by gentle pressure on the rubber teat. This micropipette is quick and easy to use after some initial practice. The instrument is less satisfactory for viscous liquids e.g. blood, than for aqueous and volatile organic liquids.

iv) An Eppendorf-Marburg micropipette.

These micropipettes are designed to deliver either five, ten, twentyfive, one hundred or two hundred microlitre samples. The sample is drawn into a Teflon tip, which fits onto the end of the body of the micropipette, and is then expelled onto the C.F.A.R. There are two modes of operation of this type of micropipette. A measured volume of sample can be drawn up into the tip of the pipette and then completely expelled. Alternatively a volume larger than that required can be drawn into the tip and a measured volume expelled. Both of these

methods are simple to use. The reproducibility of the sample delivered by a five microlitre Eppendorf-Marburg micropipette was measured (for both of these modes of operation) by direct weighing of twenty replicate samples. For the first mode the relative standard deviation was 2.15%; for the second it was 2.84%. The relative standard deviation is defined by:-

$$\text{R.S.D.} = \frac{1}{\bar{x}} \sqrt{\frac{\sum_{i=1}^n (x_i - \bar{x})^2}{n-1}} \quad \underline{3.1}$$

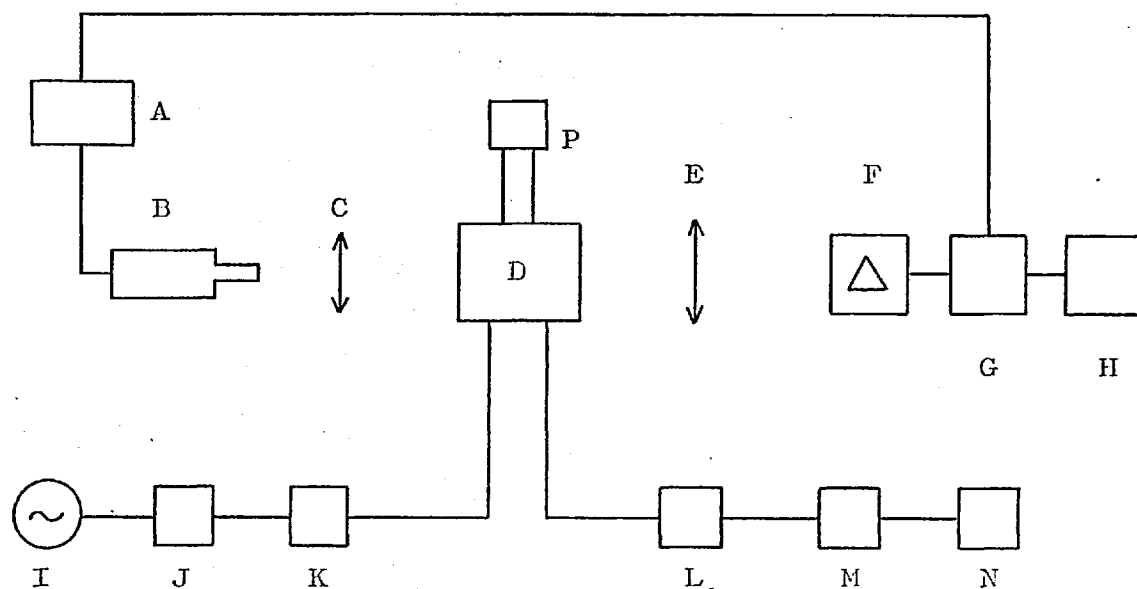
where x is the measured parameter and \bar{x} is the mean value of n replicates of x .

In view of the ease of use, their capacity to handle viscous liquids and the good reproducibility, these pipettes were used in preference to the other three.

Instrumentation.

The burner-nebuliser unit of a Varian-Techtron A.A.4. was replaced by the C.F.A.R. The arrangement is shown diagrammatically in Figure 3.2. The lens C is positioned to focus light from the hollow cathode lamp at a spot just above the middle of the carbon filament. The lens E is positioned to re-focus the light at the monochromator entrance slit. This arrangement ensures that the maximum light intensity enters the monochromator slit. Alternative arrangements in which one or other or both lenses are omitted have been tried and found to be less effective.

Figure 3.2.



Key:

- A Hollow cathode lamp power supply.
- B Hollow cathode lamp.
- C,E Lenses.
- D C.F.A.R.
- F Monochromator and photomultiplier tube.
- G Amplifier.
- H Recorder.
- I Mains electricity supply.
- J 1.2 kW. stepdown transformer.
- K Variac variable transformer.
- L Rotameter flow gauge.
- M Aspirator.
- N Gas cylinder.(Nitrogen or argon)
- P Water supply

Optimum Conditions to Determine Lead.

Monochromator Slit.

The atomic absorption spectrum of lead shows two intense lines, one or other of which is frequently used for the A.A.S. analysis of lead. One of these lines is at 283.3 nm., the other at 217.9 nm. The usefulness of the two lines is considered later in this chapter.

The purpose of the monochromator in atomic absorption spectrometry is to isolate the absorption line from the other radiation which the hollow cathode lamp emits (e.g. non-absorption lines in the lead atomic emission spectrum and emission from the filler gas). A wide entrance slit on the monochromator allows the maximum light intensity to reach the photomultiplier tube and therefore allows a low 'gain' (i.e. potential difference across the photomultiplier tube) to be used, which in turn means a low background noise level. However, if the monochromator entrance slit is too wide, the photomultiplier tube 'sees' radiation from non-absorption lines. The maximum width of the entrance slit which resolves the absorption line from the nearby emission lines is determined empirically.

Experimental

The lead hollow cathode lamp was switched on and focused onto the monochromator slit. The slit was fully opened (i.e. 0.3 mm.). The photomultiplier tube was switched on at minimum gain. The wavelength selector was set at 283.3 nm. and the gain adjusted to give the

maximum signal which could be displayed on the read out. The wavelength selector was then moved through 0.1 nm. intervals and the photomultiplier tube output recorded at each step. The relative intensity (i.e. photomultiplier tube output) of the hollow cathode lamp was plotted against the wavelength. This procedure was repeated at three more slit widths (0.2 mm., 0.1 mm. and 0.02 mm.). The whole experiment was repeated for the absorption line at 217.1 nm., except the 0.02 mm. slit width was ignored.

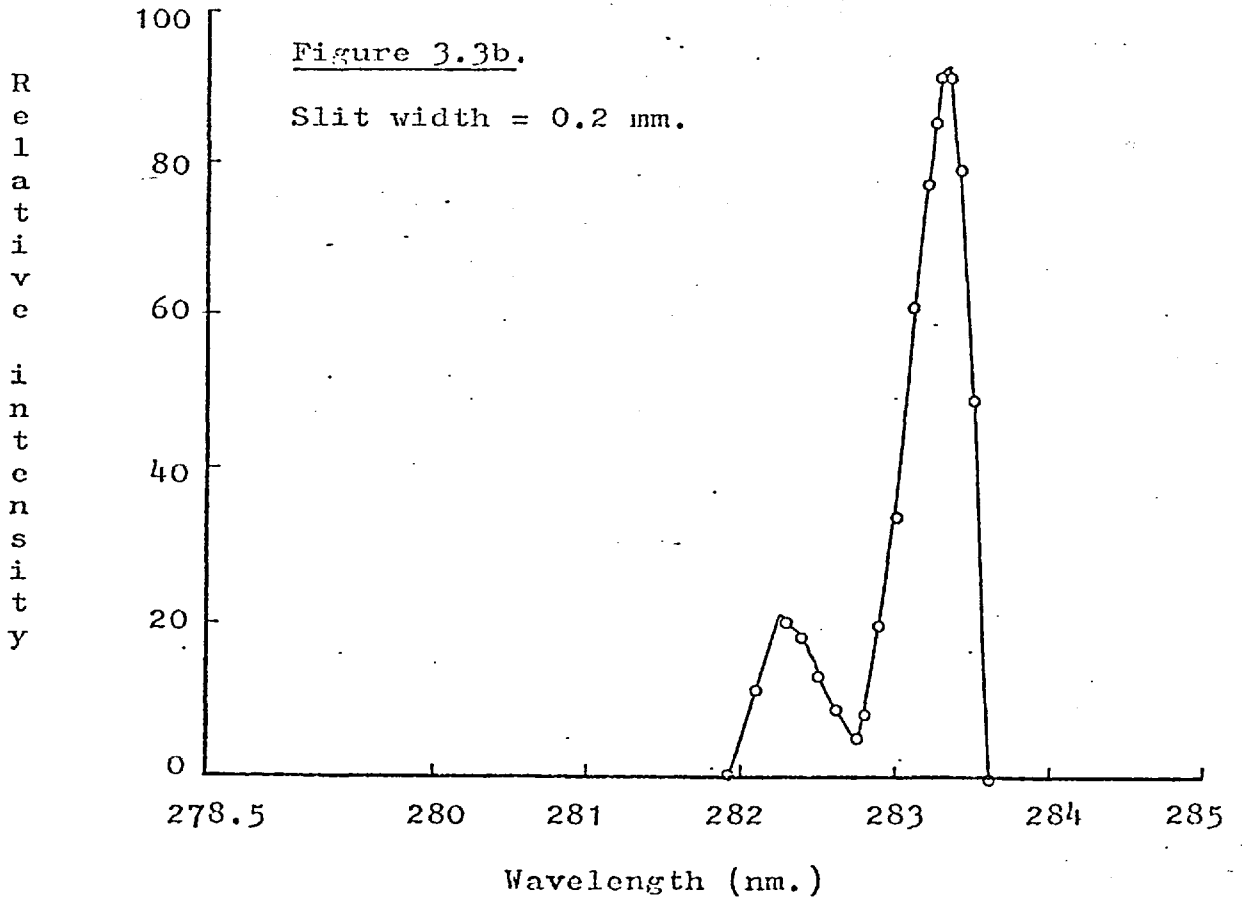
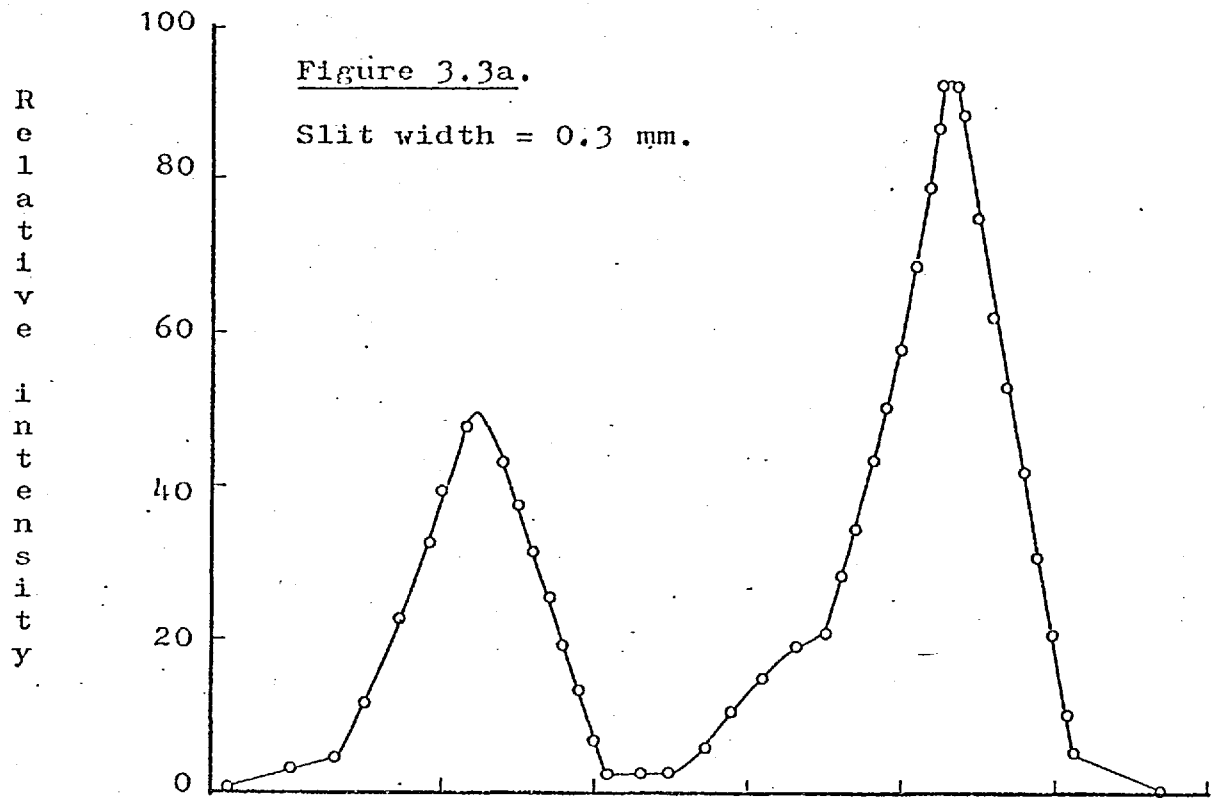
Results and Conclusion.

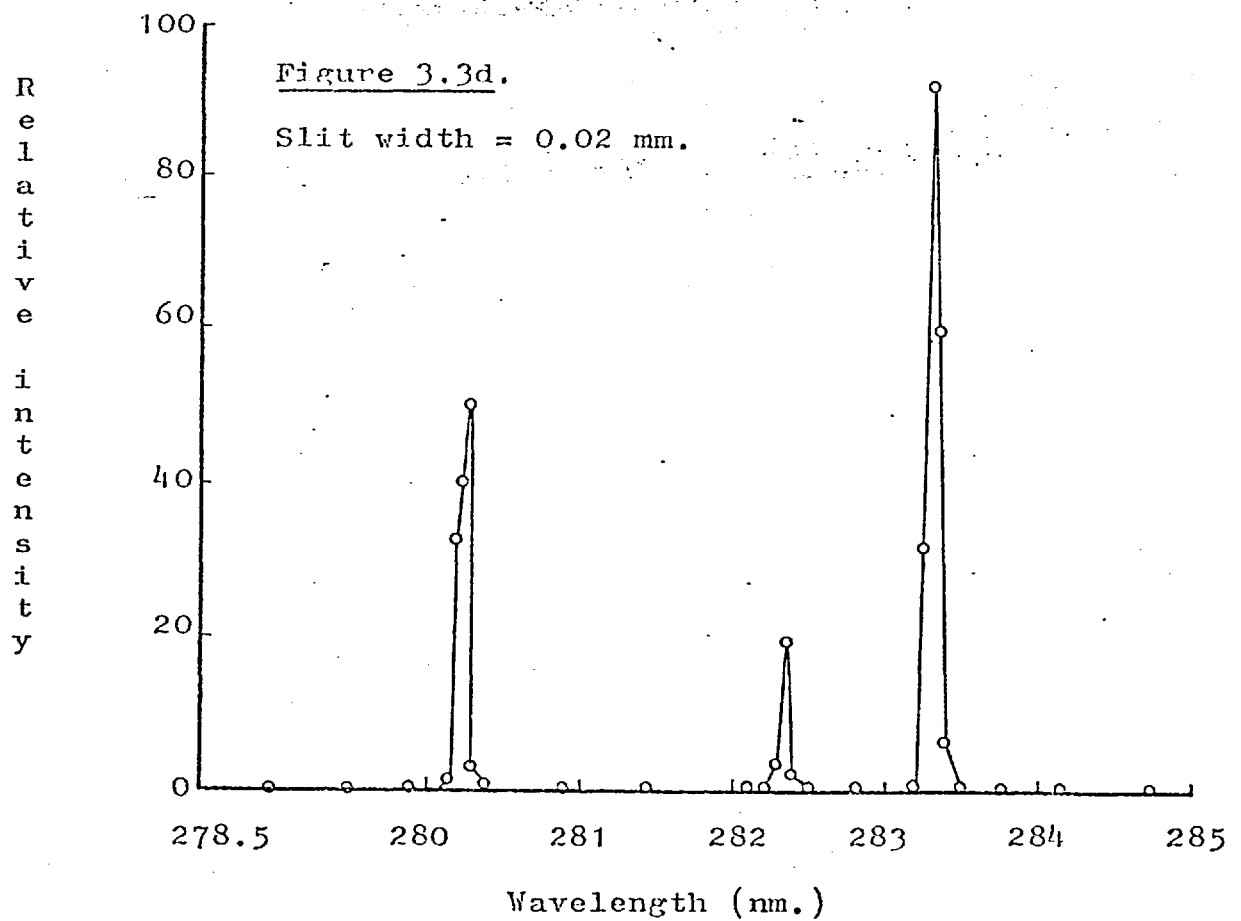
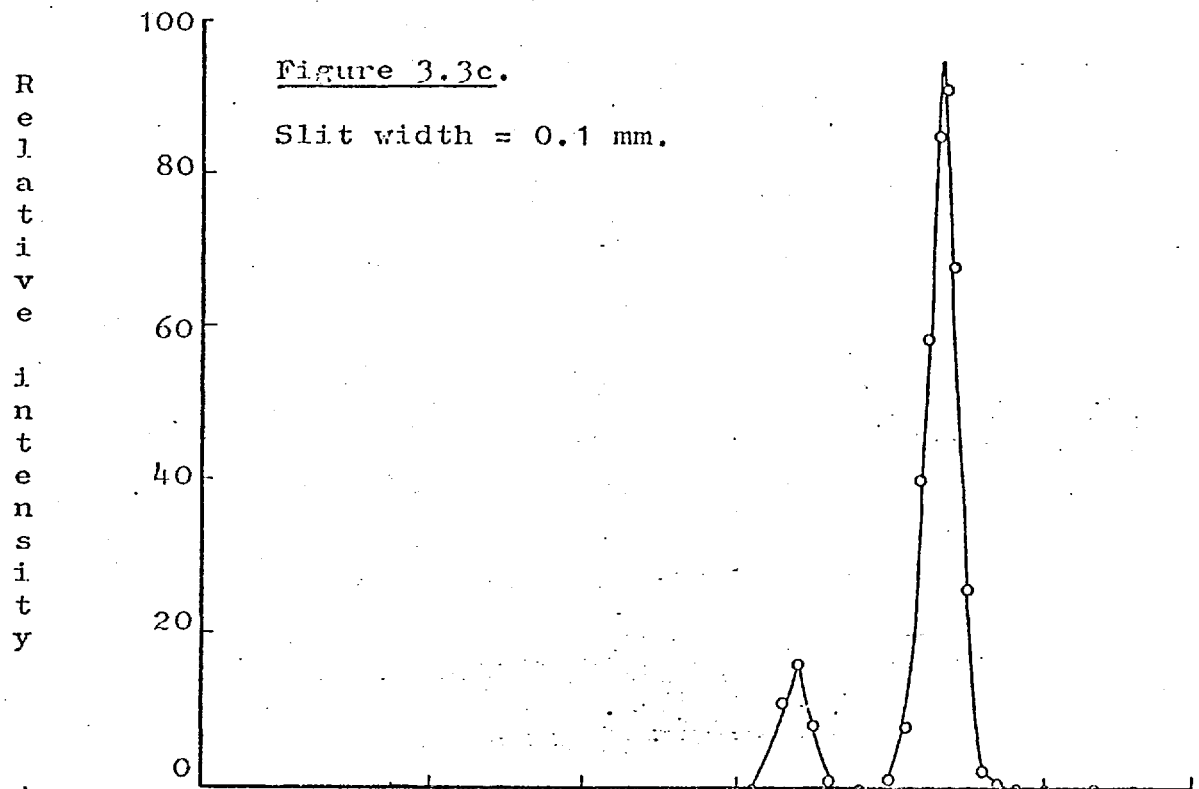
The results for the 283.3 nm. line are shown in Figures 3.3a - d. The maximum slit width which completely resolves the emission lines centred on 283.3 nm. and 282.4 nm. respectively is just less than 0.2 mm.

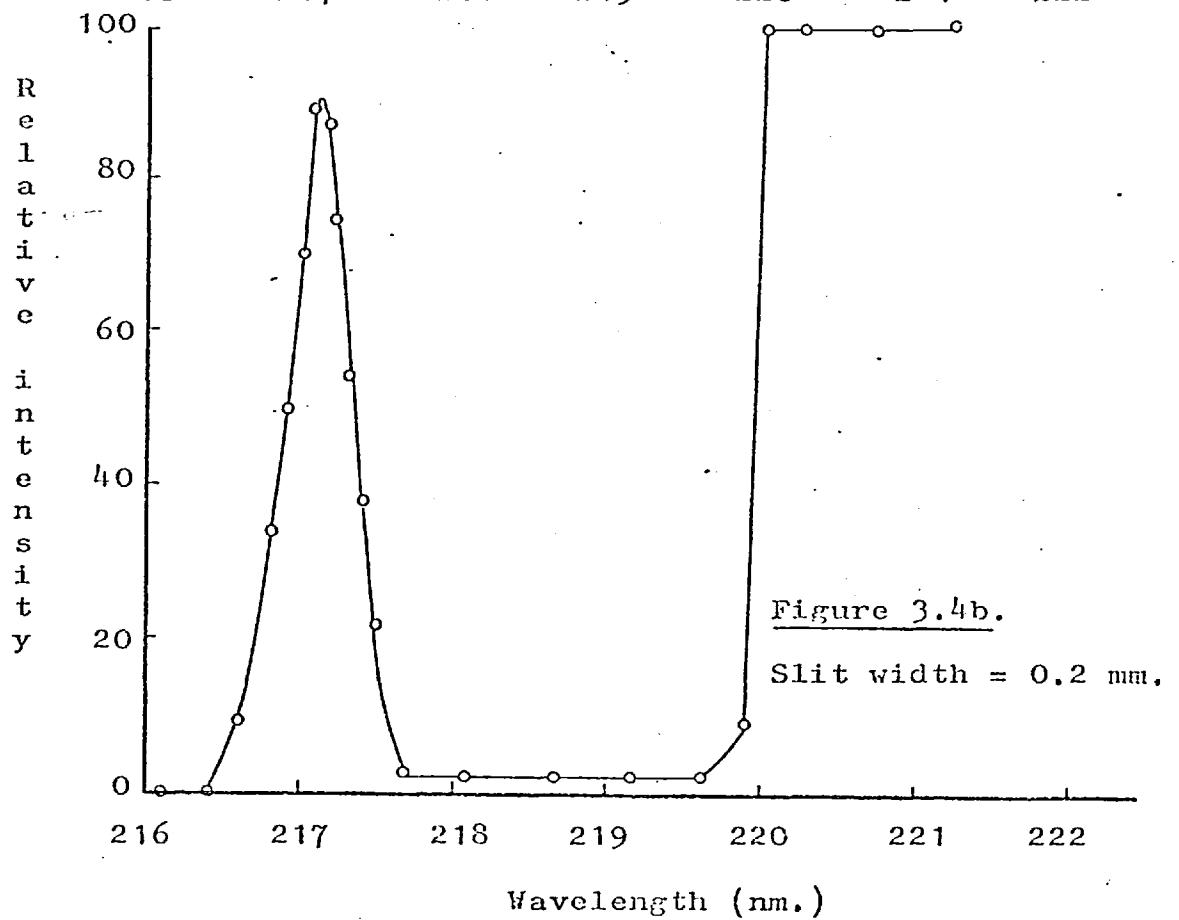
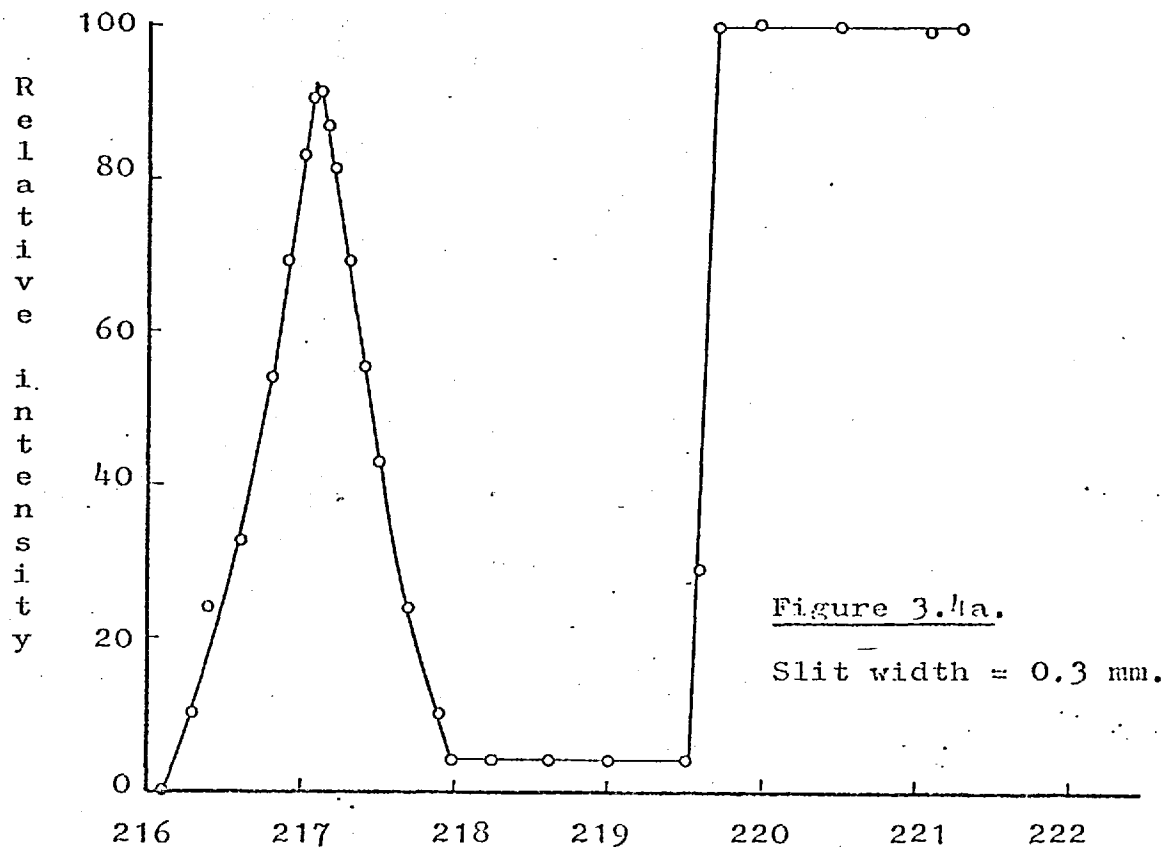
The results for the 217.1 nm. line are shown in Figures 3.4a - c. The maximum slit width which completely resolves the 217.1 nm. line from the continuum beginning at 220.0 nm. is again just less than 0.2 mm.

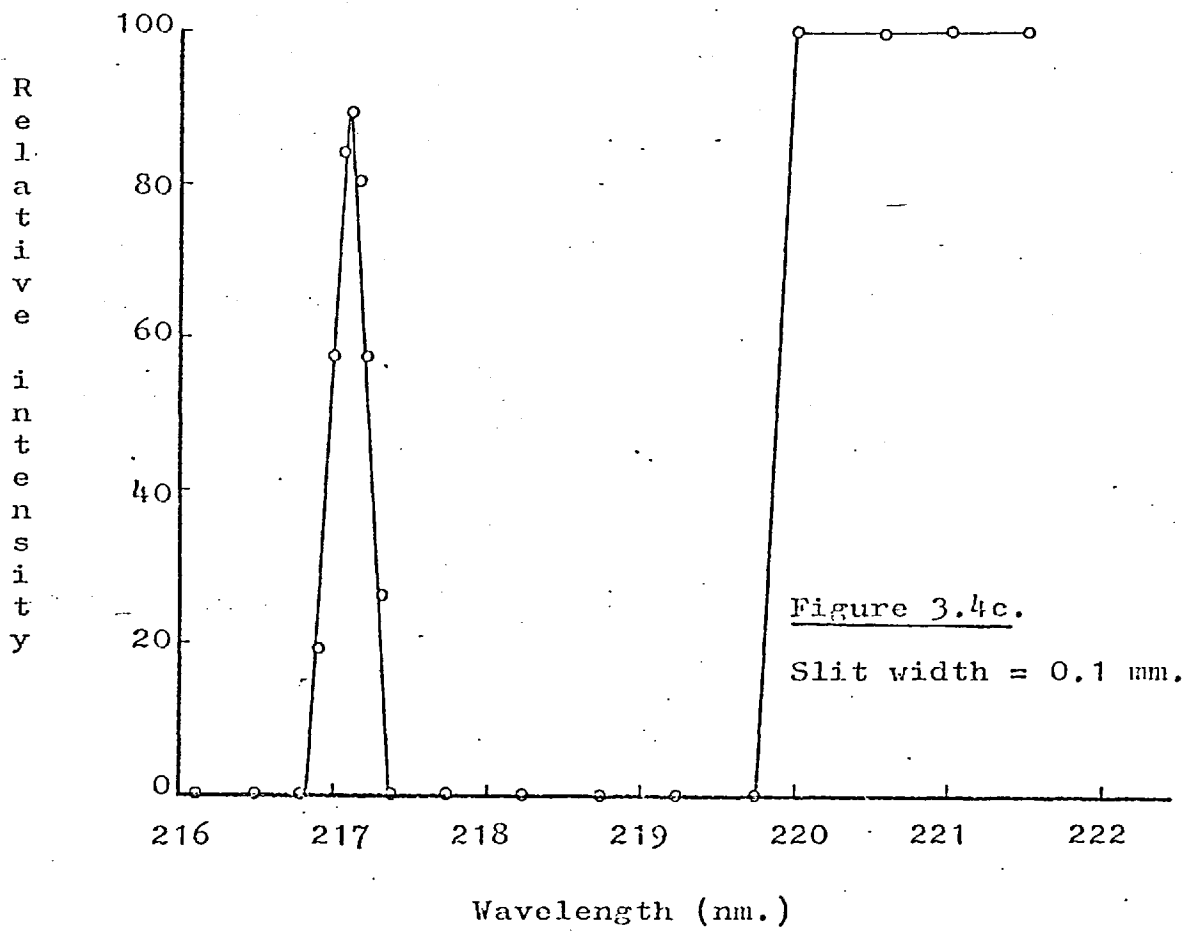
Amplifier and Recorder.

The Techtron A.A.4. includes a tuned a.c. amplifier which is synchronised with the hollow cathode lamp modulation. The use of a modulated hollow cathode lamp with a tuned amplifier is not necessary when the flame is replaced by the C.F.A.R. since the monochromator slit can be shielded from the incandescence of the filament. However the tuned a.c. amplifier was used as normal. In routine use the amplified signal is displayed on a moving coil galvanometer. Obviously, a signal last-









ing several seconds, such as that produced by a flame atom reservoir, can be accurately recorded from a galvanometer. A transient signal, from the C.F.A.R., must be recorded.

Two types of recorder have been used:-

i) The Honeywell 1706 Visicorder Oscillograph.

This instrument is a very high speed response recorder. The signal is fed into a galvanometer which rotates a small mirror. The mirror reflects a beam of intense U.V. light, which is focused onto a moving strip of U.V. sensitive paper. This type of recorder has been used to record signals due to atomic absorption by lead, but is more useful when used in conjunction with involatile metals (e.g. cobalt) which give rise to very short lived signals.

ii) The 'Servoscribe' Potentiometric Recorder.

This instrument employs a moving pen and moving chart and has a much slower response than the 'Visicorder'. If the signal is finished before the pen has completed its movement a low reading is obtained. This can cause curvature of the calibration graph.

The signal displayed on the recorders is the relative intensity of the light falling on the photomultiplier tube. This is converted first to a percentage absorption, by comparison with the signal obtained by covering the monochromator slit, and then to absorbance from tables. The calibration graphs obtained by plotting absorbance against mass of lead, for each recorder, shown in Figure 3.5, indicate the curvature due to the slow response of the recorder. The pen re-

Figure 3.5

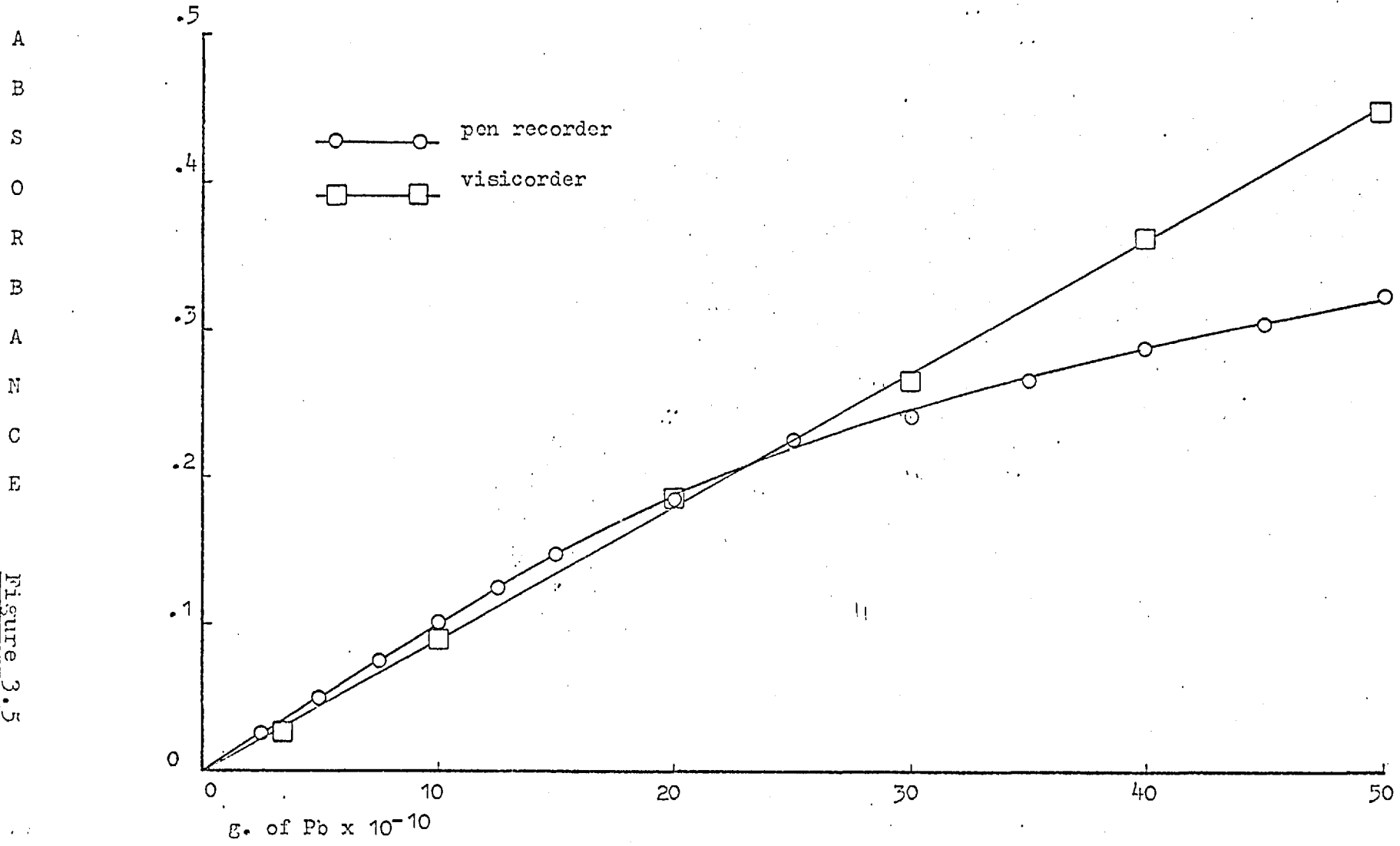


Figure 3.5

corder, however, possesses two advantages over the 'Visicorder'. Since the pen recorder has a slow response time it filters the high frequency noise from the photomultiplier, allowing a greater photomultiplier gain to be used. Secondly it is possible to 'expand the scale' on the pen recorder by increasing the recorder sensitivity so that although the 100% absorption signal is off-scale its position is accurately known. (e.g. If the 100% absorption signal is 200 mm. from the 0% absorption signal with a recorder sensitivity of 1 mV. per 40 mm. of chart, then a recorder sensitivity of 1 mV. per 100 mm. of chart can be used. The 100% absorption signal will be 500 mm. from the 0% absorption line, well off-scale, but accurately known). This enables very small absorption signals to be measured. The 'Visicorder' cannot be adjusted in this way.

The Inert Atmosphere.

The filament is protected from atmospheric oxygen by a flow of inert gas. Nitrogen and argon have both been used. Argon is preferred to nitrogen for atomic fluorescence studies since the diatomic nitrogen molecule can quench the fluorescence. For atomic absorption studies either gas is satisfactory, but argon was used in all the experiments described here.

As described above, the argon is transferred from a cylinder via an aspirator and Rotameter flow gauge to the laminar flow box below the filament. The optimum rate of flow of the argon was determined empirically. Figure 3.6a. shows how the absorbance due to

Figure 3.6

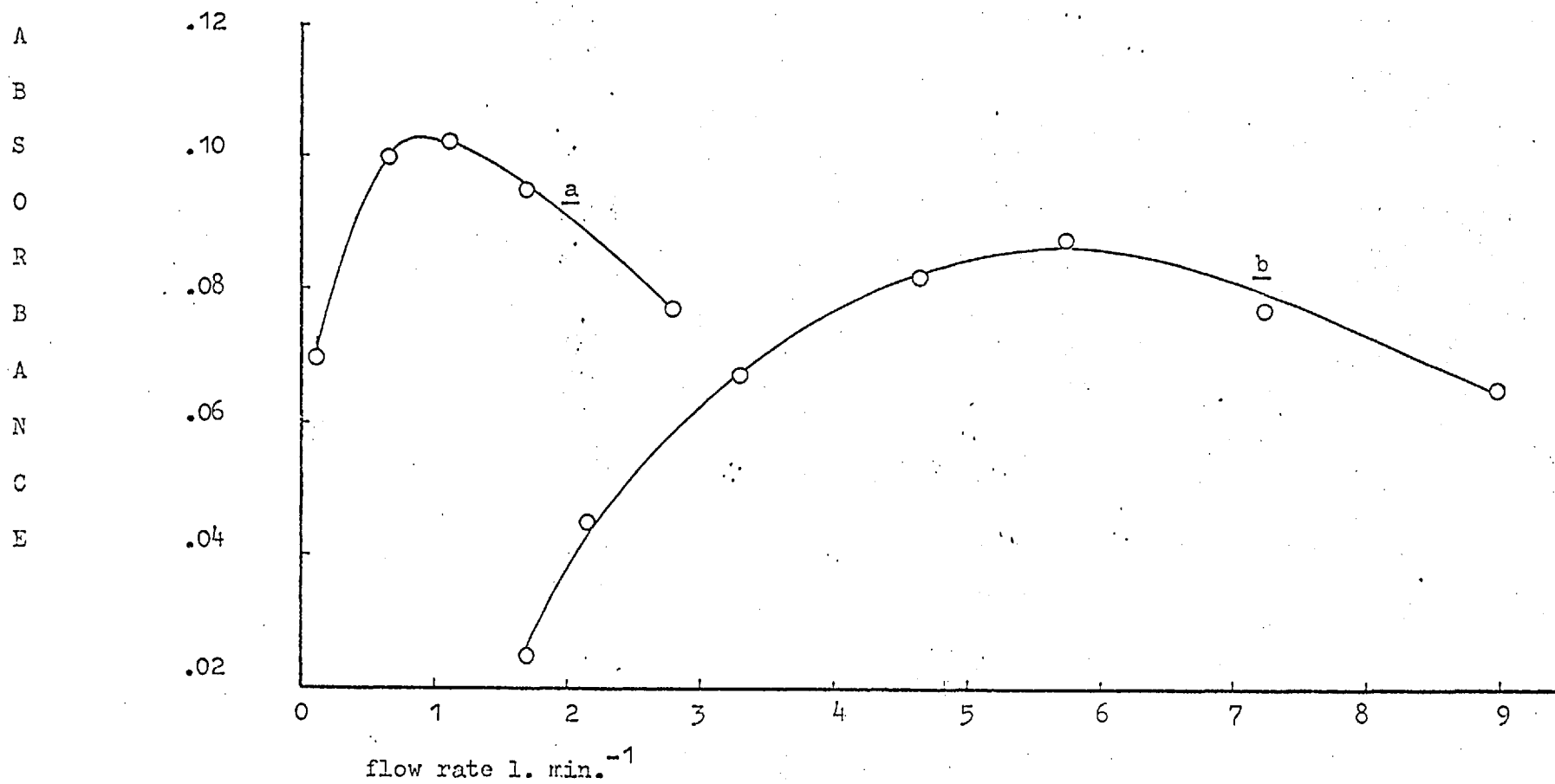


Figure 3.6

A
B
S
O
R
B
A
N
C
E

10^{-9} g. of lead varies with argon flow rate for the open-topped cell., Figure 3.6b. for the completely open cell. The shape of these curves can perhaps be explained in terms of two factors. At very low flow rates, the argon may not completely protect the atomic vapour from atmospheric oxygen, so at first the absorbance signal will be increased by a faster flow of argon. However equation 2.4 indicates that the peak atomic population in the observed volume depends on τ_2/τ_1 , (where τ_2 is the average lifetime of a single atom in the observed volume) as shown in Figure 3.7. If τ_1 is constant then the peak atomic population decreases as τ_2 decreases. As the argon flow rate increases, τ_2 will probably decrease, since the atomic vapour will be swept through the observed volume more quickly, and therefore the peak absorbance will decrease. Figure 3.7 shows clearly that the effect of τ_2 on peak atomic population only becomes marked when τ_2 becomes very small. It is reasonable to suppose that at low flow rates the change in the peak atomic population, due to a change in τ_2 , is small, so that protection from oxygen is the determining factor. As the flow rate increases the change in peak atomic population, due to a change in τ_2 , becomes larger, so that τ_2 becomes the determining factor. The displacement of the peak for the open cell probably reflects the greater openness to atmospheric oxygen.

The Potential Difference applied across the Filament.

The voltage applied across the filament has a large effect on the heating rate and hence on the peak

atomic population. This is controlled between zero and twelve volts, by a Variac variable transformer. The relationship between absorbance, and therefore atomic population, and applied potential is shown in Figure 3.8 for a sample of 10^{-9} g. of lead. The shape of the curve can be explained by reference to Figure 3.7. This time τ_2 will be constant and τ_1 (the duration of the atomization process) is decreased as the applied voltage is increased. At low applied voltages, (large τ_1 values), the change in peak atomic population is large for a small change in τ_1 , but at high applied voltages (low τ_1 values), the change in peak atomic population is small for a large change in τ_1 . Therefore the curve flattens off. The lifetime of the filament is related to the applied voltage chosen for routine use. Frequent use of a very high voltage reduces the lifetime of the filament. Replacement of the filament is not serious but may be time consuming. A compromise of 8.2 volts was found to be satisfactory.

The Carbon Filament.

The dimensions and electrical resistivity of the filament have been discussed in Chapter 2. Before use in the C.F.A.R. a small notch, approximately 3 mm. long is filed in the centre of the filament. This enables the sample to be deposited on the same spot each time, and prevents the sample from simply falling off the filament.

Figure 3.7

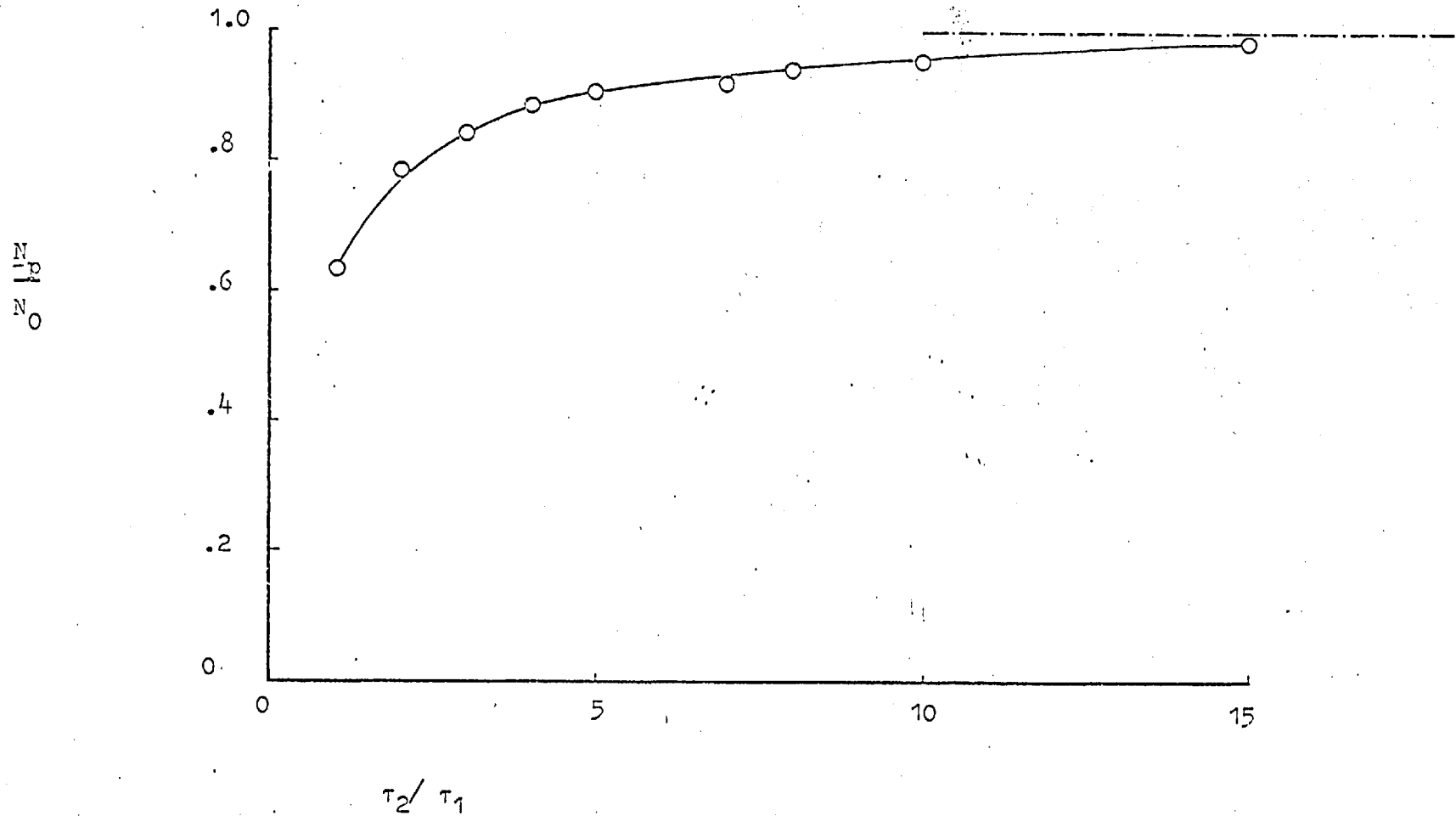
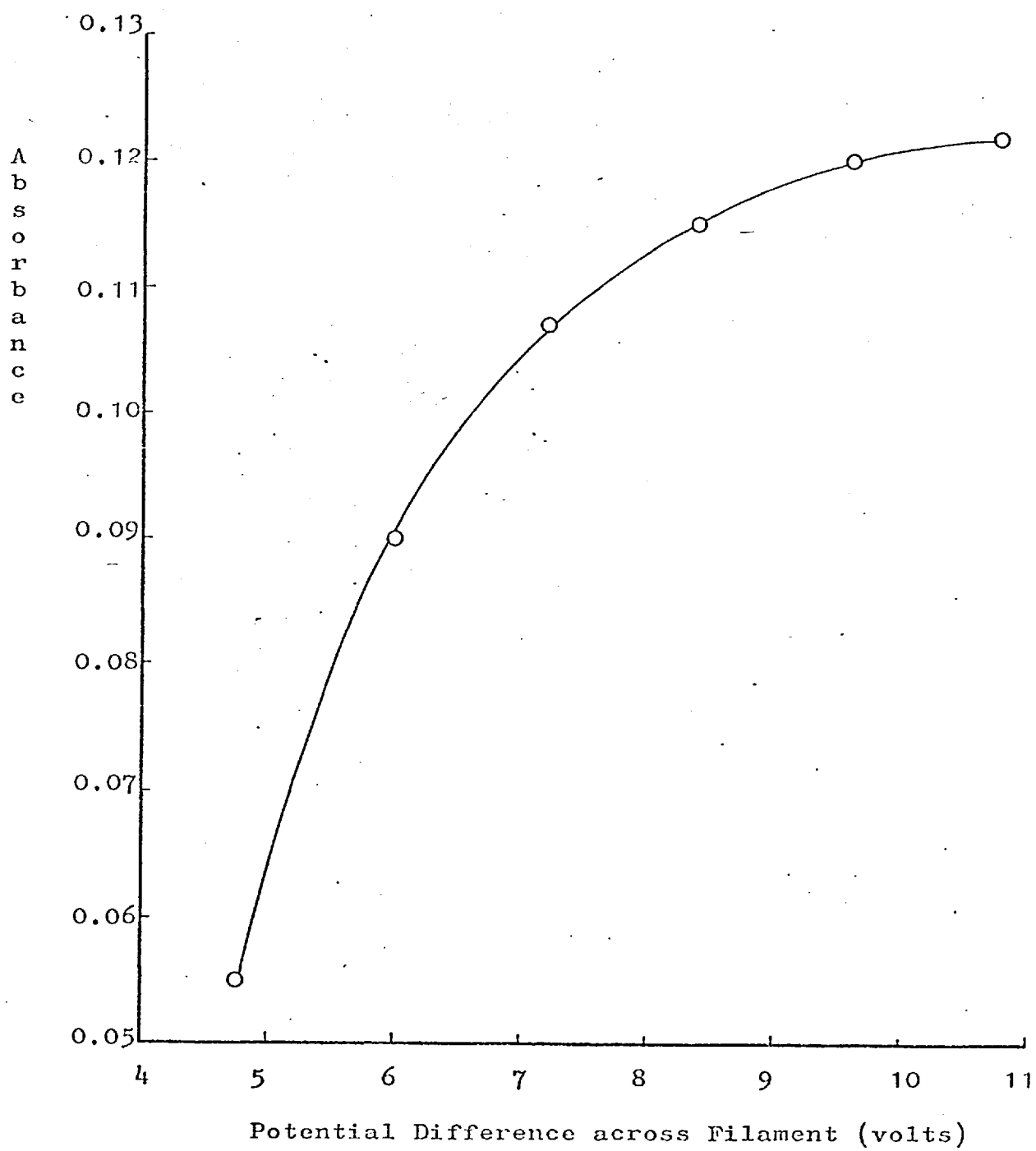


Figure 3.7

Figure 3.8

The Hollow Cathode Lamp

Two types of hollow cathode lamp have been used:-

i) A Walsh and Sullivan type High Intensity Hollow Cathode Lamp. (Atomic Spectral Sources Ltd.)

This type of lamp achieves high intensity by use of secondary electrodes. The primary cathode gives rise to an atomic vapour. This extends beyond the cathode (a fact which leads to reduction of intensity due to self absorption in normal hollow cathode lamps) and is excited by collisions with inert gas-ions between the secondary electrodes. The result of this is a large, relatively diffuse light source. When used with a flame atom reservoir this is quite satisfactory, since the atomic vapour in a flame is diffuse, but the atomic vapour generated by the C.F.A.R. is very restricted in volume.

ii) A Westinghouse Hollow Cathode Device, Type WL(Pb) High Spectral Output.

The Westinghouse Device achieves the same (or better) high intensity output as the Walsh-Sullivan lamp, (without the use of secondary electrodes), and can be easily focused to a circular spot with a diameter of approximately 3 mm. As a result it may be used without any 'slits' in between the lamp and the monochromator entrance, which in turn means that a low photomultiplier gain can be used and background noise reduced.

Optical Alignment.

It has already been stated that the light from the hollow cathode lamp is focused above the fila-

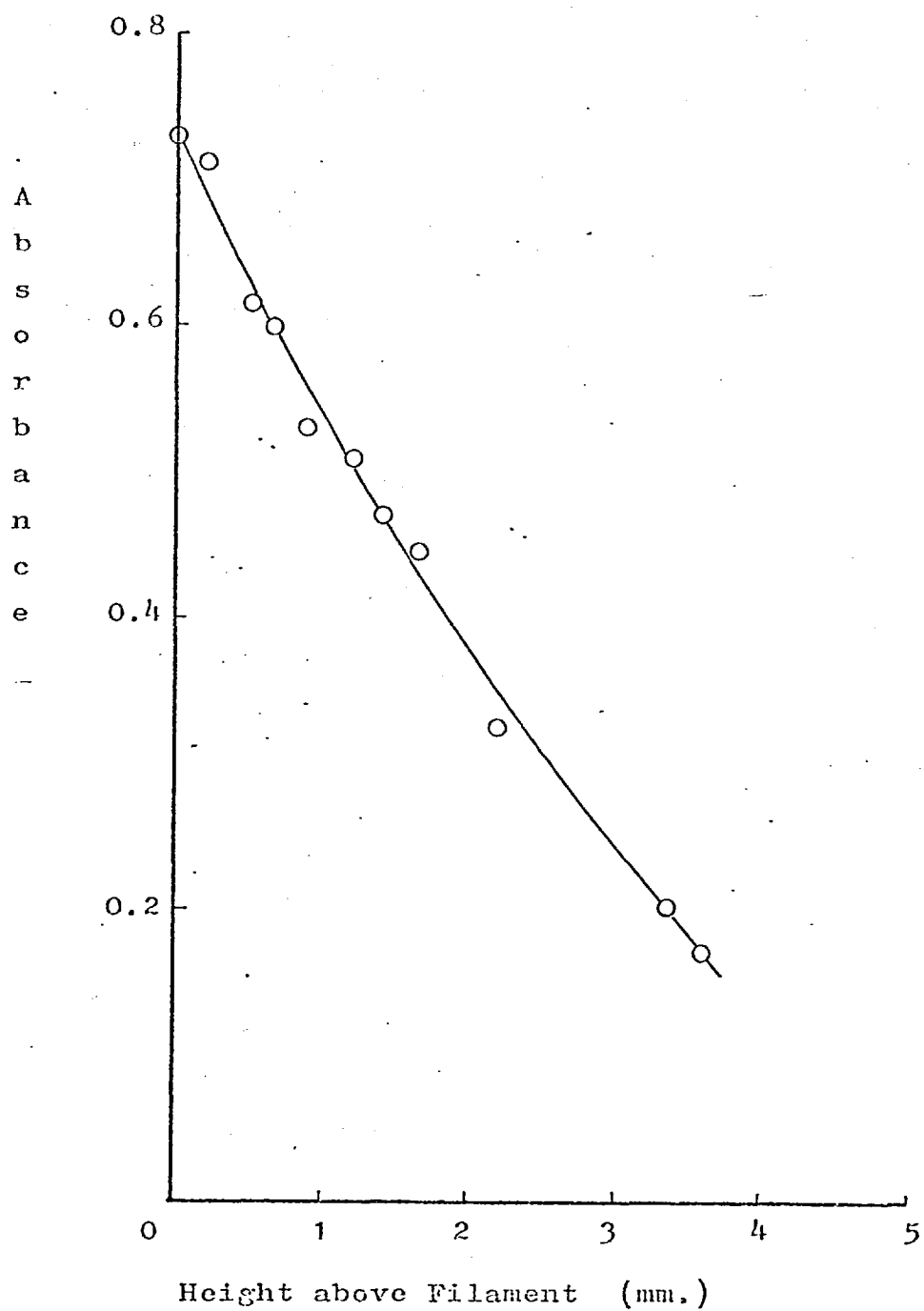
ment and re-focused at the monochromator entrance slit, but the vertical position of the focused spot has not been considered.

Experimental.

A metal disc with a slit (10 mm. by 0.5 mm.) was placed in front of the hollow cathode lamp. The resultant rectangle of light was focused onto a sheet of white card held above the filament. A travelling microscope was placed along side the hollow cathode lamp and focused on the image of the slit. The distance between the filament surface (which was filed flat) and the bottom of the image of the slit was measured with the travelling microscope. The card was removed and the image of the slit re-focused at the monochromator entrance slit. A sample (5×10^{-9} g. of lead in 5 μ l. of solution) was placed on the filament, dried and atomized and the absorbance measured. This was repeated twice and the average calculated. The height of the C.F.A.R. was adjusted and the new distance between the filament surface and the bottom of the image of the slit measured. The absorbance measurement was repeated. This procedure was repeated at several heights above the filament and a graph was plotted of absorbance against height above the filament.

Result and Discussion.

The result is shown in Figure 3.9. The concentration of the atomic vapour clearly decreases continuously above the filament. Two reasons are immediately apparent. Firstly the atomic vapour will spread out away from the observed volume as it rises and secondly it will cool rapidly and perhaps condense. Therefore a

Figure 3.9

light beam grazing the filament will give rise to the most intense absorption and this arrangement is used.

Analysis of Pure Aqueous Samples.

Experimental.

A stock solution of lead nitrate (100 p.p.m. Pb) was made from AnalaR grade lead nitrate and distilled, deionised water. Dilute solutions (down to 0.01 p.p.m. Pb) were made up as required. The apparatus was set up as shown in Figure 3.2. The Westinghouse hollow cathode lamp was used without any slits. The amplifier was connected to the Honeywell Visicorder. The lamp current was set at 8 mA. (the recommended maximum current) and the light focused above (grazing) the filament and re-focused at the monochromator entrance slit. The argon flow rate was adjusted to 1 L. per minute. The cooling water was switched on (also at a rate of approximately 1 L. per minute). The monochromator slit was set at just below 0.2 mm. and the wavelength selector at 283.3 nm. The photomultiplier gain was adjusted to give a full scale deflection of the recorder trace for 100% absorption. The sample (1.0 p.p.m. Pb, 5 μ l.) was deposited on the notch at the centre of the filament with an Eppendorf micropipette. A potential difference of 0.5 volts was applied across the filament to evaporate the water. The power was switched off and the variable transformer adjusted to produce 8.2 volts. The recorder was switched on. The power was switched on and then off as soon as the signal was seen to be completed. A card was placed in front of the monochromator slit to obtain a signal to represent 100% absorption.

This procedure was repeated until three consecutive readings were within 10% of their own mean. The peak absorbance was calculated and plotted against mass of lead. The procedure was repeated for several solutions including pure water. The entire experiment was repeated with the wavelength selector set on 217.1 nm. The absorption signal due to a 0.05 p.p.m. lead solution was measured at 283.3 nm. for sixteen replicates.

Results and Discussion.

The calibration curves for both absorption lines are shown in Figure 3.10. The sensitivity of the method (defined as the sample needed to produce a 1% absorption, i.e. an absorbance of 0.00476) is seen from these curves to be 2×10^{-11} g. of lead for the 217.1 nm. absorption line and 5×10^{-11} g. of lead for the 283.3 nm. absorption line.

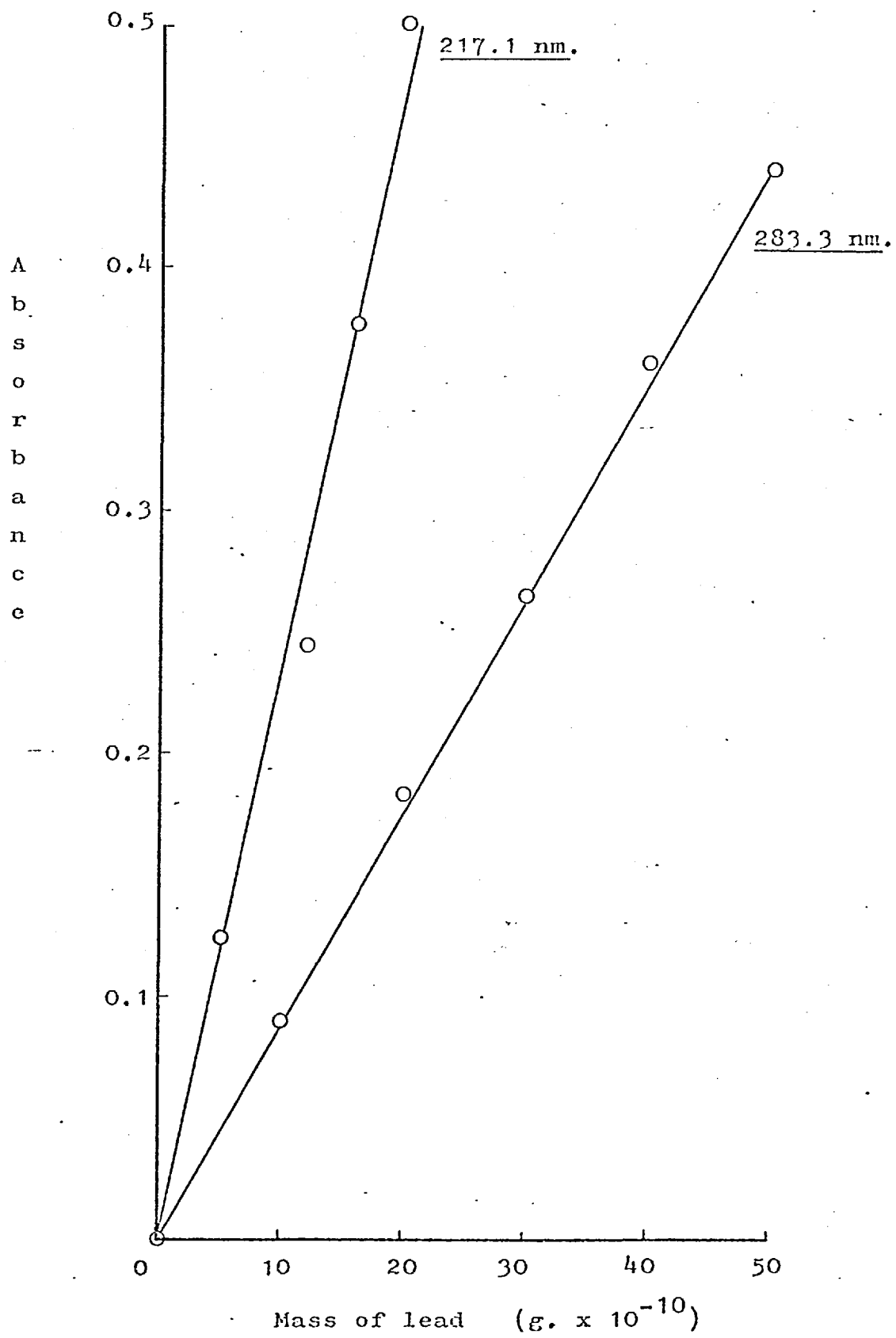
The relative standard deviation of the sixteen replicate signals was 21.7% of the mean signal. The limit of detection (i.e. the sample required to produce a relative standard deviation of 50%) was calculated as

$$\underline{21.7} \times 2.5 \times 10^{-10} \text{ g. of lead, (since } 5 \mu\text{l. of}$$

50

a 0.05 p.p.m. solution contains 2.5×10^{-10} g. Pb), i.e. 1.1×10^{-10} g. of lead. This calculation was valid because the sample used was of the same order of magnitude as the limit of detection. The signals were not converted to absorbance values because at that low level (≈ 0.01 absorbance units) the measured signal is proportional to absorbance.

The detection limit at 217.1 nm. was not

Figure 3.10

measured. Although that line exhibits a greater sensitivity, the emission from the hollow cathode lamp is not so intense as that at 283.3 nm. Hence a high photomultiplier gain must be employed in conjunction with the 217.1 nm. line. This results in a high background noise level and a low limit of detection. The limits of detection of both lines have been measured in another experiment (see below).

Extension of working curve by use of alternative recorder.

As mentioned previously, the substitution of a Servoscribe Potentiometric recorder for the Visicorder results in less background noise and permits an expanded scale to be used. The disadvantage of the pen recorder is its slow response, which sometimes causes the recorded signal to be lower than the true signal. Figure 3.5 shows that the loss of magnitude of the signal due to the slow response of the recorder is negligible below 0.15 on the absorbance scale. An absorbance of 0.15 represents an absorption of approximately 30%. Since the curve in Figure 3.5 was obtained by using a full scale deflection on the pen recorder it may be assumed that any signal which takes up less than 30% of the full scale of the Servoscribe is accurate. If the pen has to travel beyond 30% of the full scale deflection the recorded signal will be less than the true signal.

Experimental.

The Visicorder was replaced by the pen recorder; otherwise the apparatus was unchanged. The wavelength was set on 283.3 nm. The photomultiplier gain was set to produce approximately 100 mV. at 100% transmission and the

recorder sensitivity set to 100 mV. for a full scale deflection. i.e. The difference between 0% and 100% absorption produced a full scale deflection. The recorder sensitivity was then increased to 50 mV. for a full scale deflection. A five microlitre sample of lead nitrate solution (0.1 p.p.m.) was placed on the filament and the solvent evaporated. The recorder was switched on and the sample atomized. The signal was converted to percentage absorption, then to absorbance. This was repeated twice for the same solution. The whole procedure was repeated for four more solutions (down to 0.01 p.p.m. Pb) and a pure water blank. The absorption signals due to the 0.01 p.p.m. of lead solution and then the 0.05 p.p.m. of lead solution were determined for sixteen replicate samples each.

The wavelength selector was adjusted to 217.1 nm. and the absorbance of a 0.03 p.p.m. of lead solution was determined. The absorption signal for a 0.02 p.p.m. of lead solution was measured for sixteen replicate samples.

Results and Discussion.

The calibration curve for the range 0.01 to 0.1 p.p.m. lead solutions, using the 283.3 nm. line is shown in Figure 3.11. The sensitivity of the method was calculated from this graph as 5×10^{-11} g. of Pb.

The 0.03 p.p.m. solution gave an absorbance of 0.03621, at 217.1 nm. Therefore an absorbance of 0.00476 (i.e. 1% absorption) will be given by a 0.004 p.p.m. solution (i.e. 2×10^{-11} g. of lead.)

The detection limits calculated as above from absorption signals of the 0.01 and 0.02 p.p.m. lead

Figure 3.11

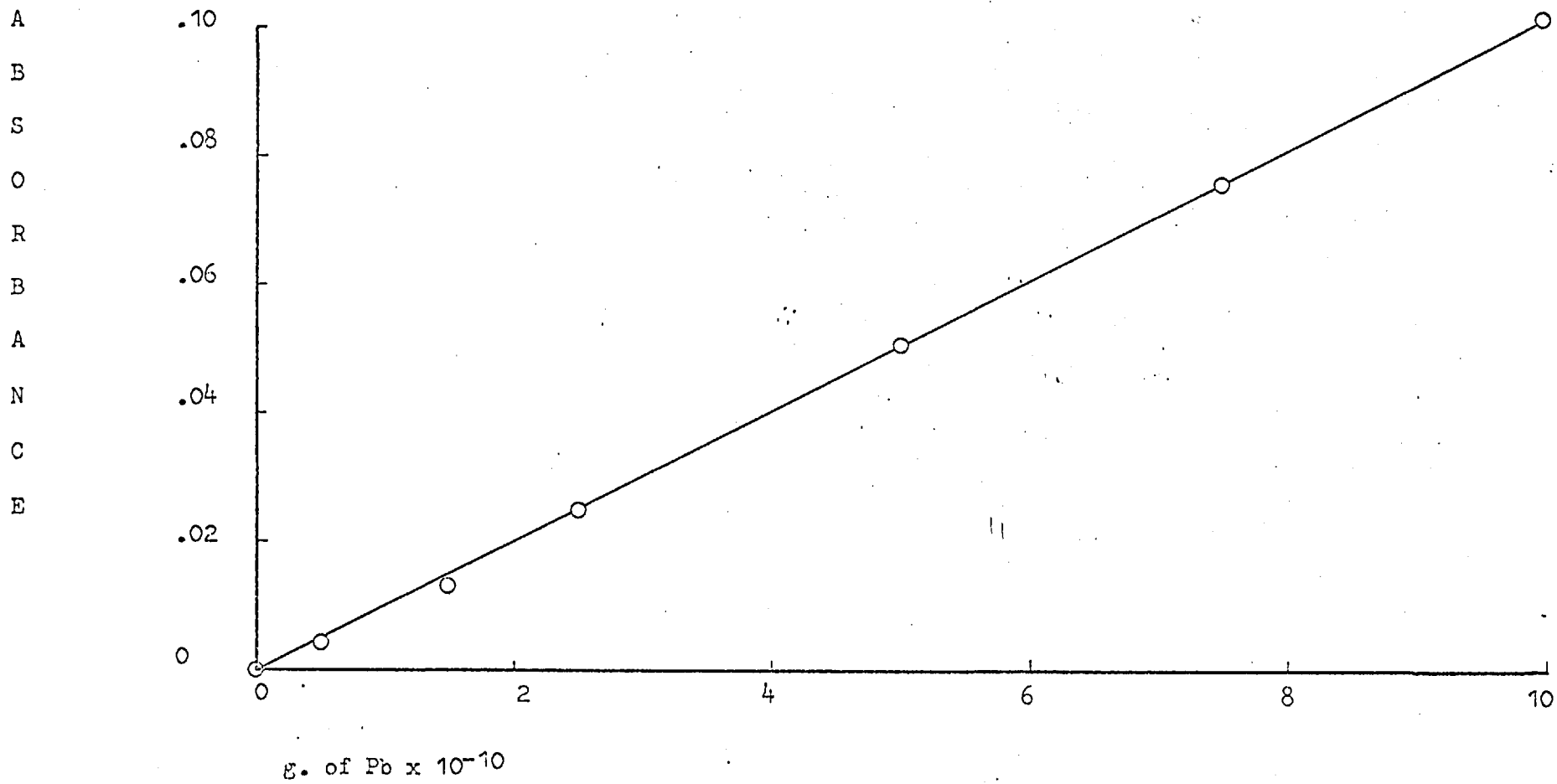


Figure 3.11

solutions were 1.5×10^{-11} g. of lead and 6.3×10^{-11} g. of lead for the 283.3 nm. line and the 217.1 nm. line respectively.

The relative standard deviation of the replicate signals for the 0.05 p.p.m. lead solution was calculated as 7.44%. i.e. the reproducibility of the measurements at about the middle of the working range is 7.44%.

Summary of these results.

Wavelength (nm.)	Visicorder		Servoscribe	
	Sensitivity (g. Pb)	Limit of Detection (g. Pb)	Sensitivity (g. Pb)	Limit of Detection (g. Pb)
217.1	2×10^{-11}		2×10^{-11}	6.3×10^{-11}
283.3	5×10^{-11}	1.1×10^{-10}	5×10^{-11}	1.5×10^{-11}

The 217.1 nm. line is more sensitive than the 283.3 nm. line but the 283.3 nm. line is more useful because the hollow cathode lamp emits much more intensely at this wavelength. The Honeywell Visicorder gives a more accurate measure of the absorption signal than the Servoscribe pen recorder due to its speed of response, but the latter is more useful in practice. A method of determining lead down to 5×10^{-11} g. in pure aqueous solutions has been established.

Chapter Four

The Determination of Lead
on the
Carbon Filament Atom Reservoir
by
Atomic Fluorescence Spectrometry

One of the advantages of atomic fluorescence spectrometry (A.F.S.) over A.A.S. is that the fluorescence signal can be electronically amplified while absorbance cannot, since it is the logarithm of the ratio of two intensities. A severe limitation on this advantage is the fact that any background emission is amplified along with the fluorescence signal. Therefore methods of reducing background emission become particularly useful. The C.F.A.R. has a low background emission in comparison with a conventional flame atom reservoir. Lead exhibits relatively intense atomic fluorescence at 405.8 nm. and 283.3 nm. The emission observed at 283.3 nm. is resonance fluorescence, whereas that observed at 405.8 nm. is direct line fluorescence. The direct line fluorescence is excited by photons whose energy corresponds to a wavelength of 283.3 nm. Emission at both wavelengths has been investigated.

Instrumentation

Almost the same arrangement of instruments is used in atomic fluorescence investigations as was used in the atomic absorption studies. The major differences are as follows:-

i) The hollow cathode lamp is moved through a right angle. This can be done in two planes. The lamp may be placed above the filament or at the side of the filament. In the latter case the filament itself must be rotated through 45° . Otherwise the electrodes supporting the filament obscure the incident radiation. Also an additional silica window must be fitted in the glass

envelope around the cell. For greater convenience the lamp is placed above the filament. Over extended periods of heating the lead may melt, and in this vertical position be lost from the hollow cathode. In either arrangement the light from the hollow cathode lamp is focused to a spot just above the filament.

ii) In A.F.S. the purpose of the monochromator is the isolation of the fluorescence signal from the general background radiation. (c.f. In A.A.S. the monochromator isolates the absorption line from other radiation emitted from the hollow cathode lamp). Since the background emission of the C.F.A.R. is low, the maximum monochromator slit width was used in all A.F.S. studies.

iii) A metal tube (20 mm. long by 6 mm. internal diameter) held in sheet of card is placed between the C.F.A.R. and the lens leading to the monochromator. This simple device shields the monochromator slit from the incandescence of the filament and from any light reflected from the hollow cathode via the filament to the monochromator.

Determination of lead by A.F.S.

Experimental.

Lead nitrate solution was prepared as described previously and the apparatus set up as described above. The optimum argon flow rate and potential difference across the filament were determined in the same way as in the A.A.S. study, and the same results were obtained. (i.e. 1 l. per minute of argon and 8.2 volts). The monochromator was set at 283.3 nm., the photomultiplier gain

set to a maximum and the Honeywell Visicorder used. A 5 μ l. sample of lead nitrate solution (2.0 p.p.m. Pb) was placed on the filament and dried by applying 0.5 volts. The recorder was started and the sample atomized. This was repeated twice. The whole procedure was repeated for solutions down to 0.1 p.p.m. Pb and a water blank. The experiment was repeated with the wavelength selector set at 405.8 nm.

The Visicorder was replaced by the pen recorder and the experiment repeated, at 405.8 nm., with solutions down to 0.01 p.p.m. Pb. The fluorescence signals at 405.8 nm. were measured for sixteen replicate samples of a 0.003 p.p.m. lead solution and also for a 0.001 p.p.m. lead solution.

Results and Discussion.

The fluorescence signal was taken to be the displacement on the recorder chart in arbitrary units.

The calibration graphs over the relatively wide range measured with the Visicorder (2.0 - 0.1 p.p.m. of lead) are shown in Figure 4.1. The 283.3 nm. line is more curved than the 405.8 nm. line. This can be explained in terms of self-absorption. Since the 405.8 nm. line is not a resonance line it will not be absorbed by the atomic vapour. The low range calibration graph is shown in Figure 4.2.

The detection limits calculated from the 0.003 p.p.m. lead (i.e. 1.5×10^{-11} g. Pb) and the 0.001 p.p.m. lead (i.e. 5×10^{-12} g. Pb) solutions are 6.34×10^{-12} g. Pb and 5.96×10^{-12} g. Pb respectively.

Figure 4.1

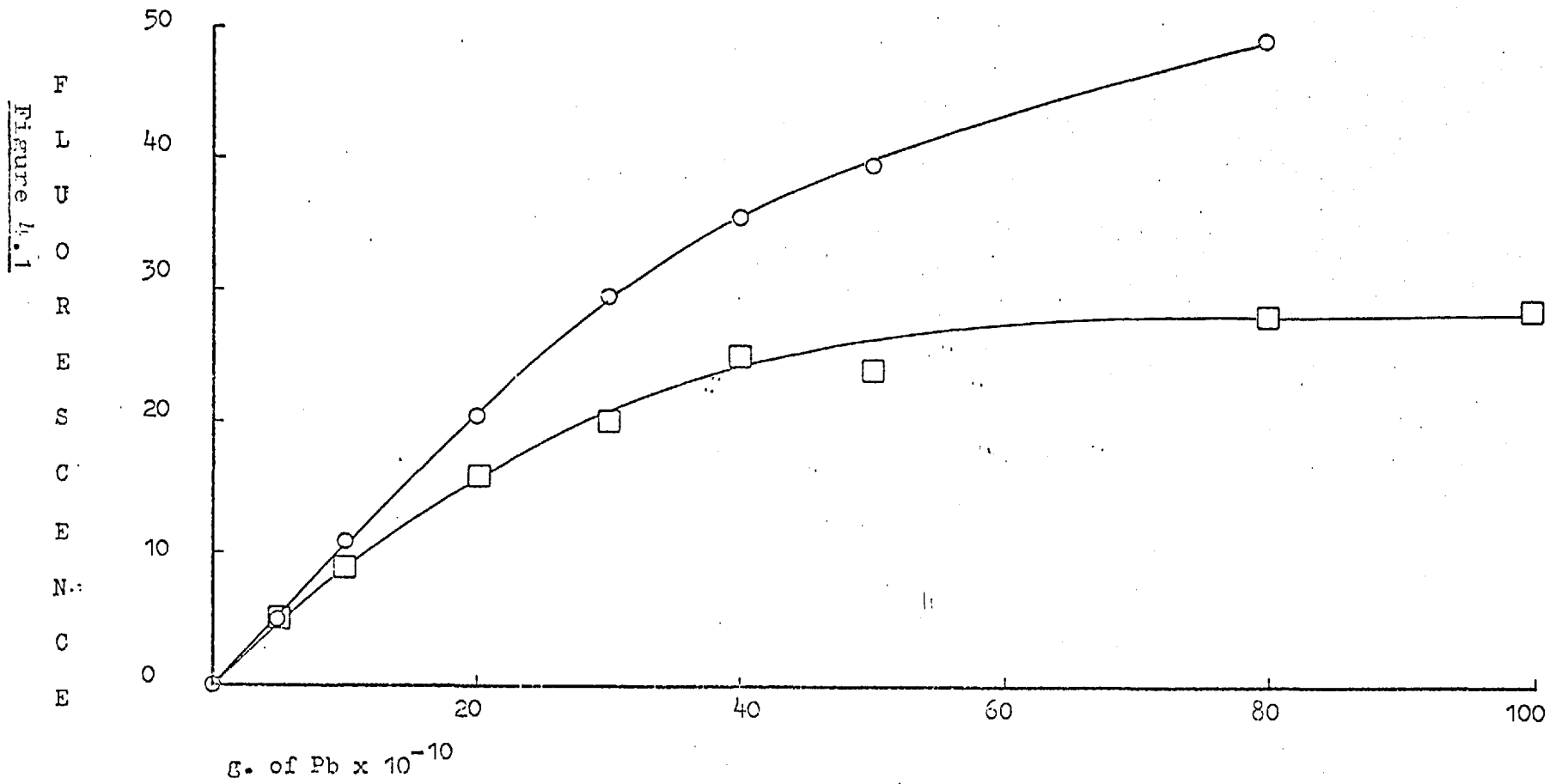
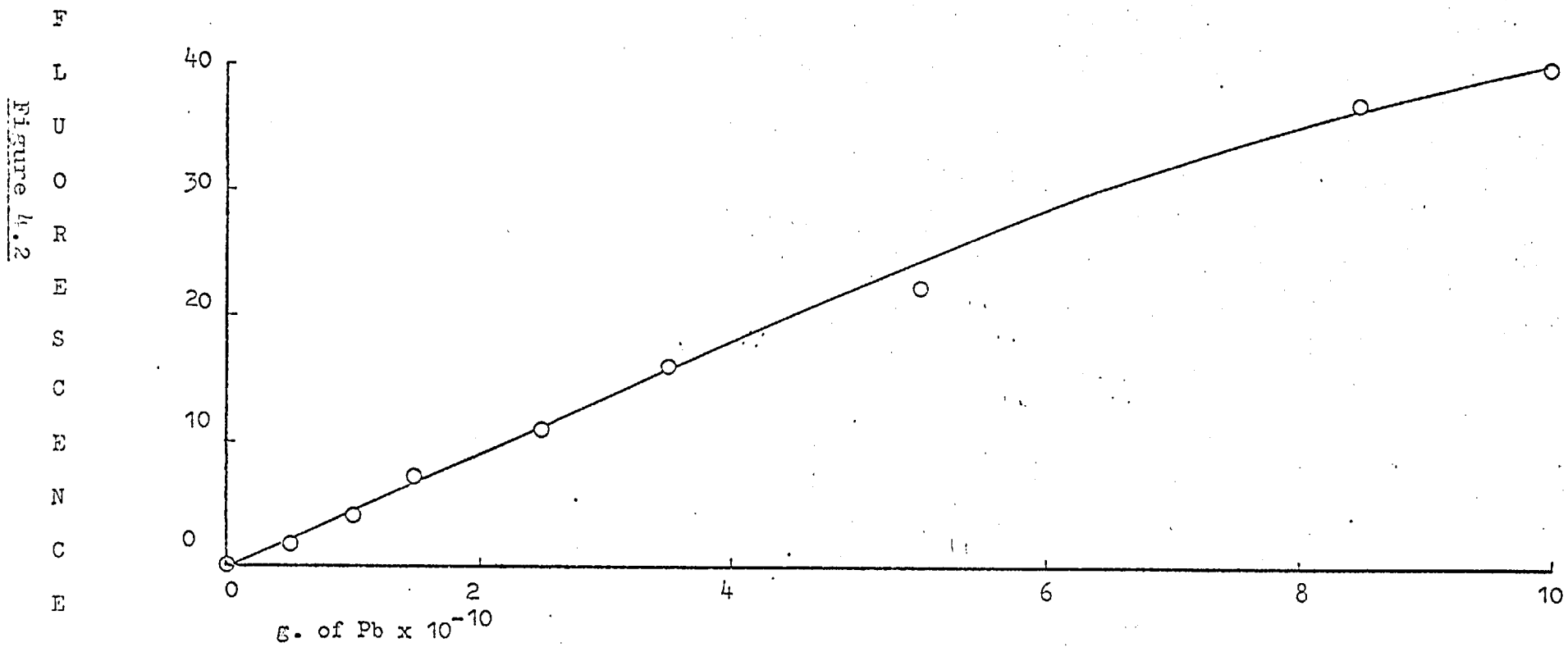


Figure 4.2



Conclusion.

Lead can be determined by A.F.S. from pure aqueous solution with a detection limit of 6×10^{-12} g. Pb (c.f. A.A.S.; 1.5×10^{-11} g. Pb). In both A.F.S. and A.A.S. the smallest sample for a practical analysis is about 5×10^{-11} g. Pb.

Chapter Five

Interference Studies
with the
Carbon Filament Atom Reservoir

The low probability of overlap between atomic absorption lines ensures that spectral interference in A.A.S. or A.F.S. is very rare. Those cases in which the presence of one element affects the A.A. or A.F. signal due to another element are usually examples of a chemical or physical interaction between the elements which affects the free atom population. This sort of interference is more liable to occur with the C.F.A.R. than with a flame or furnace atom reservoir because the temperature of the atomic vapour drops above the filament.

Blood contains a relatively high concentration of sodium and potassium ions (approximately 4000 p.p.m. c.f. approximately 0.1 p.p.m. of lead). Since the ultimate aim of this work was to determine lead in blood, the effects of these two metals on the A.A. and A.F. signals of lead were investigated.

Experimental.

Lead nitrate solutions were prepared as described previously. Sodium nitrate and potassium nitrate solutions were made up from AnalaR grade sodium and potassium nitrates and distilled, de-ionised water. Solutions containing 2 p.p.m. of lead with 10 fold, 100 fold and 1000 fold excess sodium were prepared by dissolving sodium nitrate in lead nitrate solutions and diluting. Corresponding solutions with excess potassium were similarly prepared. Solutions containing 0.1 p.p.m. lead with the same ratios of sodium and potassium were also prepared. The apparatus was set up for A.F.S. as described previously, and the atomic fluorescence signals

due to five microlitre samples of each solution measured repeatedly at 405.8 nm.

Results and Discussion.

The pure sodium nitrate and potassium nitrate solutions gave no measureable fluorescence signal.

Interference, I_n , is defined by:-

$$I_n = \frac{S_p - S_I}{S_p} \times 100 \% \quad \underline{5.1}$$

where S_p is the signal from the pure sample and S_I is the signal from the sample containing foreign ions.

The pure lead solutions gave reproducible signals. Fluorescence signals of considerable irreproducibility were observed for the solutions containing lead and sodium (or potassium). The interference due to the sodium (or potassium) was calculated from the average of three or four signals. The results are summarized in Table 5.1.

	Interference (%)	
	2.0 p.p.m. Pb	0.1 p.p.m. Pb
1000 fold excess Na	75	45
1000 fold excess K	68	33.5
100 fold excess Na	23	16
100 fold excess K	63	14
10 fold excess Na	10	0
10 fold excess K	24	9

Table 5.1

Both metals cause a reduction of the fluorescence signal due to lead. The magnitude of this reduction

was related to the excess of interfering metal over lead, and to the absolute concentrations of the solution.

Height above the Filament.

If the interference is due to chemical or physical interaction between the atoms, the degree of interference should be least when the atomic vapour is hottest, i.e. when it first leaves the filament.

Experimental.

Solutions containing 0.5 p.p.m. of lead and a mixture of lead (0.5 p.p.m.) and sodium (4000 p.p.m.) were prepared. The apparatus was set up for A.A.S. with a 0.5 mm. slit placed in front of the hollow cathode lamp and focused above the filament, as described previously. Absorption measurements due to five microlitre samples of both solutions were made, with the slit focused at various heights above the filament. These heights were measured with a travelling microscope.

Results and Discussion.

The results of the experiment are shown in Table 5.2. Each absorbance is an average of three measurements.

The figures indicate both the great irreproducibility of the interference and the general trend that the interference is least immediately above the filament.

Selective Volatilisation of the Elements from the Filament.

If the interfering elements could be removed from the filament, and the lead left behind, by controlled

Height above filament (mm.)	Absorbance due to pure lead solution	Absorbance due to mixture	Interference (%)
0.00	0.7321	0.3420	53
0.18	0.7101	0.3420	58
0.50	0.6149	0.2776	55
0.66	0.5983	0.2310	61.5
0.88	0.5334	0.2404	55
1.08	0.5110	0.2551	50
1.38	0.4712	0.1970	58
1.64	0.4446	0.1263	71.5
2.08	0.2748	0.1129	59
3.06	0.1698	0.0584	65.5

Table 5.2

heating, the interference problem would be solved.

Experimental.

Solutions containing 2.0 p.p.m. of lead, 200 p.p.m. of sodium and 2.0 p.p.m. of lead plus 200 p.p.m. of sodium were prepared. The apparatus was set up for A.F.S. and the fluorescence signal due to a five microlitre sample of pure lead solution was measured. Another sample of pure lead solution was placed on the filament and dried. The variable transformer was set to produce a potential of 1.8 volts across the filament and the power switched on for one minute. The variable transformer was re-adjusted to 8.2 volts and the

fluorescence signal measured. This procedure was repeated several times, increasing the pre-heating voltage by 0.6 volts each time, until some lead was lost during the minute of heating.

The lead lamp was replaced with a sodium hollow cathode lamp and the experiment repeated with the sodium solution.

Result.

No lead was lost from the filament by applying a potential of 3.0 volts or less for one minute, but some was lost when a higher potential was applied. The sodium was lost from the filament when a potential of 2.4 volts was applied.

Experimental.

The lead hollow cathode lamp was replaced in the apparatus. A sample of the mixed solution was placed on the filament, dried and heated for one minute at a potential of 2.8 volts. The variable transformer was reset at 8.2 volts and the fluorescence signal measured. This was repeated several times. Each time the potential for the one minute heating was reduced by 0.12 volts.

Results and Discussion.

Some lead was lost from the mixture on the filament during the one minute heating process even when a potential of less than 2.4 volts was applied.

It appears to be impossible to separate the metals in this manner.

Chapter Six

Integrated Absorption Measurements_
with the
Carbon Filament Atom Reservoir

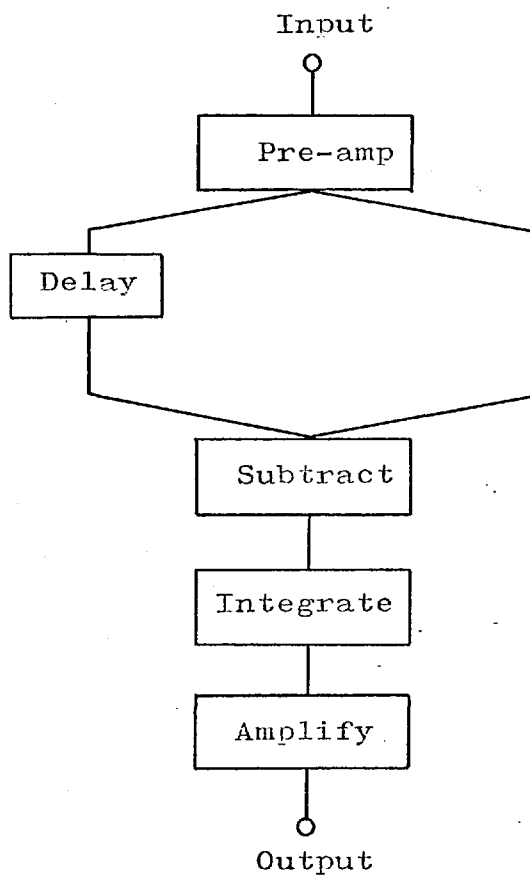
Chapters Three, Four and Five have been concerned with the measurement of peak atomic absorption or atomic fluorescence signals. The integrated absorbance or fluorescence can also be related to the mass of the analyte. (see Equation 2.3)

$$\int_0^{\tau_3} x \cdot dt \propto N_0 \quad \underline{2.3}$$

This integral is independent of τ_1 , the duration of the atomization process.

An electronic integrator designed by R. Stevens,⁽¹¹⁹⁾ formerly a member of the Analytical Chemistry Department at Imperial College, and built by D. Alger (a member of the same department), has been used to measure the integrated absorption signal due to lead samples atomized from the C.F.A.R. This device integrates not the absorbance, but the change in output from the photomultiplier tube. Figure 6.1 is a block diagram of the integrator. If a constant signal is fed into the input this is first amplified, then bisected. Half the signal is delayed and half is fed directly through the subtract unit. When the delayed half reaches the subtract unit it is subtracted from the original half to give a zero resultant. Thus a steady input produces a zero output. If the input signal suddenly decreases and then returns to normal, the change in signal is delayed then subtracted from the normal signal. The resultant is then integrated with respect to time, amplified and fed out to a recorder. The change in input may be very short lived, but the output is not and can be recorded on a slow recorder. The duration of the delay is of great importance and therefore the device is fitted with a choice of three delay periods.

Figure 6.1



If the integrator output is designated Q , then

$$Q = a \int_0^{\tau_3} (I_0 - I) dt \quad \underline{6.1}$$

where a is a constant.

but

$$I = I_0 \exp(-k_v l) \quad \underline{1.2}$$

Therefore

$$Q = a \cdot I_0 \int_0^{\tau_3} (1 - e^{-k_v l}) dt \quad \underline{6.2}$$

If $k_v l$ is small,

$$e^{-k_v l} \simeq 1 - k_v l \quad \underline{6.3}$$

Therefore

$$Q = a \cdot I_0 \int_0^{\tau_3} k_v l \cdot dt \quad \underline{6.4}$$

but

$$k_v l \propto N \quad \underline{1.3}$$

Therefore

$$Q \propto \int_0^{\tau_3} N \cdot dt \quad \underline{6.5}$$

But

$$\int_0^{\tau_3} N \cdot dt \simeq N_0 \tau_2 \quad \underline{2.1}$$

Therefore

$$Q \propto N_0 \tau_2 \quad \underline{6.6}$$

i. e.

The integrator output is directly proportional to the total mass of analyte for low values of $k_v l$ and constant τ_2 , and should be independent of τ_1 .

The Integrated Absorption Signal and τ_1 .

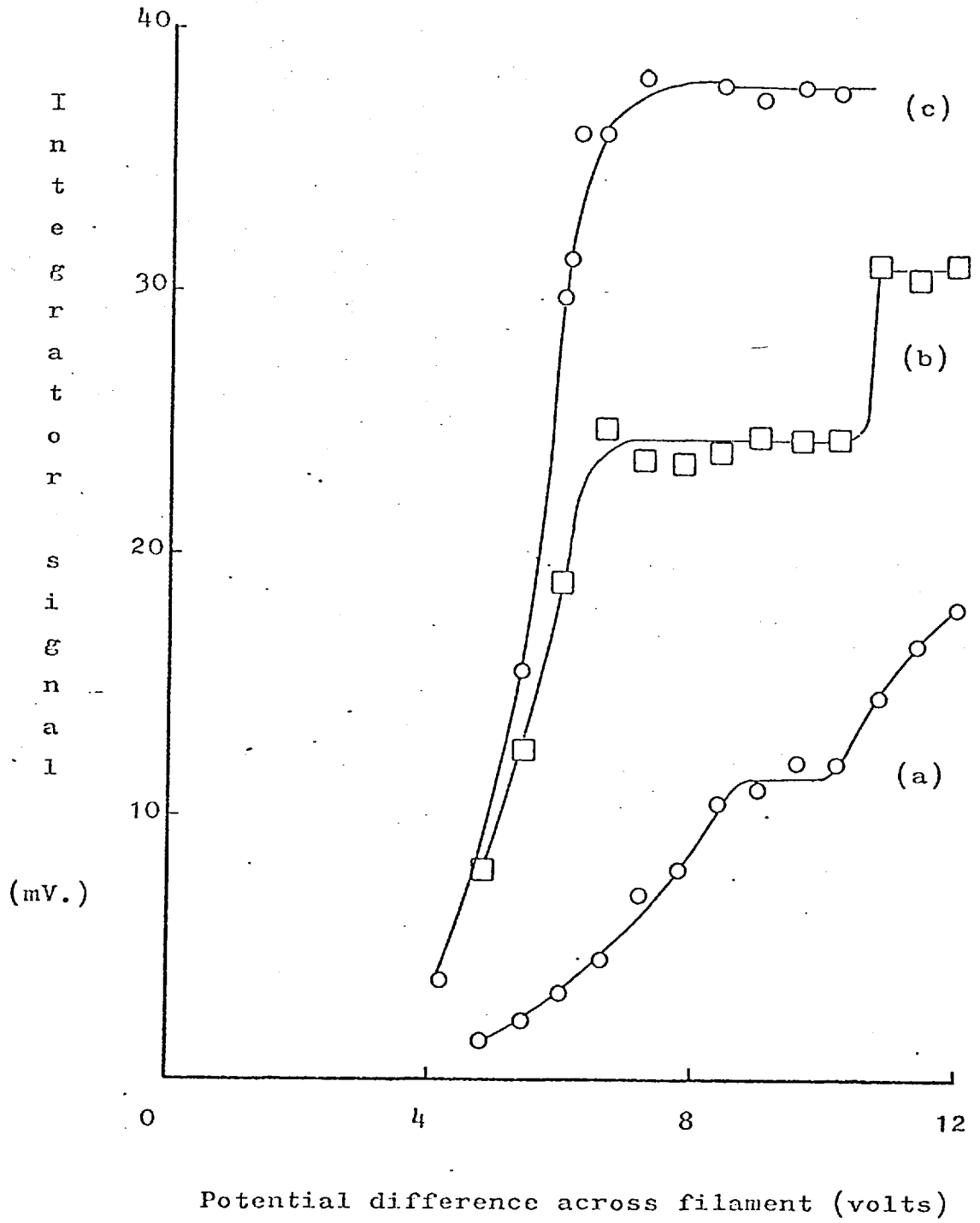
Experimental.

Solutions of lead nitrate were prepared as before. The apparatus was set up for A.A.S. with the photomultiplier tube connected directly to the integrator. The power supply to the hollow cathode lamp was not modulated. The integrated absorption due to five microlitres of a solution containing 0.1 p.p.m. of lead was measured using an atomization potential of 4.2 volts and the shortest of the delay periods on the integrator. This was repeated several times at increasing atomization potentials. The experiment was then repeated using the two other delay periods on the integrator.

Results and Discussion.

Figure 6.2 shows that over a certain range of applied potentials, and therefore of τ_1 values the integrated signal is independent of the potential. The three curves (a), (b) and (c) represent the three different delay periods of the integrator. Curve (a) was

Figure 6.2



obtained using the shortest delay periods, curve (c) the longest. The steeply sloped part of the curves, before the plateau, can be explained by the relatively long duration of the signal with respect to the integrator delay time. Thus the sloping section extends to the highest potential, for the curve obtained using the shortest delay time. The sloping sections of curves (a) and (b), beyond the plateau are difficult to explain. Curve (c) was not investigated beyond 10.2 volts since at higher potentials the integrator did not resolve the absorption signal from the incandescence of the filament.

The delay period was set at the longest value and atomization potential of 8.4 volts was used for the following experiments.

Calibration Curve, Detection Limit and Reproducibility.

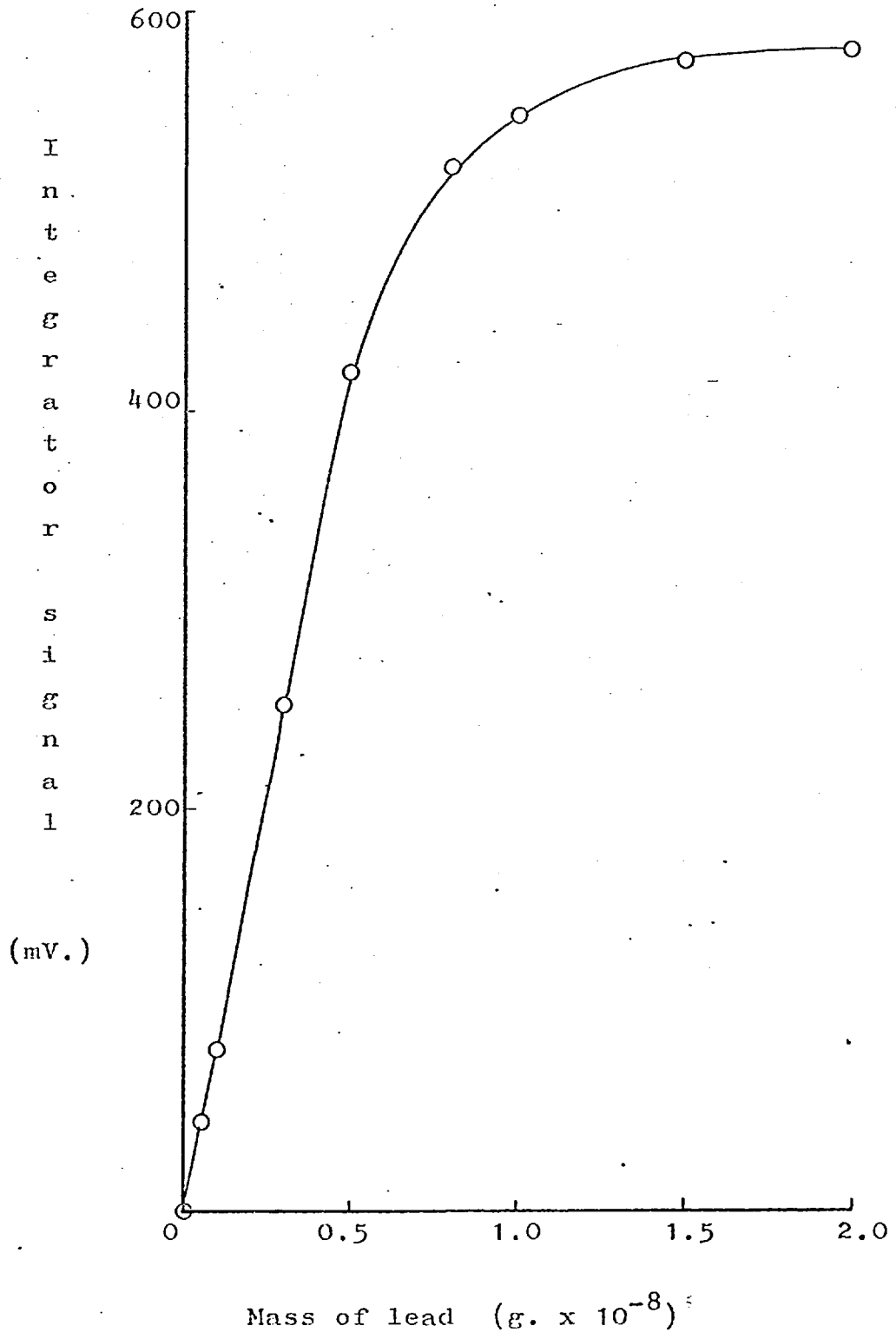
Experimental.

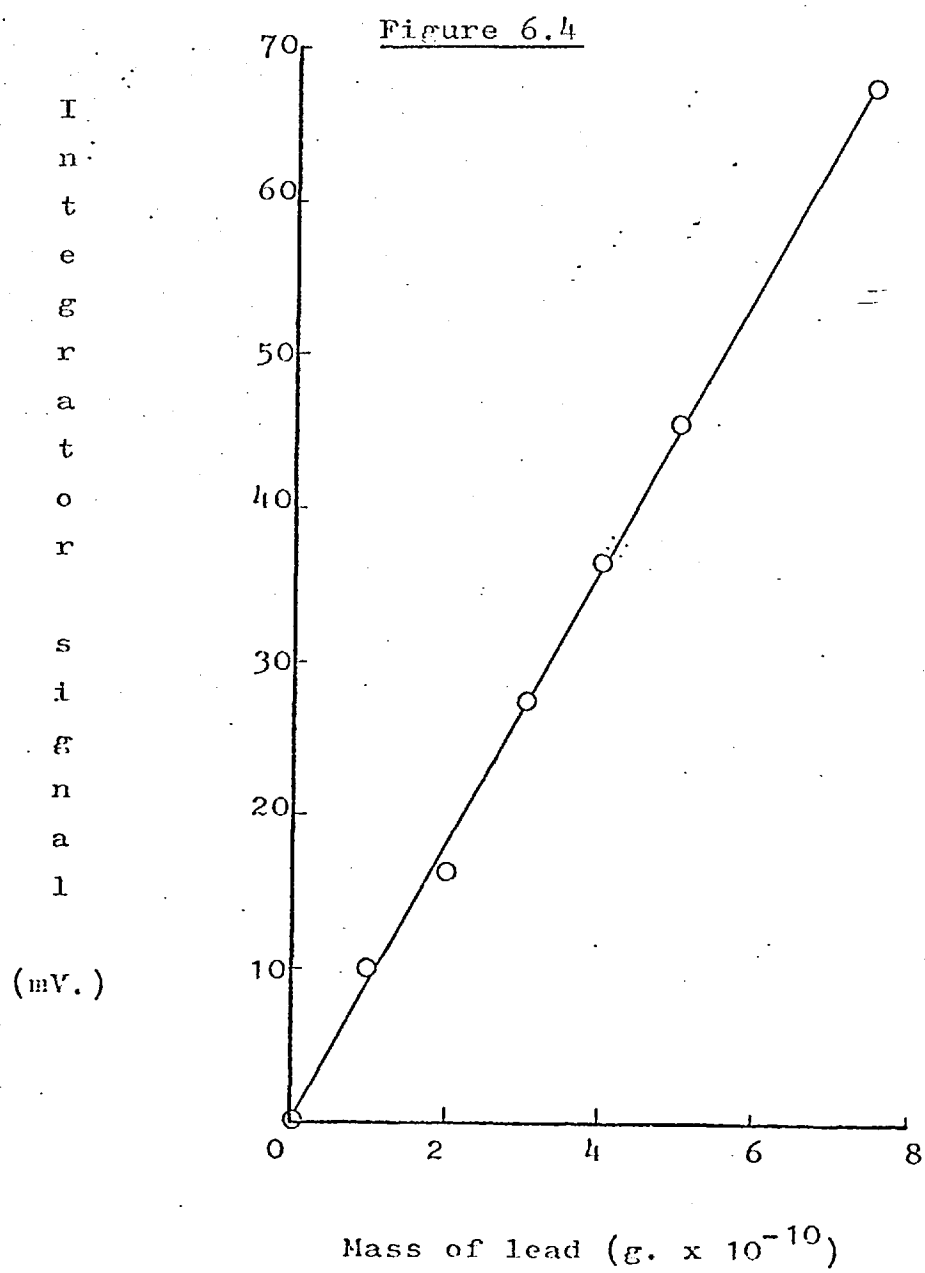
The integrated absorption signals due to five microlitre samples of a series of solutions of lead nitrate ranging from 0.02 p.p.m. of lead to 4.0 p.p.m. of lead were measured. The signals due to solutions containing 0.05 p.p.m. of lead and 0.005 p.p.m. of lead were measured sixteen times each.

Results and Discussion.

Figure 6.3 is the calibration graph over a wide range and Figure 6.4 over a small range. The curvature of Figure 6.3 can be explained by the fact that Equation 6.6 is valid only for small absorption signals.

The relative standard deviation of the signal due to the 0.05 p.p.m. of lead solution (2.5×10^{-10} g. Pb)

Figure 6.3



was 5.3%. (c.f. 7.4% without the integrator). The detection limit calculated (as before) from the replicate signals due to the solution containing 0.005 p.p.m. of lead (2.5×10^{-11} g. Pb) was 2.5×10^{-11} g. Pb. (c.f. 1.5×10^{-11} g. Pb : best figure without the integrator).

The integrated absorption signal was found to be independent of the atomization potential over a limited range, as predicted. The relative standard deviation of the signal due to a sample from about the middle of the working range is a little less than that obtained without the integrator. (5.3% vs. 7.4%). The detection limit obtained using the integrator is a little higher than that obtained without the integrator. (2.5×10^{-11} g. Pb vs. 1.5×10^{-11} g. Pb).

Chapter Seven

The Determination of Lead in Blood

Lead Poisoning.

The danger of lead poisoning has been discovered, forgotten and re-discovered throughout human history. Recently the mechanism of lead poisoning has been a subject of medical research. The exact details of the action of lead in the body are not yet understood, but three main effects are known. Firstly, lead inhibits the action of δ -aminolevulinic acid dehydrase, an enzyme involved in the biosynthesis of haem and hence of haemoglobin. This results in an anaemic condition as long as the excessive lead remains in the body. Secondly, lead damages the kidneys in such a manner that essential substances, e.g. phosphates, are excreted excessively. This effect also lasts while excess lead remains in the body. Thirdly, permanent damage to brain cells can be caused by lead poisoning. The extent to which lead poisoning is responsible for mental sub-normality in children is not known, but is suspected by some workers⁽¹²⁰⁾ to be considerable. The treatment of lead poisoning is simple and effective. Lead chelating agents, e.g. E.D.T.A., penicillamine, are taken orally and the lead is rapidly excreted. The problem associated with lead poisoning is early diagnosis. The medical symptoms of the disease are non-specific. Measurement of the concentration of lead in the blood or soft tissue is the only certain test. Until recently the smallest blood sample which could be used for a lead analysis was 10g.⁽¹²⁰⁾ Delves⁽³²⁾ has recently developed a method of lead analysis which requires a very small volume of blood.

The concentration of lead in the blood of a

healthy adult is approximately 0.1 p.p.m. of lead. A concentration of 2 p.p.m. of lead in the blood would indicate a very sick person. These concentrations come within the working range of the method of determining lead by atomic spectrometry using the C.F.A.R. previously described. Therefore the method was adapted to deal with blood samples instead of pure aqueous samples.

All blood samples were supplied by the Hospital for Sick Children, Great Ormond Street, London.

The blood was haemolized, i.e. the cell walls were ruptured, so that a homogenous liquid was produced, by repeated freezing and melting of the blood before all experiments.

Preliminary Experiment.

The apparatus was set up for A.A.S. A five microlitre blood sample was transferred to the filament via an Eppendorf-Marburg micropipette and a potential of 0.5 volts was applied to dry the sample. The sample was then atomized by application of an 8.2 volt potential, and the absorption signal recorded.

Result and Discussion.

A 100% absorption signal was recorded. The signal did not return to zero absorption. A cloud of smoke was seen to form on the filament when the 8.2 volt potential was applied and a charred residue was left on the filament, partially blocking the light beam. It seems reasonable to suppose that the organic material in the blood gives rise to the smoke and the charred residue. If the atomic absorption signal due to the

lead is to be clearly observed this organic material must be removed from the sample before the lead is atomized.

Controlled Heating of Blood.

Experimental.

A blood sample was placed on the filament and dried by application of a potential of 0.5 volts. A potential of 2.0 volts was applied for one minute. The sample was then atomized by a potential of 8.2 volts and the absorption signal recorded. The procedure was repeated several times, increasing the potential applied for one minute by 0.12 volts each time, up to 3.92 volts.

Results and Discussion.

A puff of smoke accompanied the atomization process even when the maximum ashing potential was used. Again the atomic absorption signal due to the lead was partially or completely obscured by the signal from the smoke. (The smoke gave rise to a much broader signal than that due to the atomic lead.) Since pure lead nitrate is lost from the filament by heating for one minute at just over 3.0 volts it seems likely that some of the lead will be lost when a potential of almost 4.0 volts is applied. Clearly simple heating of the sample is not sufficient to separate the organic material from the lead. Three chemical agents have been used to attempt to break up the organic material in the blood.

Chemical Breakdown of Blood.

Concentrated perchloric and nitric acids were first considered. Both acids were found to react with

the lead as well as the blood. The effects of these two acids on the absorption signals due to pure lead nitrate samples were investigated. In both cases addition of the acid resulted in lead being lost from the filament at very low temperatures, e.g. by heating for one minute at a potential of 1.0 volt.

Hydrogen peroxide was next considered. First the effect of hydrogen peroxide on pure lead nitrate samples was investigated. Addition of up to fifteen microlitres of 100-volume hydrogen peroxide (Hopkin and Williams, Atomic Absorption Grade) to the dried lead nitrate sample on the filament had no effect on either the absorption signal due to the lead or the minimum temperature at which the lead was lost from the filament. The action of hydrogen peroxide on blood was investigated. A five microlitre drop of 100-volume hydrogen peroxide was added to an equal drop of blood on the filament. A vigorous reaction ensued, causing an expansion of the sample along the filament and upwards. When the reaction ceased a 'froth' was spread along the filament and sometimes fell off. Subsequent heating for one minute by applying a potential of up to 4.0 volts failed to remove all the organic material, but reduced the quantity considerably. The absorption signal due to smoke (measured at 280.3 nm., which is not a lead absorption line, but is strongly emitted by the lead hollow cathode lamp) was reduced by this treatment.

Attempts to reduce the spreading and frothing of the blood by using diluted hydrogen peroxide were only partially successful. The blood was dried before adding

the hydrogen peroxide in another attempt to prevent spreading and frothing but this reduced the effectiveness of the hydrogen peroxide. Dilution of the blood instead of the hydrogen peroxide seemed an apt way to reduce the absorption signal due to smoke and perhaps avoid the problem of spreading and frothing. Since healthy blood contains approximately 0.1 p.p.m. and a solution containing roughly 0.01 p.p.m. of lead is the most dilute five microlitre sample which can be analysed, a dilution of one part blood plus ten parts water was used.

Experimental.

The apparatus was set up for A.A.S. with the pen recorder, as previously described. An Eppendorf-Marburg micropipette was used to measure 200 μ l. of distilled de-ionised water into a small beaker (5 ml.) Another Eppendorf-Marburg micropipette was used to add 20 μ l. of haemolised blood to the water. The liquids were mixed by shaking the beaker. A 5 μ l. sample of the diluted blood was transferred to the filament via a third Eppendorf-Marburg micropipette. A potential of 0.72 volts was applied. Hydrogen peroxide was immediately added to the sample. The 5 μ l. micropipette was used, but only about half the five microlitres of hydrogen peroxide was delivered, to prevent excessive frothing. When the sample was reduced to a white ash the power was switched off. A potential of 1.5 volts was applied for one minute to remove the organic material and then the sample was atomized and the absorption measured at 280.3 nm. (the non-lead absorption line) to estimate the non-atomic

absorption due to the remaining organic material. This procedure was repeated several times, increasing the potential applied for one minute by 0.12 volts each time.

Result and Discussion.

The absorption signal due to the organic material was reduced by increasing the applied potential to 2.28 volts. By heating at this voltage for one minute the non-atomic absorption signal was reduced to 0.7% absorption, and was reproducible. Increasing the voltage did not reduce this signal.

A potential of 2.28 volts for one minute did not remove pure lead nitrate from the filament but did cause lead nitrate in the presence of sodium nitrate to be lost. The chemical environment in the case of blood is so different from the cases of pure lead nitrate and mixed lead and sodium nitrates, that one cannot predict whether or not the lead will be lost from blood.

Experimental.

The preceding experiment was repeated with a blood sample whose lead content was known (0.66 p.p.m.). A potential of 2.28 volts was used for the one minute heating. The absorption signals at 283.3 nm. and 280.3 nm. were measured.

Result and Discussion.

The absorption at 280.3 nm. was subtracted from that measured at 283.3 nm. and the signal converted to absorbance. This gave the figure of 0.0269 absorbance units. An equivalent pure lead nitrate sample (3×10^{-10} g. Pb) gave rise to a signal of 0.03 absorbance units (see Chapter Three). This suggests that the lead may not be

lost from the blood under these conditions.

When the experiment was repeated the absorption signal at 283.3 nm. (but not at 280.3 nm.) was very low and remained low for subsequent repeats. After various other unsuccessful approaches it was discovered that the absorption signal due to a pure lead nitrate solution was also much reduced if a blood sample had been atomized from the filament immediately before. This reduction of the atomic absorption signal was avoided by scraping clean the filament surface with a sharp edge, before applying the sample. The absorption due to the blood sample returned to 0.0269 absorbance units when this procedure was adopted.

Calibration Graph and Reproducibility.

Diluted samples were prepared from five blood samples with a known lead content. The absorption signals due to each sample at 283.3 nm. and at 280.3 nm. were measured three times for each sample at each wavelength, using the following procedure:-

1. A five microlitre sample was placed on the filament.
2. A potential of 0.72 volts was applied and two microlitres of hydrogen peroxide were immediately added to the sample.
3. When the sample had been reduced to ash the power was switched off and the filament allowed to cool for two minutes.
4. A potential of 2.28 volts was applied for one minute.
5. The sample was atomized at 8.2 volts and the absorption signal recorded.

6. The filament surface was scraped with a razor, heated at 8.2 volts again and then allowed to cool for two minutes before addition of the next sample.

Sixteen replicate measurements were made using one of the samples.

Results and Discussion.

Whole blood sample number	Lead content before dilution (p.p.m.)	Lead content after dilution	
		(p.p.m.)	(10^{-10} g.) [*]
I	0.22	0.020	1.00
II	0.40	0.036	1.80
III	0.66	0.060	3.00
IV	0.87	0.079	3.95
V	0.105	0.095	4.73

* Refers to a five micro-litre sample.

Table 7.1a.

Figure 7.1 (a) is the calibration graph drawn from the figures shown in Tables 7.1a and b. Figure 7.1(b) is the calibration graph obtained from pure aqueous samples (see also Figure 3.11). If Figure 3.11 is used as a working curve to calculate the lead content of unknown blood samples the calculated level would be approximately 11% too high.

The relative standard deviation of the absorp-

Sample number	Average Absorption (%)		Difference (%)	Absorbance
	at 283.3 nm.	at 280.3 nm.		
I	2.62	0.68	1.94	0.0086
II	4.35	"	3.67	0.0162
III	6.68	"	6.00	0.0269
IV	8.57	"	7.89	0.0356
V	9.88	"	9.20	0.0419

Table 7.1b.

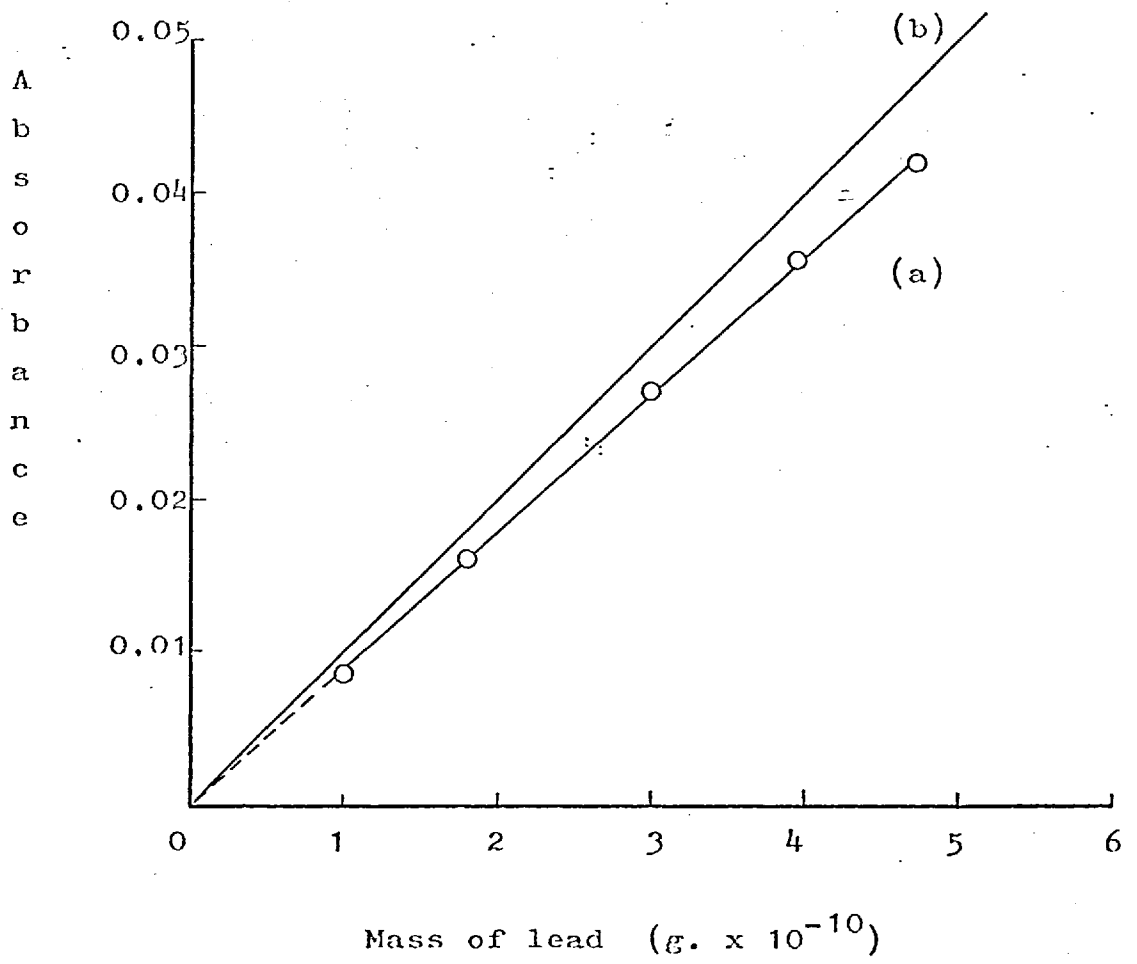
tion signal due to Sample V was 7.16%. (c.f. 7.4% for pure aqueous lead samples.)

Method of Standard Additions.

A preliminary investigation into the use of standard additions for determining lead in blood suggested that the method would be unsuitable. Further attempts to use the method were not made. The preliminary experiment is described here.

Experimental.

A blood sample containing approximately 1.0 p.p.m. Pb was diluted with water as described above and also with a lead nitrate solution containing 0.06 p.p.m. Pb. Thus the diluted lead samples contained approximately 0.09 p.p.m. Pb and 0.15 p.p.m. Pb respectively. The atomic absorption signals due to these samples were measured as described above.

Figure 7.1

Result and Discussion.

The sample containing approximately 0.09 p.p.m. Pb gave rise to an absorption signal at 283.3 nm., of 19%. The sample containing approximately 0.15 p.p.m. Pb gave rise to an absorption signal at 283.3 nm. of 17%. Both samples gave a signal of approximately 0.7% absorption at 280.3 nm.

Clearly the added lead did not add to the absorption signal. Presumably therefore it was lost from the filament during the one minute heating period. It was noted earlier that lead nitrate in the presence of sodium nitrate was lost from the filament by heating for one minute at lower potentials than the 2.28 volts employed here. In the light of this, it is not the loss of the added lead, but the retention of the lead originally in blood which is surprising.

No attempt to explain the loss of lead nitrate in the presence of sodium nitrate was made in Chapter Five, but the first approach to be considered involves postulating the formation of mixed crystals of lead, sodium and nitrate ions. If the lead is firmly bound to some organic chelate (as may be the case in blood) then the mixed crystals could not form. This tentative explanation is pure speculation. No systematic investigation of the problem has been attempted.

Conclusion.

The lead content of blood can be determined by A.A.S. with the C.F.A.R. provided a set of standard blood samples is available. If an error of the order

of 10% can be tolerated then aqueous lead nitrate standards can be used. The method of standard additions to the unknown blood sample appears to be unsuitable.

References

1. B.V.L'vov, 'Atomic Absorption Spectrochemical Analysis', Hilger, 1970.
2. A.Mitchell and M.Zemansky, 'Resonance Radiation and Excited Atoms', Cambridge, 1934.
3. A.Walsh, Spectrochim. Acta, 1955, 7, 108.
4. E.L.Nichols and H.L.Howes, Phys. Rev., 1924, 23, 472.
5. A.L.Boers, C.Th.J.Alkemade and J.A.Smit, Physica, 1956, 22, 258.
6. J.W.Robinson, Anal. Chim. Acta, 1961, 24, 254.
7. C.Th.J.Alkemade, 'Excitation and Related Phenomena in Flames', p.143, Proceedings, Xth Colloquium Spectroscopium Internationale, Washington D.C., 1963.
8. D.J.Winefordner and T.J.Vickers, Anal. Chem., 1964, 36, 161.
9. D.J.Winefordner and R.A.Staab, Anal. Chem., 1964, 36, 165.
10. Idem., ibid., 1964, 36, 1367.
11. J.M.Mansfield, D.J.Winefordner and C.Veillon, ibid., 1965, 37, 1049.
12. J.M.Mansfield, J.D.Winefordner, C.Veillon and M.L.Parsons, ibid., 1966, 38, 204.
13. R.M.Dagnall, T.S.West and P.Young, Talanta, 1966, 13, 803.
14. R.M.Dagnall, K.C.Thompson and T.S.West, Anal. Chim. Acta, 1966, 36, 269.
15. Idem., Talanta, 1967, 14, 551.
16. Idem., ibid., 1967, 14, 557.
17. Idem., ibid., 1967, 14, 1467.

18. C.Th.J.Alkemade, Pure and Applied Chem., 1970, 23, 1.
19. H.P.Hoomayers, Spectrochim. Acta, 1968, 23B, 567.
20. J.D.Winefordner, Anal. Chem., 1968, 40, 26A.
21. Idem., Spectrochim. Acta, 1968, 23B, 37.
22. Idem., ibid., 1971, 26B, 161.
23. L.J.Cline, V.Svoboda and J.D.Winefordner, 'Critical Reviews in Analytical Chemistry', August, 1970, p.232.
24. J.B.Willis, Nature, 1965, 205, 715.
25. M.D.Amos and J.B.Willis, Spectrochim. Acta, 1968, 22,
413.
26. G.F.Kirkbright, A.Semb and T.S.West, Talanta, 1967,
14, 1011.
27. K.Fuma and B.L.Vallee, Anal. Chem., 1963, 35, 942.
28. T.V.Ramakrishna, Anal. Chim. Acta, 1967, 37, 20.
29. D.N.Hingle, G.F.Kirkbright and T.S.West, Talanta,
1968, 15, 199.
30. R.A.White, Int. Atomic Absorption Spectroscopy Conference, Sheffield, July, 1969.
31. Bo.G.Danielson and H.R.Ulfendahl, ditto.
32. H.T.Delves, Analyst, 1970, 95, 431.
33. F.J.Fernandez and H.L.Khan, Atomic Absorption Newsletter, 1971, 10, 1.
34. J.D.Kerber, Atomic Absorption Newsletter, 1971, 10, 116.
35. S.G.Elfbaum, R.Juliano, R.E.MacFarland and R.D.Pfeil, Clin. Chem., 1972, 18, 316.
36. R.D.Ediger and R.L.Coleman, Atomic Absorption Newsletter, 1972, 11, 33.
37. A.A.Cernik and M.P.H.Sayers, Brit. J. Industr. Med.,
1971, 28, 392.

38. D.Clark, R.M.Dagnall and T.S.West, Anal. Chim. Acta,
1972, 58, 1972.
39. Idem., *ibid.*, 1972, 60, 219.
40. C.D.West and D.N.Hume, Anal. Chem., 1964, 36, 412.
41. S.Greenfield, I.L.Jones and C.T.Berry, *Analyst*,
1964, 89, 713.
42. S.Greenfield and P.B.Smith, Anal. Chim. Acta, 1972,
59, 341.
43. R.H.Wendt and V.A.Fassel, Anal. Chem., 1965, 37, 920.
44. K.Kitangawa and T.Takeuchi, Anal. Chim. Acta, 1972,
60, 309.
45. R.Maurodineanu and R.C.Hughes, Spectrochim. Acta,
1963, 19, 1309.
46. R.M.Dagnall, D.J.Smith, S.Greenfield and T.S.West,
Anal. Chim. Acta, 1971, 54, 397.
47. H.C.Hoare and R.A.Mostyn, Anal. Chem., 1967, 39, 1153.
48. K.M.Aldous, R.M.Dagnall, B.Sharp and T.S.West,
Anal. Chim. Acta, 1971, 54, 233.
49. H.Brandenburger, Chimica, 1968, 22, 449.
50. S.Greenfield, P.B.Smith, A.E.Breeze and N.M.D.Chilton,
Anal. Chim. Acta, 1968, 41, 385.
51. C.Veillon and N.Margoshes, Spectrochim. Acta, 1968,
23B, 503.
52. K.E.Friend and A.J.Diefenderfer, Anal. Chem., 1966,
38, 1763.
53. R.H.Wendt and V.A.Fassel, Anal. Chem., 1966, 38, 337.
54. R.D.Hudson, Phys. Rev., 1964, 135, 1212.
55. S.P.Choong and W.Loong-Seng, Nature, 1964, 204, 276.
56. F.S.Tomkins and B.Ercoli, Appl. Optics, 1967, 6, 1299.
57. A.S.King, Astrophys. J., 1908, 27, 353.

58. B.V.L'vov, J. Engng. Phys., 1959, 2, 44.
59. Idem., ibid., 1959, 2, 56.
60. Idem., Spectrochim. Acta, 1961, 17, 761.
61. Idem., Optica. Spectrosk., 1961, 19, 507.
62. Idem., Zavodsk. Lab., 1962, 28, 931.
63. B.V.L'vov and G.G.Lebedev, Zh. Prikl. Spectrosk.,
1967, 7, 264.
64. Idem., 'Symposium on Theoretical Spectroscopy',
Yerevan, 1966.
65. B.V.L'vov, Spectrochim. Acta, 1969, 24B, 53.
66. B.V.L'vov and A.D.Khartsyzov, J.A.C.U.S.S.R., 1969,
24, 636.
67. H.Massmann, Spectrochim. Acta, 1968, 23B, 215.
68. Idem., Z. Analyt. Chem., 1967, 225, 203.
69. D.C.Manning and F.Fernandez, Atomic Absorption
Newsletter, 1970, 9, 65.
70. D.A.Segar and J.G.Gonzalez, Anal. Chim. Acta, 1972,
58, 7.
71. E.Norval and L.R.P.Butler, Anal. Chim. Acta, 1972,
58, 47.
72. R.Woodriff and R.W.Stone, Appl. Optics, 1968, 7,
1337.
73. R.Woodriff, R.W.Stone and M.A.Held, Appl. Spectrosc.,
1968, 22, 408.
74. R.Woodriff and G.Ramelow, Spectrochim. Acta, 1968,
23B, 665.
75. R.Woodriff, B.R.Culver and K.W.Olson, Appl. Spectrosc.
1970, 24, 250.
76. R.Woodriff and D.Shrader, Anal. Chem., 1971, 43, 1918.
77. R.Woodriff and J.F.Lech, ibid., 1972, 44, 1323.

78. J.B.Headridge and D.R.Smith, Talanta, 1971, 18, 247.
79. Idem., ibid., 1972, 19, 833.
80. S.H.Omang, Anal. Chim. Acta., 1971, 55, 439.
81. Idem., ibid., 1971, 56, 470.
82. J.P.Pemsler, E.J.Rapperport, and E.Adler, Rev. Sci. Instr., 1970, 41, 1168.
83. J.P.Pemsler and E.J.Rapperport, Anal. Chim. Acta, 1972, 58, 15.
84. J.D.Winefordner, Pure and Applied Chem., 1970, 23, 35.
85. M.S.Black, T.H.Glenn, M.P.Bratzel and J.D.Winefordner, Anal. Chem., 1971, 43, 1769.
86. T.S.West and X.K.Williams, Anal. Chim. Acta, 1969, 45, 27.
87. R.C.Anderson, I.S.Maines and T.S.West, ibid., 1970, 51, 355.
88. J.F.Alder and T.S.West, ibid., 1970, 51, 365.
89. J.Aggett and T.S.West, ibid., 1971, 55, 349.
90. D.Alger, R.G.Anderson, I.S.Maines and T.S.West, ibid., 1971, 57, 271.
91. R.G.Anderson, H.N.Johnson and T.S.West, ibid., 1971, 57, 281.
92. J.Aggett and T.S.West, ibid., 1971, 57, 15.
93. L.Ebdon, G.F.Kirkbright and T.S.West, ibid., 1972, 58, 39.
94. Idem., ibid., 1972, 61, 15.
95. K.W.Jackson and T.S.West, ibid., 1972, 59, 187.
96. Idem., Anal. Chem., 1973, 45, 249.
97. A.C.Oborne and T.S.West, Proc. Soc. Analyt. Chem., 1972, 2, 198.
98. J.P.Matousek, Amer. Lab. August 1970, p.33.

99. Idem., *ibid.*, p.45.
100. K.G.Brodie and J.P.Matousek, *Anal. Chem.*, 1971, 43, 1557.
101. J.P.Matousek and B.J.Stevens, *Clin. Chem.*, 1971, 17, 363.
102. J.P.Matousek, M.D.Amos, P.A.Bennet, K.G.Brodie and P.W.Y.Lung, *Anal. Chem.*, 1971, 43, 211.
103. M.Glenn, J.Savory, L.Hart, T.Glenn and J.D.Winefordner, *Anal. Chim. Acta*, 1971, 57, 263.
104. M.P.Bratzel, Jr. and C.L.Chakrabarti, *ibid.*, 1972, 61, 25.
105. M.P.Bratzel, Jr., C.L.Chakrabarti, R.E.Sturgeon, M.W.McIntyre and H.Agerrtian, *Anal. Chem.*, 1972, 44, 372.
106. M.P.Bratzel, Jr., R.M.Dagnall and J.D.Winefordner, *Anal. Chim. Acta*, 1969, 48, 197.
107. Idem., *Appl. Spec.*, 1970, 24, 518.
108. H.M.Donega and T.E.Burgess, *Anal. Chem.*, 1970, 42, 1521.
109. B.J.Russell and A.Walsh, *Spectrochim. Acta*, 1959, 15, 883.
110. B.M.Gatehouse and A.Walsh, *ibid.*, 1960, 16, 602.
111. A.Walsh, Proceedings, Xth Colloquium Spectroscopium Internationale, Washington D.C., p.127, 1963.
112. H.Massmann, p.170, Proceedings, IXth Colloquium Spectroscopium Internationale, Volume II, 1961.
113. J.A.Goleb and J.K.Brody, *Anal. Chim. Acta*, 1963, 28, 457.
114. J.A.Goleb, *Anal. Chem.*, 1963, 35, 1978.
115. N.P.Ivanov, M.N.Gusinsky and A.D.Jesikov, *Zh. Analit. Khim.*, 1965, 20, 1133.
116. H.Massmann, *Spectrochim. Acta*, 1970, 25B, 393.
117. V.G.Mossotti, K.Laqua and W.D.Hagenah, *ibid.*, 1967, 23B, 197.
118. B.Gebhart, 'Heat Transfer', Chapter 2, p.20, McGraw-Hill, 1971.

119. R.Stephens, Ph.D. Thesis, University of London, 1971

120. S.L.M.Gibson, C.N.Lam, W.M.McCrae and A.Goldberg,

Arch.Dis.Childh., 1967, 42, 573.